2020

Protocol Development and Optimization for rNLS Mouse Characteristic Assessment

Hasan Farid
Wright State University

PROTOCOL DEVELOPMENT AND OPTIMIZATION FOR RNLS MOUSE
CHARACTERISTIC ASSESSMENT

A thesis submitted in partial fulfillment of the
requirements for the degree of
Master of Science

by

HASAN FARID

B.S., University of Ontario Institute of Technology, 2017

2020

Wright State University

WRIGHT STATE UNIVERSITY

GRADUATE SCHOOL

December 4th, 2020

I HEREBY RECOMMEND THAT THE THESIS PREPARED UNDER MY
SUPERVISION BY <u>Hasan Farid</u> ENTITLED <u>Protocol Development and Optimization
for rNLS Mouse Characteristic Assessment</u> BE ACCEPTED IN PARTIAL
FULFILLMENT OF THE REQUIREMENTS FOR THE DEGREE OF <u>Master of
Science.</u>

_____
Sherif M. Elbasiouny, Ph.D., PE,
P.Eng
Thesis Director

_____
Eric S. Bennett, Ph.D.
Department Chair Neuroscience,
Cell Biology and Physiology

Committee on Final Examination:

_____
Sherif M. Elbasiouny, Ph.D., PE, P.Eng.

_____
Keiichiro Susuki, M.D., Ph.D**.**

_____
Adrian M. Corbett, Ph.D.

_____
Barry Milligan, Ph.D.
Interim Dean of the Graduate School

ABSTRACT

Farid, Hasan. MS, Deparment of Neuroscience, Cell Biology and Physiology, Wright State University, 2020. Protocol Development and Optimization for rNLS Mouse Characteristic Assessment

Protocol development and optimization are vital in the scientific method process. By having accurate protocols, one can properly assess the characteristics of their animal model for any given experiment. One animal newly adopted in our lab was the novel regulatable nuclear localization sequence (rNLS) mouse model. This novel mouse model displays symptoms of Amyotrophic Lateral Sclerosis (ALS) and Frontotemporal dementia (FTD), after the accumulation of the hTDP-43 (TAR DNA-binding protein 43) aggregate in the central nervous system. The expression of this protein occurs after the removal of deoxycycline from the mouse's food source. Once the removal of the drug, this activates a tetracycline-controlled activation system, which causes expression of hTDP-43. The ability to control the expression of hTDP-43 provides the uniqueness to this ALS/FTD mouse model allowing researchers to study these fatal neurodegenerative diseases at various time points in the mouse's timeline.

In this thesis, three different studies were conduct that either developed or optimized protocols to assess characteristics of this novel rNLS mouse. The first study investigates the development of cognitive behavioural tasks designed assess working memory and learning in this mouse model. These behavioural tasks are the Y-maze, the

NOR (NOR) and the Holeboard tests. In addition to developing behavioural task protocols suited for our mouse model, a comparison was also done between WT (WT) and NS (NS) rNLS mouse, which are mice part of the rNLS colony that do not have the bigenic mutation expressing ALS/FTD, to determine if NS rNLS could be used as control, the results confirm they can be used. In the second study, the Y-maze protocol was utilized in assessing short-term working-memory of rNLS mice 3 and 5 weeks off doxycycline. This preliminary study shows evidence of cognitive deficits in this mouse model as well as provides credibility to our developed protocol.

The third study compares the intramuscular labelling of α-MNs (α-MNs) through the usage of Fast-Blue (FB) and Cholera-toxin B (CTB) retrograde tracers under different parameters such as different concentrations and survival days. These tracers were injected into the hindlimb muscles of WT mice and showed that despite each tracer providing its own uniqueness in labeling α-MNs was no overall difference between these retrograde tracers. However, it was discovered that using less in concentration and survival day is often advantageous then utilizing standard protocol for alpha-motoneuron labeling.

TABLE OF CONTENTS

LIST OF FIGURES AND ILLUSTRATIONS

LIST OF FIGURES AND ILLUSTRATIONS (Continued)

LIST OF TABLES

LIST OF ABBREVIATION

Full Word – Abbreviation

Alpha-motoneurons – α-MNs

Amytrophic Lateral Sclerosis – ALS

Camodulin-dependent protein kinase – CamkIIa

Frontotemporal Dementia – FTD

Gamma-motoneurons – γ-MNs

Human TAR DNA-binding protein – hTDP-43

Motoneurons – MNs

Neurofilament heavy chain – NEFH

Non-symptomatic rNLS – NS-rNLS

Novel Object Recognition test – NOR test

Regulatable Nuclear Localization Sequence – rNLS

Ribonucleic Acid – RNA

TAR DNA-binding protein 43 – TDP-43

Tet operator – tetO

Transactivator – tTA

Wild-type - WT

Introduction

TDP-43 and TDP-43 Proteinopathies

Transactive response DNA binding protein-43 (TDP-43), commonly known as TDP-43, is a heterogenous ribonuclear protein that is composed of an N-terminus, C-terminus and 2 Ribonucleic Acid (RNA) Recognition Motifs that allows the protein to bind to ribonucleic acid (J. Gao et al., 2018, p. 43; Guo & Shorter, 2017; Ratti & Buratti, 2016, p. 43; Tremblay et al., 2011). This protein was originally discovered in 1995 as a repressor for the Human immunodeficiency virus-1 gene (Ou et al., 1995). Since then additional research has discovered that human TDP-43 (hTDP-43) is responsible for other functions surrounding the DNA dogma, in addition to gene regulation (J. Gao et al., 2018, p. 43; Guo & Shorter, 2017; Ratti & Buratti, 2016; Tremblay et al., 2011). TDP-43 primarily plays a role in post-transcriptional modification such as pre-mRNA splicing, mRNA translation, mRNA stability and transportation across the axon (Coyne et al., 2017). The C-terminus of TDP-43 is responsible for these functions as it regulates pre-mRNA splicing activity through the interaction of other hnRNPs and also self-regulates its transcription (Guo & Shorter, 2017). TDP-43 also plays a significant role in the processing of microRNA and formation of stress-granules to ensure that the transcription continues during oxidative stressful environments (Colombrita et al., 2009; Guo & Shorter, 2017).

In the early 2000s, researchers discovered that many patients with various neurogenerative diseases like Alzheimer's Disease, Huntington's Disease, Parkinson's Disease, Frontal Temporal-Dementia (FTD) and Amyotrophic Lateral Sclerosis (ALS) had commonalities that was the presence of aggregated TDP-43 in the cytoplasm of neurons and glial cells (Kovacs, 2016) . This discovery introduces the topic of TDP-43 proteinopathies to research, which suggests that TDP-43 plays an important role in

neurodegenerative diseases. Since its discovery, further research has been conducted to understand how TDP-43 contributes to neurodegenerative diseases.

Although there is still more research to be conducted in the pathomechanism of TDP-43 during these neurodegenerative diseases, there are some theories as to how TDP-43 goes from being helpful to harmful. In individuals without any neurodegenerative diseases, TDP-43 is observed primarily in the nucleus, with less than 30% of the total TDP-43 in the cytosol (Kabashi et al., 2010). However, in neurodegenerative diseases, TDP-43 is not observed in the nucleus but rather aggregated in the cytosol (Ratti & Buratti, 2016). This relocation of TDP-43 to the cytoplasm is caused by mutations to the *TARDBP* gene, which responsible for expressing TDP-43 protein (Kabashi et al. 2010; Janssens and Van Broeckhoven 2013, 43; Medina, Orr, and Oddo 2014, 43). Majority of these mutations are missense mutations that result in conformational structure changes of TDP-43, truncation of TDP-43 or deletion of a nuclear localization sequence (J. Gao et al., 2018; Kabashi et al., 2010; Medina et al., 2014).

The nuclear localization sequence (NLS) is primarily responsible for translocating TDP-43 back to the nucleus after translation (Janssens & Van Broeckhoven, 2013; Kabashi et al., 2010; Medina et al., 2014; Ratti & Buratti, 2016). These mutations of TDP-43 result in a loss of function mutation, where TDP-43 that is normally located in the nucleus is no longer there (Cascella et al., 2016). In addition to a loss of function mutation, there is also a gain-of-function mutation for these mutated TDP-43, where aggregation of TDP-43 outside of the nucleus becomes toxic (Cascella et al., 2016; Kapeli et al., 2017). How aggregated TDP-43 is toxic is still yet to be determined, but one theory suggested that TDP-43 still retains its ability of bind to RNA and protein and thus

sequesters other TDP-43 outside of the nucleus to aggregate in a prion-like manner contributing to toxic effects (Voigt et al. 2010). Other theories have inferred that mutated TDP-43 affects axonal transport and other dependent mechanisms, which interrupted can results in neuronal death (Ludolph & Brettschneider, 2015). Further investigation is needed into these proteins as they appear to be a primary suspect in various neurodegenerative diseases.

Amyotrophic Lateral Sclerosis

(ALS) is a fatal neurodegenerative disease that was first discovered by French neurologist Jean-Martin Charcot in 1869 (Martin et al., 2017; Ng et al., 2017; Zarei et al., 2015). It became more commonly known as Lou Gehrig's disease after the famous baseball player, Lou Gehrig, was diagnosed with ALS in 1939 (Zarei et al. 2015). This fatal neurodegenerative disease causes the death of upper and lower MNs located at the spinal and bulbar level (Ng et al., 2017). This loss of MNs results in paralysis and atrophy of muscles, which eventually leads to death due to respiratory failure within 1-5 years after disease onset (Ng et al., 2017). In addition to the fatality of this disease, only a small fraction of people are diagnosed with ALS.. In a population of 100,000 people worldwide, only 1.5-2.5 people are affected by ALS (Chiò et al., 2013). Of the people affected by ALS, the majority of them are males diagnosed between the ages of 50 and 75 (Martin et al., 2017). Currently, there are two FDA-approved drugs, Riluzole and Edaravone, that assist in treating ALS symptoms, however, there is no cure regarding this fatal disease (Jaiswal, 2019).

ALS is presented in two forms, with the common form being sporadic ALS (Zarei et al., 2015). This type of ALS occurs in 90% of the patients and has no underlying causes for the disease (Zarei et al., 2015). The other form of ALS is known as familial ALS, which accounts for 10% of all ALS cases (Zarei et al., 2015). This form of ALS does have a genetic attribution to cause symptoms of ALS (Zarei et al., 2015). The mutations that are commonly studied in research are Superoxidase dismutase gene, Fusion in sarcoma gene, Angiogenin gene, Optineurin gene, C9orf72 gene and TDP-43 gene (Kapeli et al., 2017; Zarei et al., 2015). Although TDP-43 mutations account for 5-10% of familial ALS cases, 97% of all ALS patients from sporadic and familial variants have shown cytoplasmic TDP-43 aggregation post-mortem (T. Ishihara et al., 2010; Kabashi et al., 2010). Interestingly, ALS patients lose normal TDP-43 function in the nucleus and gain neurotoxic effect by the aggregation of TDP-43 in the cytoplasm (Kabashi et al., 2010; Scotter et al., 2015, p. 43). Due to the involvement of TDP-43, ALS is also considered under the TDP-43 proteinopathy umbrella (Scotter, Chen, and Shaw 2015).

Frontotemporal Dementia

FTD is the third common dementia that follows after Alzheimer's Disease and Dementia with Lewy bodies and is the second most common dementia for patients under 65 years of age (Young et al., 2018). The term frontotemporal corresponds to the loss of neurons located primarily in the frontal and temporal regions of the brain (Olney et al., 2017). The loss of neurons in these locations results in dysfunction in executive functioning, behavior, language, episodic memory loss and motor deficits in later stages

of the disease (Olney et al., 2017; Young et al., 2018). The symptoms of FTD are difficult to effectively diagnose as many of the symptoms can show off as psychiatric disorders (Bang et al., 2015).

Within FTD there are subtypes of this disease that all vary in the initial symptoms seen in patients (Liu et al., 2004). For example, behavior variant FTD is a subtype of FTD that shows primary symptoms of behavior and personality changes that result in inappropriate social actions, lack of empathy and even impulsiveness (Bang et al., 2015). Whereas, primary progressive aphasia subtype shows symptoms that mimic Alzheimer's disease-like deficiency in memory and also presents deficits in the language (Bang et al., 2015). So far there are no current FDA treatments for FTD other than managing symptoms through hospitality care and medication for behavior symptoms (Bang et al., 2015).

Although there are many different subtypes of FTD, various cases have shown the presence of 3 different mutated proteins that contribute to the disease (Young et al., 2018). These proteins are said to play a role in the progression of FTD (Young et al., 2018). These proteins are microtubule-associated protein tau protein, TDP-43 and FUS (Young et al., 2018). Of these three proteins, TDP-43 plays a role in 50% of all FTD cases with the majority of the cases being primary progressive aphasia subtype of FTD (Sieben et al., 2012). TDP-43 observed in FTD patients have shown the same consistency as ALS patients, where there is a loss of nuclear TDP-43 accompanied by aggregation of TDP-43 in the cytoplasm that leads to toxicity, ultimately leading to neuronal death (Janssens & Van Broeckhoven, 2013).

ALS/FTD spectrum involving TDP-43

ALS and FTD patients appear to be two polar opposite diseases, however, it was later discovered that there were overlapping symptoms between these two neurogenerative diseases (Bennion Callister & Pickering-Brown, 2014). Studies have shown that 15% of all ALS and FTD patients experience behavioral, cognitive and motor deficits in the latter stages of their disease (Lillo & Hodges, 2009). These overlapping symptoms of ALS and FTD suggested some patients that develop ALS also develop FTD and that there is a commonality between these diseases (Lillo & Hodges, 2009).

In 2006, TDP-43 mutations were identified as the common source that contributed to ALS-FTD disease (Ling et al., 2013; Neumann et al., 2006). The pathomechanism of TDP-43 in ALS and FTD are still being determined, but patients that exhibit ALS-FTD all seem to show a loss of regular function of TDP-43 in the nucleus and aggregated TDP-43 in the cytoplasm (Ling et al., 2013). It is speculated that TDP-43 aggregation in the cytoplasm cause neurotoxicity in ALS-FTD patients (Ling et al., 2013).

rNLS Mouse Model

One mouse model that has gained interest in being used as an ALS-FTD mouse model is rNLS mouse model. This model was first introduced with a tetracycline transactivator (tTA) attached to a calcium camodulin-dependent protein kinase (*CamkIIa*) promotor along with a tetO (Tet Operator)-hTDP-43ΔNLS (Alfieri et al., 2014). The uniqueness of this mouse model came from the ability to express hTDP-43, after the removal of doxycycline (Alfieri et al., 2014). This would be more beneficial to study ALS-FTD than other transgenic mouse models because you can assess all aspects of

ALS-FTD symptoms at various ages and stages of diseases, as well as further investigate

role TDP-43 plays in ALS-FTD, especially after re-introducing doxycycline (Spiller,

Cheung, et al., 2016; Walker et al., 2015). In addition to the tTA system, the hTDP-43

contained the ablation of the nuclear localization sequence (NLS), this sequence was

located close to the N-terminus of TDP-43 and is responsible for shuttling TDP-43 back

into the nucleus after translation (Cascella et al., 2016). Previous literature has shown that

for ALS-FTD pathogenesis to occurs both the loss of nuclear function and gain of

toxicity through aggregation must occur (Cascella et al., 2016). Ablation of the NLS

sequence allowed for this to happen.

Although, this early hTDP-43ΔNLS mouse model showed motor deficits, these

deficits were not regards to affected MNs located in the spinal cord (Alfieri et al., 2014).

This is because the *CamkIIa* promotor facilitated the expression of hTDP-43 only in the

forebrain and not in the spinal cord (Walker et al., 2015). This expression only to the

brain led to cognitive deficits due to inclusions of hTDP-43ΔNLS seen in the

hippocampus, cortex and olfactory bulb (Igaz et al., 2011). In addition, these inclusions

were also shown to cause cognitive deficits in this model of rNLS as seen through

behavioral tests such as the Y-maze, NOR and Elevated Plus Maze with minimal motor

deficits (Alfieri et al., 2014). Furthermore, this model of rNLS showed an increase of

hTDP-43 expression 8 to 9 fold more than endogenous mTDP-43 and evidence of gliosis

by immunohistochemistry staining using glial fibrillary acidic protein (Igaz et al., 2011).

The results of this study showed that *CamkIIa* rNLS model is excellent models for FTD,

but lacked the full symptoms of ALS and therefore not considered to be an ALS-FTD

mouse model.

This then led to the development of the novel rNLS mice model, which is currently used in our lab. This rNLS mice model is unique because it contains a *NEFH* (neurofilament heavy chain) promoter attached to the tTA instead of the *CamkIIa* promotor, allowing expression of the hTDP-43 protein to occur in neurons and non-neuronal cells in the central nervous system (Spiller et al., 2019; Walker et al., 2015). Previous literature has shown that when these mice are taken off doxycycline, transcription of hTDP-43ΔNLS occurs in neurons and astrocytes of the hippocampus, cortex, olfactory bulb and MNs in the spinal cord causing severe motor function deficits in addition to suspected cognitive deficits (Spiller et al., 2019; Walker et al., 2015). Although, literature has also shown that this novel rNLS mouse model is capable of exhibiting cytoplasmic inclusions of hTDP-43 in neurons in the hippocampus and other regions of the brain (Walker et al., 2015) there has yet to be a study conducted on whether this results in the expression of FTD symptoms.

Study 1: Development of Short-Term Memory and Learning Tests

Brief Introduction

Rodents are ideally used for behavior experiments as their innate behaviors are relevant to human disease (Teegarden, 2020). Behavior experiments utilize innate behaviors of rodents to assess various functions (Teegarden, 2020). Such functions that are commonly assessed by behavioral experiments are memory (Prieur & Jadavji, 2019), learning (Kuc et al., 2006), motor function (Shiotsuki et al., 2010), sensory function (Pankevich & Bale, 2008) and addiction (Duncan et al., 2019).

Memory is defined as the ability to recall information that is already stored and learning is defined as the ability to acquire new information (Smid & Vet, 2016). In humans, we use working memory, which is a type of short-term memory that is temporally store information for the usage of everyday tasks such as remembering and using facts and data to solve problems (Hasselmo et al., 2017). Working memory can be further broaden to include spatial awareness, this is known as spatial working memory (Shrager et al., 2007). In this study, three commonly used behavioral tasks were developed to assess short-term working memory and learning in mice. These behavioral tasks are the Y-maze test, NOR test and Holeboard Discrimination test.

The Y-maze test is a maze that is set up in the shape of a "Y" with each arm having an angle of 120 degrees (Kraeuter et al., 2019). This test is frequently used as it is relatively easy to conduct and assess spatial working memory in rodents. The premise of the Y-maze test involves the use of mice's innate curiosity to explore less recently visited arms (Kraeuter et al., 2019). As a mouse is dropped into the center of the maze, it will continue to go from arm to arm without entering the previous arm it just visited. A mouse that has memory deficit will not be able to recall the arm it had just entered and will continue to enter the same arm it just visited (Kraeuter et al., 2019). The Y-maze test

requires the use of several different regions of the brain such as the hippocampus and prefrontal cortex, which are some of the affected regions in the novel rNLS mouse model (Walker et al., 2015) mice are required to recall the arm they had just visited and make decisions as to which arm to go into next (Kraeuter et al., 2019).

The NOR test is another behavioral task used in research that can assess short-term working memory. This test is conducted by using two familiar objects that a mouse thoroughly explores before one of the objects is replaced with a novel object (Antunes & Biala, 2012). The same mouse is then reintroduced to the objects, after a short interval of time, and will recall, which object is familiar and will interact with the novel object (Antunes & Biala, 2012). This test relies on a mouse's innate preference towards novelty and assesses functions related to the limbic system specifically the hippocampus, entorhinal and prefrontal cortices (Antunes & Biala, 2012). These specific brain regions are involved in object recognition and retention in mice and are the affected regions of the rNLS model (Antunes & Biala, 2012; Walker et al., 2015).

The Holeboard Discrimination test is the only test in this study that assesses spatial reference memory and learning within the mice. Spatial reference memory refers to the retention of one's location-based off a series of visual cues (Kuc et al., 2006). Interestingly, this test relies heavily on visuospatial processing as mice use distal cues to identify baited holes in the test (Kuc et al., 2006). The goal of this experiment is that mice are tested over a series of days, expected to find 4 holes that are baited with treats using distal cues attached on the side of the apparatus. Mice with hippocampal-dependent memory and learning deficits will make more errors in finding the baited holes (Kuc et al., 2006). Our modification of this test involves the use of positive reinforcement in the

form of cookie dough to encourage mice to find the baited holes. The brain structure most assessed from this test is the hippocampus, as it is the primary brain structure involved in learning as well as spatial reference memory (Vorhees & Williams, 2014).

Due to the novelty of this particular rNLS mouse model, no literature indicates this mouse model has been assessed through behavioral tests. Therefore, the purpose of this study is to develop and modify the experimental designs of the behavioral tests: the Y-maze test, the NOR test and the Holeboard Discrimination test to assess short-term memory and learning in this rNLS mice model. The reason these specific tests were chosen is because of their ability to assess different aspects of hippocampal dependent memory such as working, recognition and spatial reference memories as well as learning. To accomplish this, WT background strain of mice and NS rNLS mice were used to develop these behavioral tests after adopting common protocols from literature. Background strain were used in this study to develop these protocols as it is unsure if the either inserts, tTA-*NEFH* and tetO- hTDP-43ΔNLS, independently cause cognitive deficits. Therefore, in addition to developing behavioral tests, this study also shows if these monogenic inserts could contribute cognitive dysfunction.

Hypothesis

We hypothesized that behavioral tests developed are capable of assessing short-term memory and learning for our rNLS mice model. We also hypothesized that the WT background strain of rNLS mice are not different in cognitive performance compared to our NS rNLS mice.

Methods and Materials

Animals

rNLS mice model had the background strain B6C3F1/J, a hybrid between C57BL/6J x C3HeJ F1 mice strains. B6C3F1/J-WT had been ordered from Jackson Laboratory (Stock No. 100010) and housed at Wright State University's Laboratory Animal Care facilities. B6C3F1/J-WT and rNLS NS mice (Stock No. 028412) were used for short-term memory task development (Table X).. rNLS +/- and -/+ contained either the tTA-*NEFH* promoter or tetO-hTDP-43-ΔNLS monogenic mutation, but neither both so ALS-FTD symptoms should not appear.

Table 1 shows the sample size used for each experiment. For all sample size equal number of male and female mice were used. Same set of adult B6C3F1/J-WT and NS rNLS mice (~5 weeks of age) were used for all experiments regarding the development of these behavioral tasks. Positive control experiments were run for the Y-maze and the NOR Task. For these experiments 24 additional B6C3F1/J-WT were ordered from Jackson Laboratory (Stock No. 100010). 12 of these B6C3F1/J-WT mice were injected with 1 mg/kg (for Y-maze testing) and 3 mg/kg (for NOR) of scopolamine (Sigma Aldrich, St. Louis, USA) intraperitonally, 30 minutes before testing. The other 12

B6C3F1/J-WT mice were I.P injected with 0.09% saline solution 30 mins before testing experimentation. The purpose of scopolamine is to induce short-term memory deficits in mice by acting as an acetylcholine antagonist, decreasing the amount of acetylcholine in the brain. In most cognitive behavioral studies, scopolamine is used as a positive control as it is also used as a positive control in this study.

All mice had been housed at Wright State University's Laboratory Animal Care facilities on 12:12-h light-dark cycle. Food and water were provided *ad libitum*. All procedures followed NIH guidelines and were approved by Wright State University's Laboratory Animal Care and Use Committee (LACUC) – protocol numbers AUP 1145 and 1117.

Table 1. Sample Size Distribution For Short-term Memory Task Development.

Experiment	Experiment Iteration #1 sample size (n)	Experiment Iteration #2 sample size (n)	Experiment Iteration #3 sample size (n)
Y-maze	B6C3F1/J-WT (12) rNLS - NS (12)	N/A	N/A
NOR Test	B6C3F1/J-WT (12) rNLS - NS (12)	B6C3F1/J-WT (12) rNLS - NS (12)	B6C3F1/J-WT (12) rNLS - NS (12)
Holeboard Discrimination Test	B6C3F1/J-WT (6) rNLS -/- (6)	B6C3F1/J-WT (3) rNLS -/- (3)	B6C3F1/J-WT (6) rNLS -/- (6)

Y-maze test

Y-maze was constructed with white plexiglass in the shape of a "Y" with each of the 3 arms labelled as A, B, C and having the dimensions 39.5 x 8.5 x 13 cm (Fig 1). All mice were acclimated to testing room conditions 30 mins before starting the test. Each mouse was tested for only one trial. Each trial consisted of 10 mins. At the start of a trial, a mouse was dropped in the middle of the chamber, where 3 of the arms intersected, to

prevent starting point having an influence on the results. At the end of the trial, the mouse

was removed from the Y-maze and the apparatus was cleaned with 70% (w/v) ethanol.
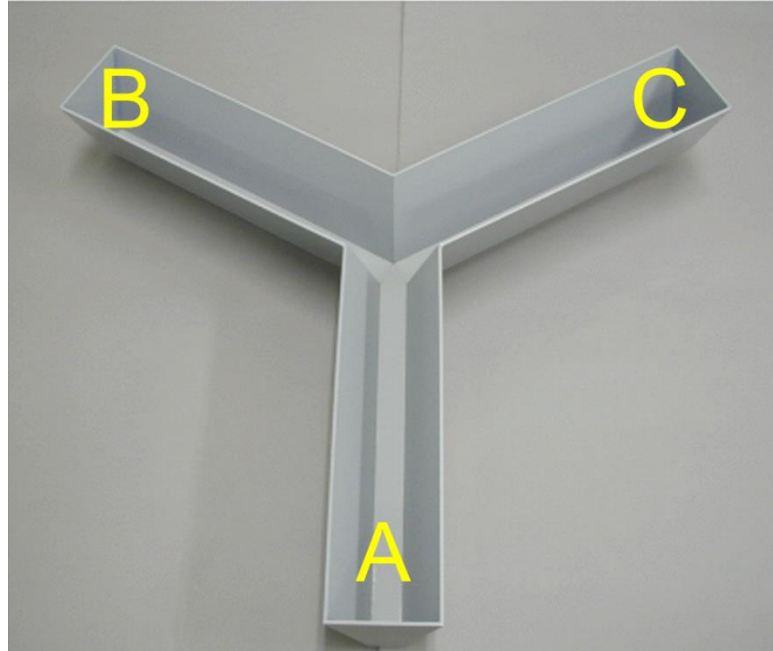
Figure 1. Image of Y-maze apparatus used for short-term memory assessment
Y-maze apparatus with Arm A, Arm B and Arm C labelled.

Animal tracking program, *Any-Maze* (Steoelting, UK) and ELP USB Camera with

1080P wide-angle fisheye lens with LED infrared (Ailipu Technology Co. LTD,

Guangdong, China) were used for determining the following: number of entries, number

of alternations and spontaneous alternations. The number of entries represents the

locomotive activity of the mouse during the trial and is defined as how many times a

mouse enters a specific arm during the trial. The number of alternations is defined as the

number of times a mouse went into each of the 3 arms consecutively to form an

overlapping triplet set ie. ABC, BCA, CAB etc. Spontaneous alternation percentage was

calculated by comparing the number of alternations relative to the number of entries of

the mouse during the trial. Spontaneous alternation percentage is calculation is represented by:

$$Spontaneous\ Alternation\ \% = \frac{(\underline{Total\ Number\ of\ Alternations})}{(Total\ Number\ of\ Entries - 2)} \times 100$$

This protocol for Y-maze was the finalized and was used for testing on rNLS +/+ mice. A positive control experiment was also conducted to determine the efficiency of this protocol. For the positive control experiment, 12 B6C3F1/J-WT were injected with 1 mg/kg of scopolamine, 30 mins before the start of the trial and 12 B6C3F1/J-WT were injected with 0.09% saline, also 30 mins before the start of the trial. Same Y-maze protocol and measurement were used to assess short-term memory.

NOR Test

NOR apparatus had 2 separate parts. Square opaque plexiglass and an open-top opaque chamber with the dimensions of 40.64cm x 40.64 cm x 38.1 cm (Fig 2). *Any-Maze* (Steoelting, UK) and ELP USB Camera with 1080P wide-angle fisheye lens with LED infrared (Ailipu Technology Co. LTD, Guangdong, China) were used to record video and the amount of time a mouse had spent with each object. NOR test development took 3 iterations to establish a proper protocol that worked for our set of mice. Before the start of each experiment, mice were acclimated to the testing room conditions for 30 mins.
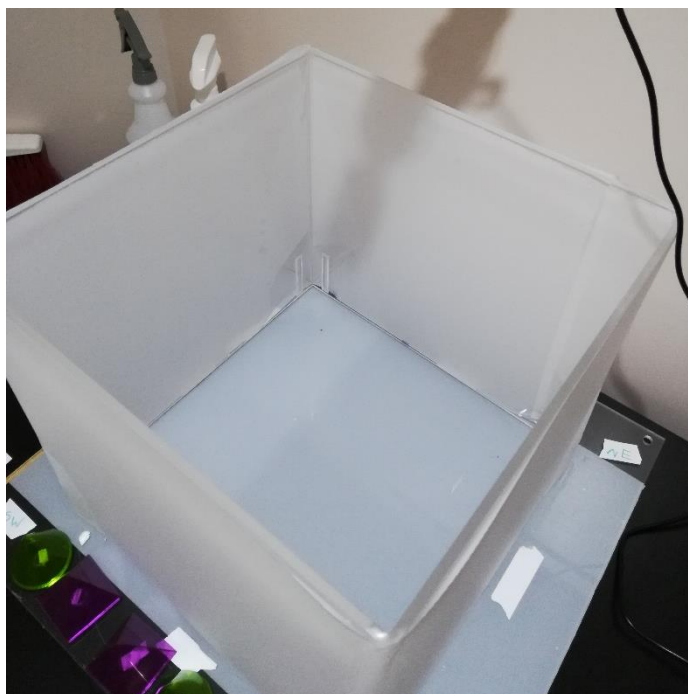
Figure 2. Image of NOR apparatus
NOR apparatus used for assessment.

The first iteration of the experiment consisted of B6C3F1/J-WT (n=12) and NS

rNLS mice (n=4 each for rNLS -/-, rNLS +/- and rNLS -/+) for a total of 24 mice. The

experiment took 2 days, the first day was for habituation in which each mouse was left in

the chamber for 10 minutes with no objects to interact with. On the second day, each

mouse was left in the chamber with two same objects in the corners of the chambers for

10 mins, this is known as the familial trial. Once the last mouse was done with the

familiar trial, the first mouse was put into the chamber again for 10 mins, however, this

time one of the objects was replaced with a new one. This portion of the experiment is

known as the novel trial. The objects used in this phase were a used pipette box filled

with rocks (Fig 2a) and 120 mL plastic cups glued at the bases with a black rubber

stopper (Fig 2b). The issue with this iteration was that the inter-trial time interval

between the familial and novel phases were too long and the mice consistently climbed

the object, which did not consider interacting with the objects.
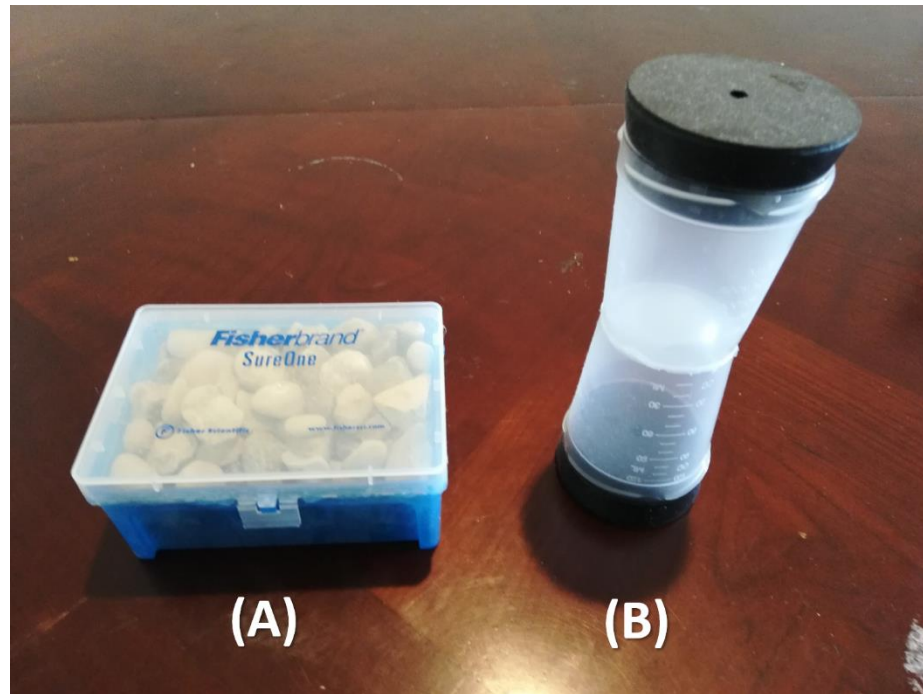
Figure 3. Objects used for first iteration of experiment for NOR Test
(A) pipette box filled with rocks (B) 120 mL plastic cups glued at the bases with black
rubber stopper.

A discrimination ratio was used to assess the short-term memory of mice and was

calculated based off timings from the novel phase of the experiment. The time a mouse

spend on top of the object was recorded and removed from the total time at the end of the

trial to give an accurate timing of interaction. The equation representing the

discrimination ratio is:

$$Discrimination\ Ratio = \frac{(Time\ spent\ with\ Novel\ Object)}{Time\ spent\ with\ Both\ Objects}$$

The second iteration of experiments was conducted to overcome the issues of the first

iteration, which were the long inter-trial interval and the objects were climbable. This

iteration was similar to the first iteration of the experiment; however, the test was

conducted over a series of days because the mice were grouped into 4 groups with a

squad of 6 mice per group. This was done so that a large cohort of mice can be tested

throughout the experiment. These 4 groups were staggered in testing as seen in Table 2.

Mice were still acclimated to testing room conditions 30 mins before the start of test each

day. Habituation was still conducted for 10 mins, the day before familial and novel trials.

On the day of familial and novel trials, each trial consisted of 10 mins with an inter-trial

interval of 2 hours, which was less than the 4 hours in the first iteration. The objects used

in this testing were 100 mL flask and 200 mL bottle with a black cap (Fig 4).

Discrimination Ratio was still used to assess short-term memory. The second

iteration had still resulted in problems with the experimental design. For this iteration, the

inter-trial time interval was still long and the objects were still climbable. Also, the mice

appeared to be interactive with their surrounds and not so much with the object.

Therefore, a third iteration was conducted to address these problems.

Table 2. Schedule of NOR Per Group

Day 1	Day 2	Day 3	Day 4
Group 1 Habituation	Group 1 Familiar/Novel	Group 2 Familiar/Novel	Group 4 Familiar/Novel
	Group 2 Habituation	Group 3 Habituation	
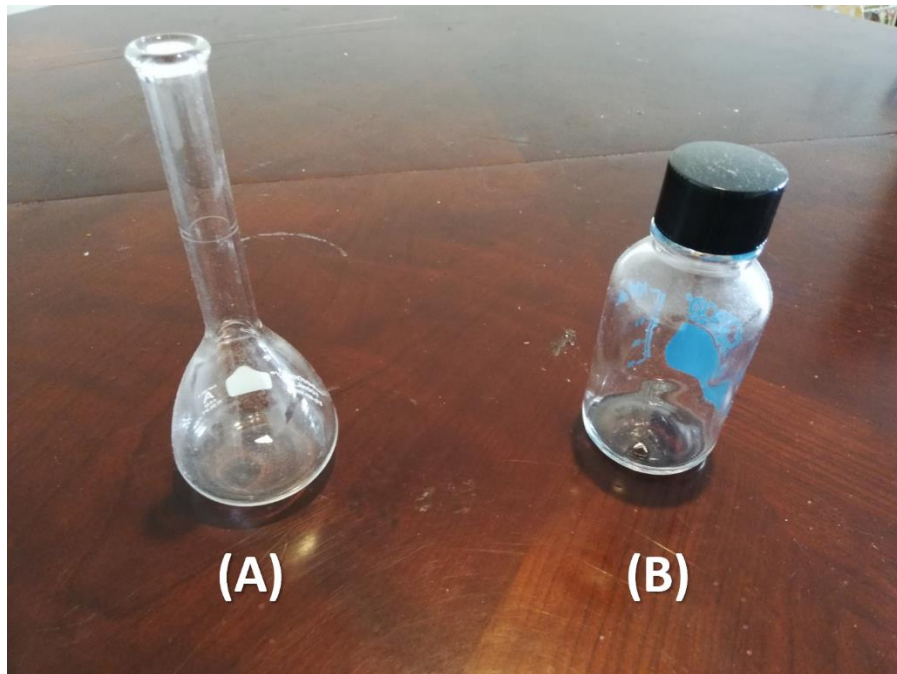
Figure 4. Objects used for second iteration of experiments for NOR.
(A) 100 mL flask and (B) 200 mL bottle with a black cap.

The third iteration of experiments was conducted to decrease the inter-trial time

interval, replace the objects with pointy geometric 3D shapes such as a cone or square-

based pyramid and increase the habituation days. These changes were done to address the

issues from the 2nd iteration, where the inter-trial interval was too long, the objects were

still climbable and the mice seemed to be distracted with their environment during

habituation. In this iteration, the protocols for acclimation, familial and novel trials were

still the same. However, 2 more habituation days were added and the inter-trial interval

was reduced to 20 mins. Grouping of 6 mice was still maintained similar to the previous

set of experiments, however, a squad of 3 mice was staggered in testing to reduce

expendable time between mice. For example, Mouse 2 and 3 ran for their familiar phase

during the 20 mins inter-trial interval of Mouse 1. The objects used in this testing were

plastic see-through colourful geometric shapes, cone (Fig 5a) and square-based pyramid

(Fig 5b). A discrimination ratio was still used to assess short-term memory. This third

phase of the experiment protocol is the finalized protocol intended to be used for testing.

A positive control experiment was also conducted using this protocol and consisted of 12

B6C3F1/J-WT I.P injected with 3 mg/kg of scopolamine 30 mins before the familiar

phase and 12 B6C3F1/J-WT I.P injected with 0.09% saline. Same protocols and

measurements were used for short-term memory assessment with NOR test.
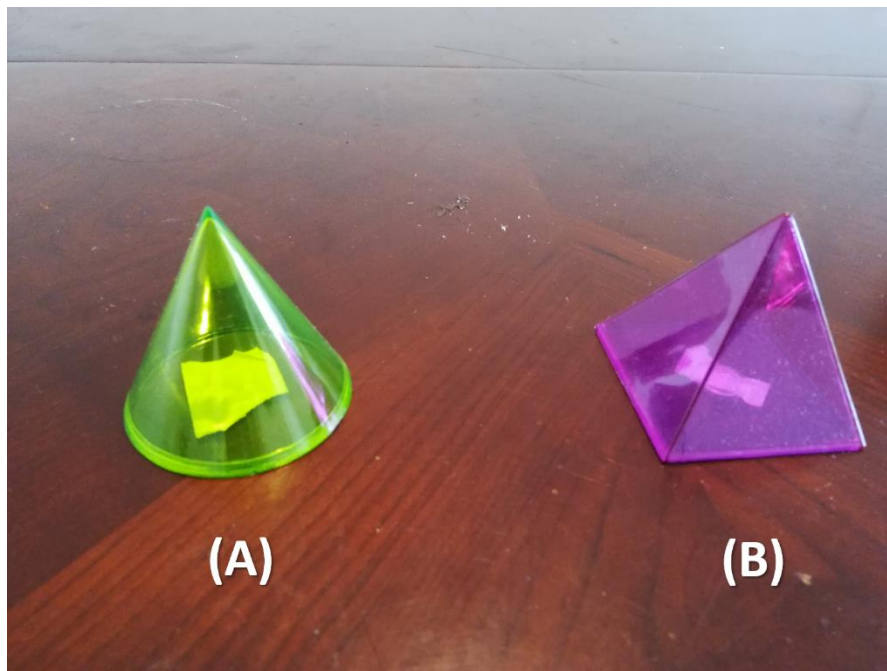
Figure 5. Objects used for third iteration of experiments for NOR test.
(A) green cone geometric shape and (B) purple square-base pyramid geometric shape.

Holeboard Discrimination Test

Holeboard Discrimination Test consisted of 16 holes on a board with the dimensions of 41.50 cm x 41.50 cm x 5 cm. The holes made in the holeboard are equal distance apart from each other and from the sides of the holeboard with a diameter of 1.8 cm and a depth of 0.6 cm. A transparent chamber with an open top-bottom is place on top of the 16 holeboard. On the north side of this chamber is a cardboard circle with a diameter of 25 cm and on the west side is equilateral cardboard triangle with a dimensions of 15 cm x 15 cm x 15 cm (Figure 6). Development of the holeboard discrimination test took 3 iterations with emphasis on not trying to fast the mice. *Any-Maze* (Steoelting, UK) and ELP USB Camera with 1080P wide-angle fisheye lens with LED infrared (Ailipu Technology Co. LTD, Guangdong, China) were used to record video throughout the experiments.

Figure 6. Image of the Holeboard Discrimination test apparatus

In the first iteration of this experiment, all mice were acclimated 30 mins before the start of the experiment. The mice were habituated by being placed into the holeboard apparatus with all 16 holes baited with whole honey-nut cheerio for 15 mins. For acquisition training, only 4 of the holes were baited with whole honey-nut cheerio in a configuration that did not change throughout the rest of an experiment. 6 trials were conducted for 4 days. Each trial was completed in 3 mins or when a mouse obtained all the baited holes. Measurements used to assess learning and memory capabilities were Reference Memory error, Working Memory error, Completion Time, 1st time to treat and Number of Treats. Reference memory error refers to the number of times a mouse nose

pokes into a hole that was never baited. This variable assesses short-term spatial reference memory of a mouse. Working memory error refers to the number of times a mouse nose pokes into a hole that was baited or is no longer baited after obtaining the treat. This variable assesses short-term working memory. This iteration presented many issues as the number of trials were too long, the time per trial was too short, the treats were too big for the mice and even the sample size tested was too big.

The second iteration of this experiment was conducted to address the issues of the first iteration which were too many trials, longer trial time, bigger treat size and large sample size testing. To overcome these issues the sample size was halved from the first iteration. The time for each trial was also extended to 4 mins and whole honey-nut cheerio was cut into ¼ size pieces. The acclimation, habituation and the number of days of testing were still the same however, the number of trials per day was decreased to 4 trials. The 4 holes baited were re-configured and kept the same throughout an experiment. The same measurements as the first iteration were used. Issues were still seen in the second iteration where the treats did not seem to appeal to the mice, the mice were not as active and avoided the center of the apparatus due to the interference of lighting and there was no learning component present. This led to a third iteration of the holeboard experiment.

The third iteration of this experiment was conducted to address the issues in the second iteration, which were the unappealing treats, lack of activity, avoiding the center of the apparatus and lack of learning. To overcome these obstacles the treats were replaced with cold 20 µg of cookie dough (Meijer Sugar Cookie Dough, 1.6 oz, Dayton, Ohio). The test was also conducted at night at around 19:00 when lights were off and a

learning component was added. To add a learning component, the 5 mL silicone-filled tubes were replaced with 5 mL tubes that had their base cut to allow a ~2 cm diameter wooden dowel insert into the tubes. The wooden dowels were placed on top of a 35 cm x 35 cm plexiglass sheet acting as a platform, which was added to the bottom of the holeboard apparatus. At the end of the trial, the wooden dowels would erect the treats exposing them for the mice to see and learn the location of the baited holes.

The time for each trial was also extended to 5 mins, the last-minute was given to raise the platform underneath the hole board to expose the baits. The acclimation, habituation, sample size and measurements used to assess this experiment were kept the same as the previous iterations. This third iteration of the experiment is the protocol that is intended to be used for short-term memory and learning assessment. Due to the interference of the COVID-19 pandemic, a positive control experiment for the third iteration of the Holeboard Discrimination test was not conducted.

Data Analysis

SPSS® (IBM Corporation, New York USA) statistical software was used for statistical analysis of all measurements. While, PRISM Graphpad (GraphPad Software, California USA) was used for all graph needs in this study. All data for behavioral task development had a normal distribution and did not reject the Levene's test ($p > 0.05$). Therefore, parametric statistical analysis was conducted for all measurements. For Y-maze and NOR Tests, independent t-test was conducted between groups. The measurements regarding Y-maze are number of entries, number of alternations, spontaneous alternations. The measurement for the NOR test is the discrimination ratio.

For Holeboard discrimination test, a Two-Way Repeated Measures ANOVA was

conducted to compare within-subjects being between Day 1 and Day 4 of testing and

between-subjects being between WT and NS rNLS mouse. Fischer's LSD was utilized

for post hoc analysis. The threshold for significance was 0.05 (α). All data is shown with

the mean $\pm$ standard error mean (SEM).

Results

Y-maze test was developed and showed no differences between* NS *rNLS and* WT *mice.

To test the short-term memory and learning of the rNLS +/+ mice, which are the

mice that exhibit ALS/FTD symptoms. Behavioral tasks must be accurately developed.

Some behavioral tasks require more refinement than others, however, having these

accurate protocols to assess short-term memory and learning will detect deficits in rNLS

+/+ mice. Y-maze test development was conducted between B6C3F1/J-WT (WT) and NS

rNLS (NS-rNLS), with equal sample sizes of rNLS -/-, rNLS +/- and rNLS -/+ within the

NS rNLS group. The reason for a NS rNLS group is because mice that contain either

monogenic mutation for the *NEFH* promoter or tetO-hTDP-43ΔNLS (rNLS +/- and rNLS

-/+) should not express any cognitive deficits and thus theoretically can be used as

controls along with rNLS -/- for behavioral experiments.

For Y-maze development, NS rNLS mice did not show any difference in

spontaneous alternation when separated by genotype and were therefore pooled into a

single "NS group". For the results regarding Y-maze development, mice did not show a

significant difference in the number of entries (p=0.07) (Fig 7a), the number of

alternations (p=0.433) (Fig 7b) and spontaneous alterations (Fig 7c) between B6C3F1/J-

WT and NS rNLS (p=0.904), suggesting that there are no cognitive deficits within the NS

rNLS mice.as p-values were greater than 0.05. When a positive control group of

B6C3F1/J-WT injected with 1 mg/kg of scopolamine was compared against B6C3F1/J-

WT injected with 0.09% saline there was a significant difference only in spontaneous

alteration (p<0.05, p=0.002) (Fig 8c). This suggests that the scopolamine injected mice

exhibited short-term memory deficits, which is reflected in the Y-maze test. Therefore,

from our results, it appears our current Y-maze protocol and apparatus is suitable for

short-term working memory assessment of our rNLS +/+ mice.
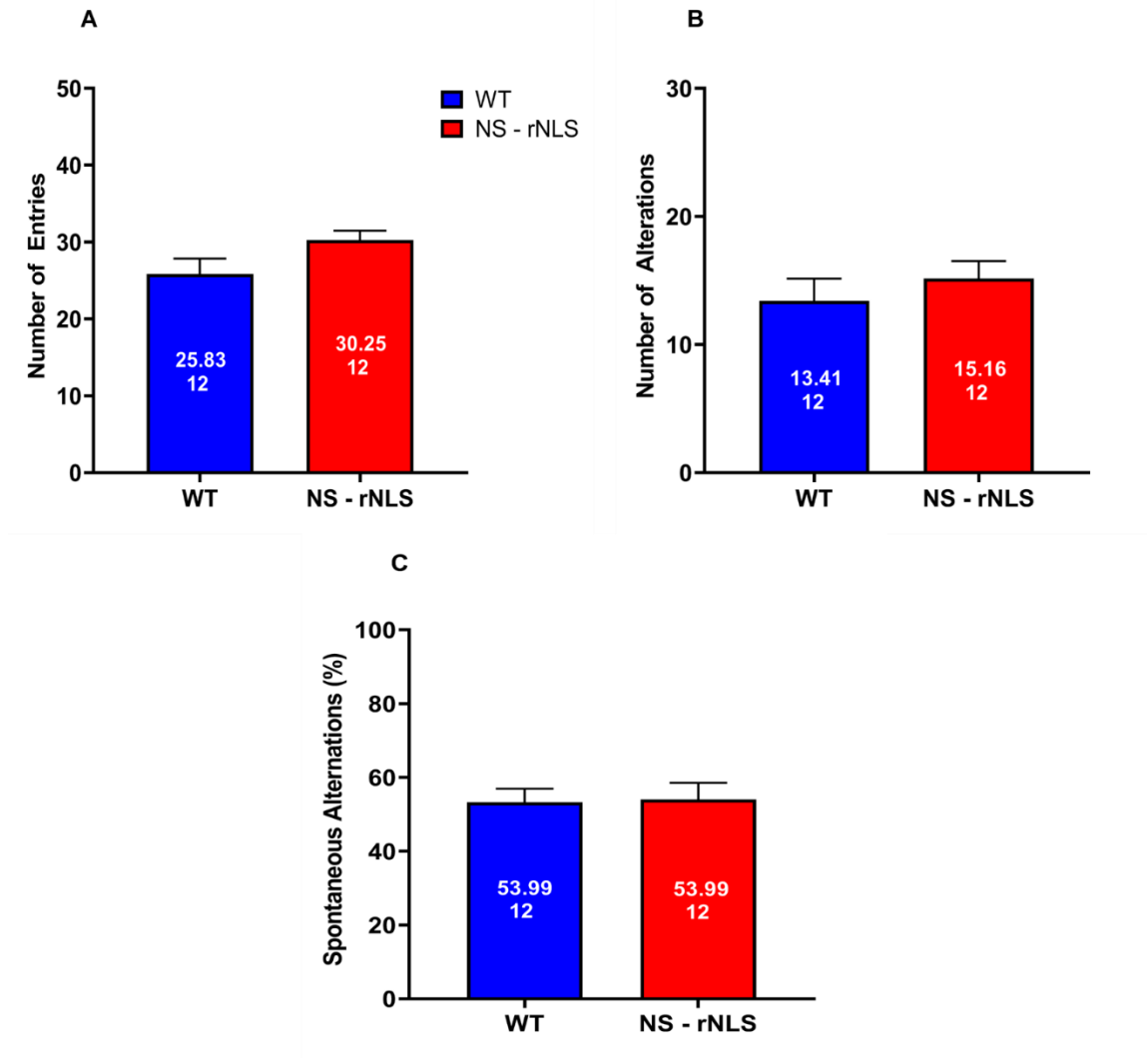
Figure 7. Y-maze assessment between B6C3F1/J-WT and NS - rNLS.
Two groups are B6C3F1/J-WT (WT) and NS rNLS (rNLS) with (A) average number of entries, (B) average number of alternations and (C) spontaneous alternations (%) duration of the trial. Numbers inside the bar indicates mean (top) and sample size (bottom). Data represents mean $\pm$ SEM.
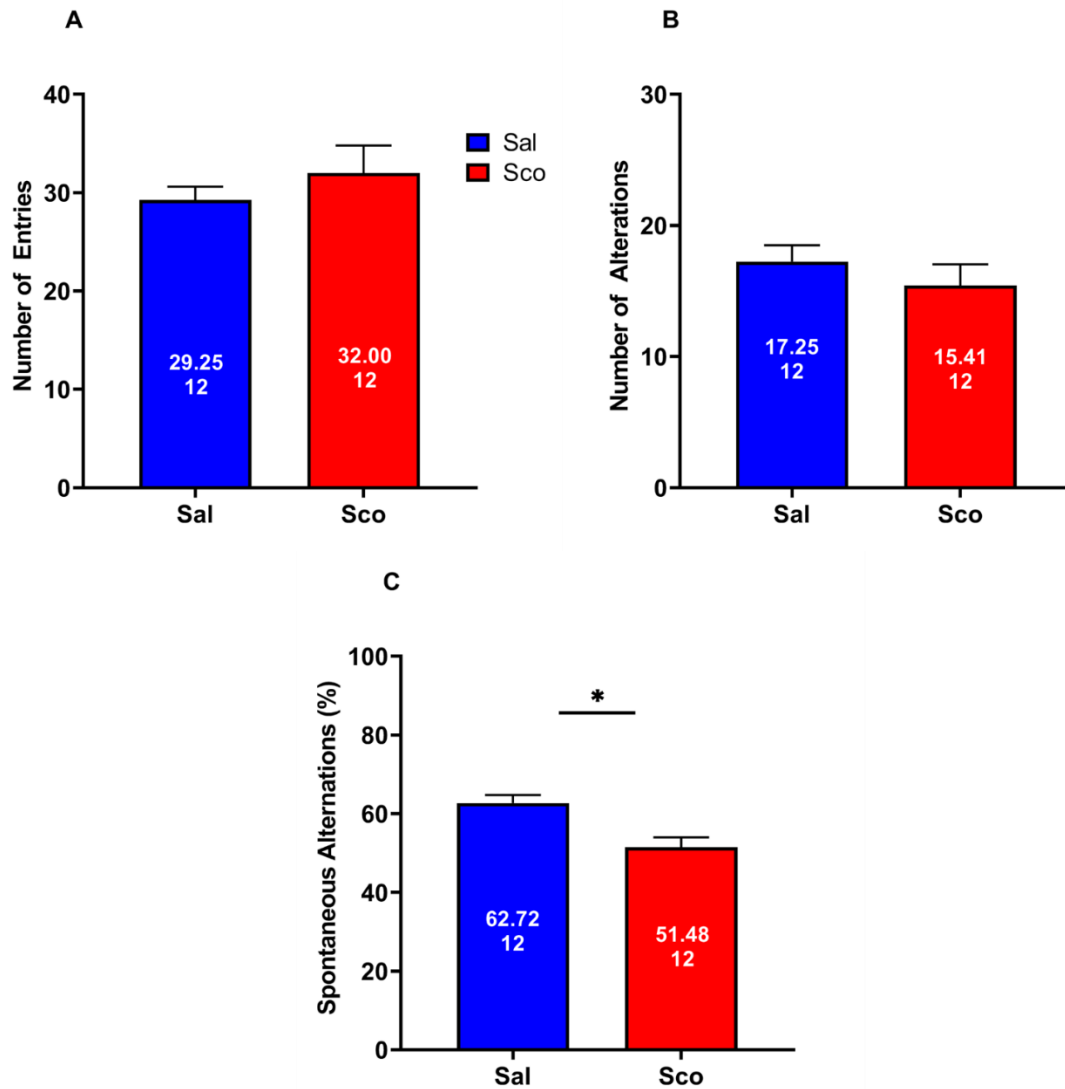
Figure 8. Y-maze assessment between saline-injected or scopolamine injected B6C3F1/J-WT mice.
Two groups injected with either 0.09% saline (Sal) or 1 mg/kg scopolamine-injected (Sco) B6C3F1/J-WT mice with (A) average number of entries, (B) average number of alterations and (C) spontaneous alternations (%) duration of the trial. Numbers inside the bars indicate mean (top) and sample size (bottom). * denotes as $p<0.05$. Data represents mean $\pm$ SEM.

NOR test was developed in three iteration and showed no difference between **NS** *rNLS* *and* **WT** *mice*

For NOR, multiple iterations were conducted to establish a working protocol. In our first iteration of the experiment, we assessed the short-term memory of WT and NS rNLS mice by comparing discrimination ratio between these groups. Within this first iteration of the experiment, the inter-trial was 4 hours long due to how the animals were serially tested and the results of the experiment show that there was no significant difference ($p>0.05$, $p=0.345$) between WT and NS rNLS mice. Our results also showed that the discrimination ratio was too low for both groups (Fig 9a). From figure 9a, the discrimination ratio for WT is -0.074 and for NS rNLS is – 0.098. Negative discrimination ratio usually indicates that a group did not learn the task or forgot which object was familiar (Sj & Jr, 2014). This suggests that the mice could have spent too long in an inter-trial interval that made them forget which object was familiar. Also, one major problem identified in this iteration of the experiment was the objects used in the experiment. These objects were not tall enough for the testing mice and therefore they were able to climb and sit on top of them. This resulted in time being deducted as it was not considered to be interaction with the object.
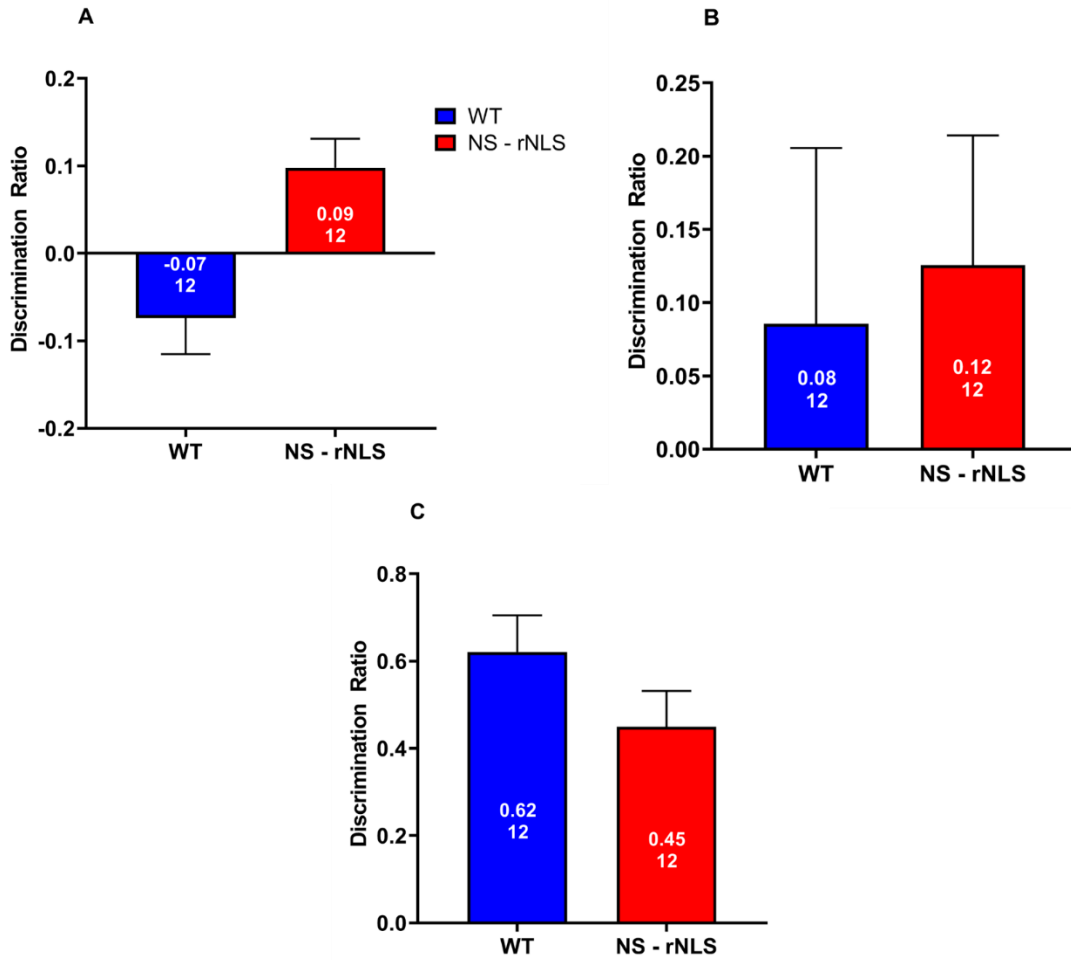
Figure 9. Discrimination ratio for the NOR test.
Discrimination ratio shown by iterations between B6C3F1/J-WT (WT) and NS rNLS
(rNLS). (A) shows the first iteration. (B) shows the second iteration and (C) shows the
third iteration Numbers inside the bars indicate mean (top) and sample size (bottom).
Data represents mean $\pm$ SEM.

For the second iteration of the experiment, the same set of animals were used

because results from the first iteration of the experiment showed that there is no

recollection of familial or novel object past 4 hours. In the second iteration, the decrease

in the inter-trial interval to 2 hours had helped increase the discrimination ratio (Fig 9b).

From figure 9b, the discrimination ratio for both groups were 0.38 for WT and 0.28 for

NS rNLS. These discrimination ratios are positive but are still low. However, there is still

no statistical difference between the groups, WT and NS rNLS (p>0.05, p=0.326). The second iteration still had a problem with mice climbing up and sitting on the objects and with being too distracted with the apparatus chamber. Therefore, better objects were still needed and the inter-trial interval was decreased to 20 minutes with three additional habituation days.

In the third iteration of the experiment, the results show that the discrimination ratio is high enough to be optimal for testing (Fig 9c). From figure 9c, the third iteration of the experiment showed that the discrimination ratio was 0.62 for B6C3F1/J-WT and 0.45 NS rNLS. These results also show that there is no statistical difference between B6C3F1/J-WT and rNLS -/- (p>0.05, p=0.224) (Fig 9c) and were similar to what is normally seen in literature (Arias et al., 2015). The introduction of 2 more habitation days had benefitted the mice, their behavior was a lot calmer and less distracted then the previous iterations of the experiment. The replacement of the object to geometric shapes like cones and square-based pyramid prevented the mice from climbing on top of the objects. The third iteration was established as the NOR protocol used for testing. From our positive control results, we see that the discrimination ratio between WT (scopolamine) and WT (saline) was significantly different (p<0.05, p=0.001) (Fig 10). The discrimination ratio for WT (scopolamine) mice were 0.38 compared to WT (saline) mice, which was 0.63 (Fig 10). Therefore, the NOR test has been successfully developed.
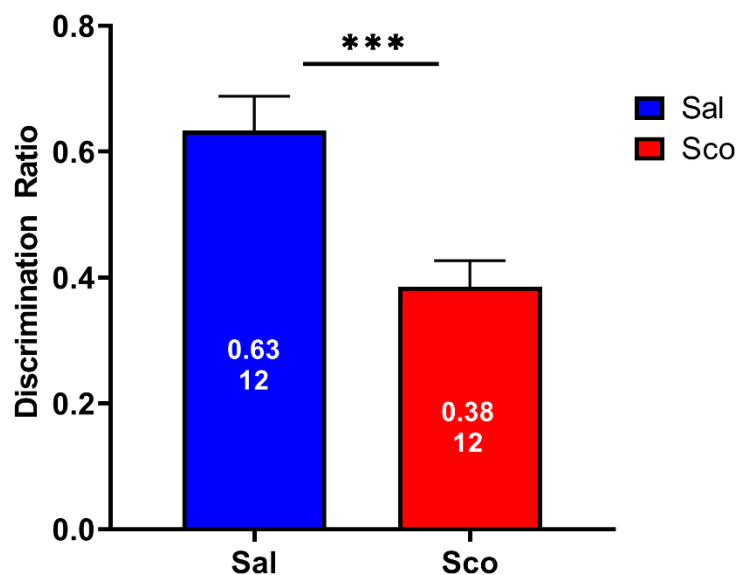
Figure 10. Discrimination ratio for saline-injected or scopolamine injected B6C3F1/J-WT groups.
Results show the discrimination ratio for 0.09% saline-injected (Sal) and 3 mg/kg scopolamine (Sco). Numbers inside the bars indicate mean (top) and sample size (bottom). *** denotes as $p<0.001$. Data represents mean $\pm$ SEM.

Holeboard Discrimination Test was developed in three iteration and showed no difference between **NS** *rNLS and* **WT** *mice.*

Holeboard experiment was more difficult than the other tests because of the complexity of the test as well as the lack of fasting, which is normally required to motivate mice to find the food. In the first iteration of the experiment, the results showed that both groups had obtained <1 treat, suggesting that majority of the mice did not find all four treats throughout the days of the experiment (Fig 11a). Reference memory error was also low as rNLS group had 2.69 errors at Day 1 and 1.5 errors at Day 4 (Fig 11b). Having low errors suggest that mice were not active throughout the experiment. Interestingly, there was no statistical difference ($p>0.05$) in reference memory errors between Day 1 and Day 4 within and between WT and rNLS groups (Fig 11b). Working

memory errors also had a low number of errors with rNLS group having the highest number of errors, 0.6 errors on Day 1 (Fig 11c). There was also no statistical difference (p>0.05) between Day 1 and Day 4, within and between WT and rNLS groups (Fig 11c). The results suggest that the mice did not seem to learn the objective of the task nor were active during experimentation. Due to the incompletion of the experiment trials for the first iteration, there was also no data obtained for 1st time to treat and completion time. The first iteration of experimental testing also took a long time and so the sample size was reduced for the next iteration.
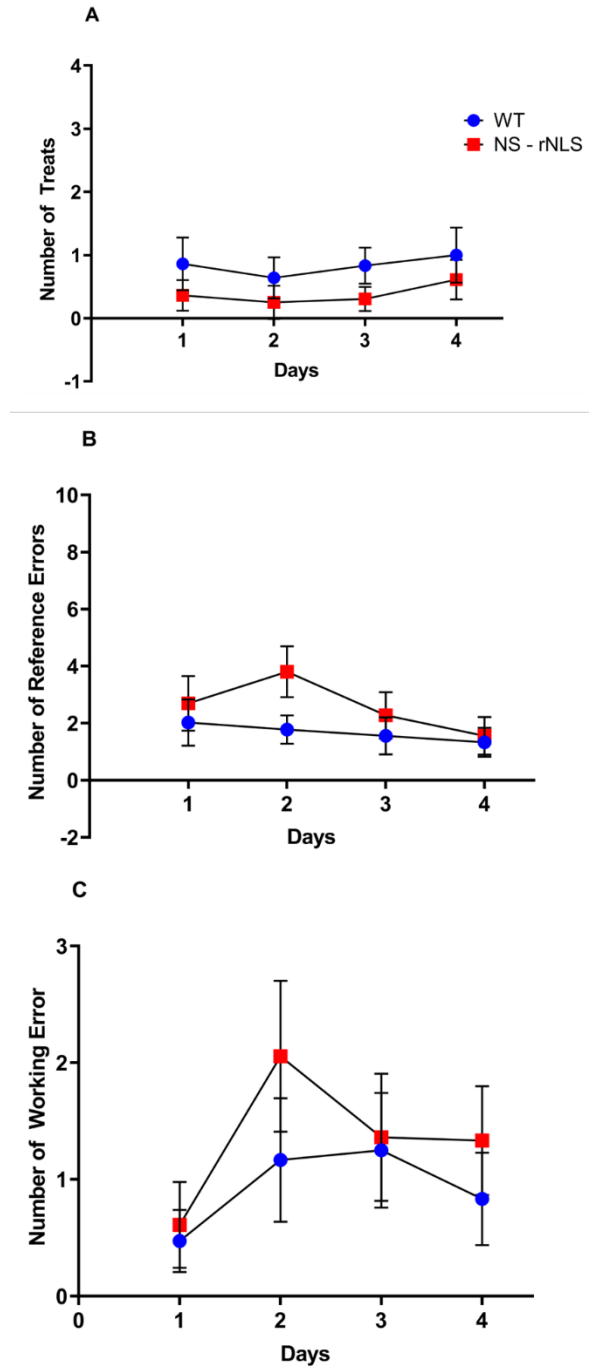
Figure 11. Results for the first iteration of the Holeboard Discrimination Test.
Results show (A) the average number of treats (B) the average number of reference
memory errors (C) the average number of working memory errors obtained per day
(Days 1-4) for B6C3F1/J-WT (WT) and NS rNLS (rNLS) groups. Data represents mean
$\pm$ SEM.

For the second iteration, both groups showed a downward trend for reference memory errors (Fig 12a). However, both groups also exhibited a low number of errors as the highest error for reference memory was 4.5 errors belonging to rNLS on Day 1 (Fig 12a). Working memory indicates no trends from Day 1 to Day 4 for both groups but also exhibits low errors with the highest number of errors being 2 errors on Day 1 for rNLS (Fig 12b). Both reference memory errors and working memory errors do not have any statistical difference ($p>0.05$, $p=0.237$ and $p=0.559$) between Day 1 and Day 4 for within and between WT and rNLS groups (Figs 12a and 12b). The number of treats obtained in the second iteration of the experiment had an upward trend only for the rNLS group, this group obtained 3 treats by Day 4 (Fig 12c). This upward trend was not significant ($p>0.05$, $p=0.078$) from Day 1 to Day 4 (Fig 12c). The 1st time to treat result reflects this as a downward trend is seen for rNLS group from Day 1 to Day 4, this trend was not significant ($p>0.05$, $p=0.477$) (Fig 12d). This suggests that the possibility of learning from the rNLS groups because of the trends seen in figure 12. Subsequentially, these trends were not observed for WT group for all measurements at any time point. Both groups had no completion time result as neither group completed the entire task.

Figure 12. Results for the second iteration of experiments for Holeboard Discrimination test.
Results show the (A) the average number of reference memory errors, (B) the average working memory errors, (C) the average number of treats and (D) the average 1st time to treat per day (Day 1-4) for B6C3F1/J-WT (WT) and NS rNLS (rNLS) groups. Data represents mean $\pm$ SEM.

In the third iteration of the experiment, results show much improvement as a decreasing trend was seen for reference memory errors from Day 1 to Day 4 for both groups. Reference memory error was the highest for the rNLS group with 7 errors starting at Day 1. Interestingly, both groups were significantly different ($p<0.05$, $p=0.00$) in reference errors from Day 1 to Day 4 within groups, but not significantly different ($p>0.05$, $p=0.805$) between groups (Fig 13a). Working memory did not show a

decreasing trend from Day 1 to Day 4 for both groups (Fig 13b). The number of errors for working memory was still low as WT and rNLS groups both started with 2.2 errors on Day 1 of testing (Fig 13b).

Interestingly, there is no statistical difference ($p>0.05$, $p=0.177$) between Day 1 and Day 4 for WT and rNLS groups regarding working memory errors (Fig 13b). Results also show that the number of treats had an upward trend, where all 4 treats were obtained by Day 4 for both groups (Fig 13c). Between Day 1 and Day 4 there was a statistical difference ($p<0.05$, $p=0.000$) in the number of treats (Fig 13c). However, there was not a statistical difference ($p>0.05$, $p=0.113$) between WT and rNLS at each of those days (Fig 13c). This was also reflective in the first time to treat and the completion time which had a decreasing trend from the Day 1 and Day 4 (Figs 13d and 13e), the results from Day 1 were significantly different ($p<0.05$, $p=0.000$ and 0.000) than Day 4 for both groups (Figs 13d and 13e). Also, rNLS group was not statistically different ($p>0.05$, $p=0.588$ and 0.849) compared to WT at any days of experimentation for 1st time to treat and completion time (Figs 13e and 13d) Therefore, changes made to the third phase was effective as this protocol for Holeboard Discrimination test has shown results that suggest mice with no short-term memory deficits can learn and retain the objectives of the Holeboard Discrimination test over 4 days.
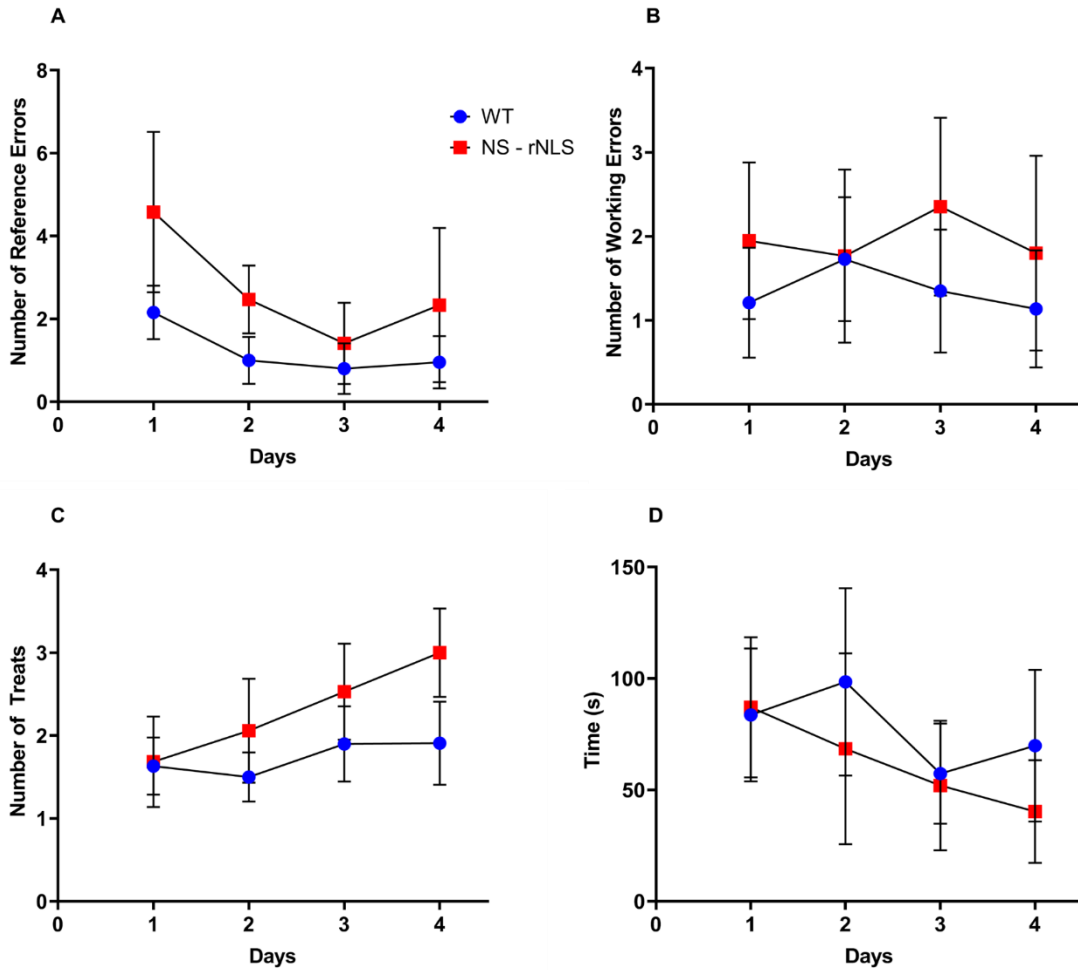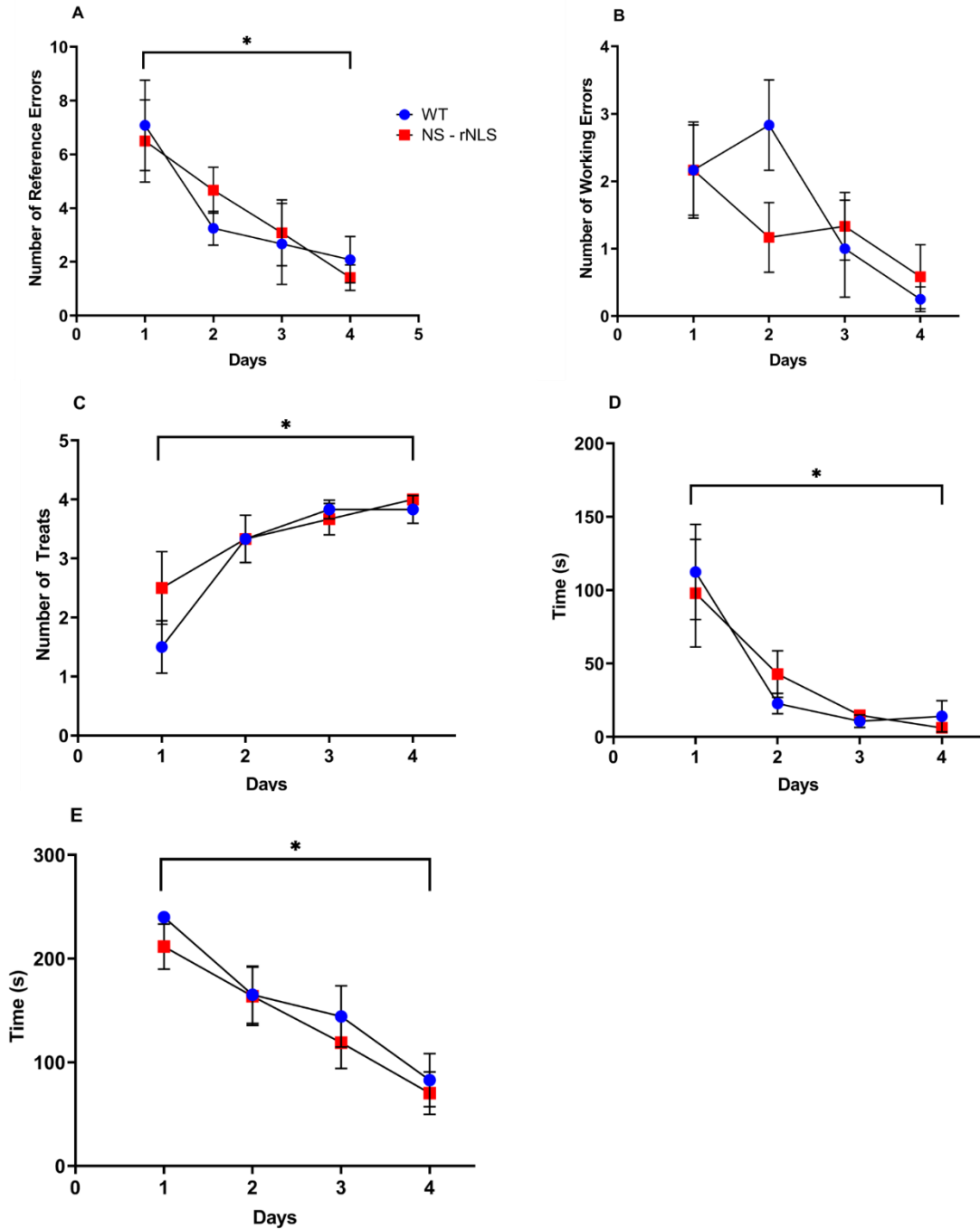
Figure 13. Results for the third iteration of experimentation for Holeboard Discrimination test.
Results show the (A) the average reference memory errors (B) the average working memory errors (C) the average number of treats, (D) the average 1st time to treat and (E) the average completion time obtained per day (Day 1-4) for B6C3F1/J-WT (WT) and NS rNLS (rNLS) groups. ******* denotes $p<0.001$. Data is represents mean $\pm$ SEM.

Specific Discussion

The purpose of this first study was to accurately develop protocols for three behavioral tasks, which will be used to assess short-term memory and learning in rNLS +/+ mice. For this study, we had decided to use a combination of rNLS -/-, rNLS +/- and rNLS -/+ as our rNLS group. The reason for this choice was because rNLS +/- and rNLS -/+ did not have the bigenic mutations that would result in expressing symptomatic ALS-FTD symptoms. Therefore, these mice did not show symptoms of FTD and can be used as potential controls, since rNLS -/- breeding is just as difficult as rNLS +/+, with ¼ chances of obtaining the desired genotype. In addition to that, there are additional possible controls that could be used for this mouse model, which also includes rNLS +/+ on doxycycline.

Results from our study have shown that for the developed protocols there is no difference between our NS rNLS and B6C3F1/J-WT groups for all three behavioral experiments. B6C3F1/J-WT Jackson ordered mice were necessary to use as a background control because it contains no transgenic insert and will determine if this strain of mice capable of behavioral testing. For this study, we utilized published works of literature as a reference point for starting our protocols (Denninger et al., 2018; Kuc et al., 2006; Prieur & Jadavji, 2019). We also utilized the results in these published pieces to determine if our results are optimal. For example, our results obtained from the Y-maze is similar to those commonly found in literature (Garcia & Esquivel, 2018; Griffiths et al., 2019; Stover et al., 2015). This suggests that our protocol for the Y-maze is optimal for testing. Whereas the results of our first iteration for NOR did not resemble what was obtained in literature (Arias et al., 2015; Lueptow, 2017; Sik et al., 2003) and thus was determined that the

protocol was not optimal and refinement in methodology was still needed. To further verify if our protocols were optimal, we had conducted positive control experiments through the intraperitoneal injection of scopolamine. Scopolamine is an acetylcholine (ACh) antagonist that decreases the amount of ACh activity in the brain resulting in symptoms of memory deficits seen in Alzheimer's disease (AD) (Skalicka-Wozniak et al., 2018). Scopolamine used as a positive control for AD-related research is common (Balmus and Ciobica 2017; Kim et al. 2017; E. Kim et al. 2016).

The idea of slightly varying experimental designs is not uncommon in the field of behavioral neuroscience. Many studies have adjusted their protocols for specific reasons or to ensure it works efficiently (Onaolapo & Onaolapo, 2015; Post et al., 2011; Prieur & Jadavji, 2019; Stover et al., 2015). This need to slightly vary experimental design could be contributed to the background strain of mice. Studies have suggested that some strains of mice do significantly better at performance in behavioral experiments than other strains (Garcia & Esquivel, 2018; Heyser et al., 1999; Sik et al., 2003). Therefore, the need to optimize behavioral experimental for the B6C3F1/J strain of mice is necessary for future short-term memory assessment.

Study 2: Assessment of Short-Term Memory in rNLS Mice Model

Brief Introduction

Previous rNLS mouse model contained a Calcium/Calmodulin Dependent Protein Kinase II Alpha (*CamkIIa*) promoter used to solely express TDP-43 in the brain (Alfieri et al., 2014; Philips & Rothstein, 2015). This led to cognitive dysfunction, where mice were showing symptoms of FTD. In addition to the cognitive dysfunction, these mice were also showing slight motor deficits, however, it was difficult to claim these motor deficits were the result of ALS as TDP-43 inclusions were not seen in MNs located in the spinal cord (Walker et al., 2015). This led to the development of the novel rNLS8 mouse model with a bigenic mutation inserts of tTA-*NEFH*/tetO-hTDP-43ΔNLS. Using a similar mechanism of expressing hTDP-43 as in the previous model, the *NEFH* promotor ensures that TDP-43 inclusions are expressed in all types of neurons located in both the brain and the spinal cord (Walker et al., 2015). Current research conducted on this newer rNLS mouse model has shown motor deficits with TDP-43 inclusions in MNs located in the spinal cord, similar to ALS-like pathogenesis (Walker et al., 2015). Although there is evidence to suggest cognitive dysfunction from TDP-43 inclusions seen in the hippocampus and other brain structures, there has yet to be any cognitive testing conducted on this novel rNLS mouse model. Therefore, protocols that were established using the background strain of this novel rNLS in the first study are used to assess the short-term memory and learning of this novel rNLS mouse to determine if FTD symptoms are exhibited along with ALS symptoms.

Hypothesis

We hypothesize that the rNLS +/+ mice will exhibit short-term memory deficits at around or past 4 weeks off doxycycline in this preliminary study.

Methods and Materials

Animals

rNLS -/- and rNLS +/+ were used for short-term memory assessment. rNLS -/- mice contains neither monogenic mutations of tTA-*NEFH* promoter (+/-) and *tetO*-hTDP-43ΔNLS. Whereas, rNLS +/+ mice contains both tTA-*NEFH* promoter (+/-) x *tetO*-hTDP-43ΔNLS (-/+) monogenic mutations. rNLS +/+ mice express disease symptoms after the removal of rodent chow containing doxycycline (Dox Diet #3888, Doxycycline 200mg/kg, Bio-Serv). Due to the difficulty in breeding large sample size of mice, short-term memory assessment of rNLS +/+ mice was conducted in two cohorts of mice labelled as Group A and Group B. With both groups the total sample size was 31 mice, which are broken down into rNLS mice +/+ (n=13, 6 male and 7 female mice) and rNLS -/- (n=18, 9 male and 9 female mice). Both of these groups did not differ in body weight or condition before the removal of doxycycline.

When the youngest mice in each cohort had reached the age of P35, all the mice in that cohort had their doxycycline rodent chow replaced with regular rodent chow. The age range of animals tested was ~5-9 weeks with a difference of 4 weeks between the oldest and youngest mice. All mice had been housed at Wright State University's Laboratory Animal Care facilities on 12:12-h light-dark cycle. Food and water were provided *ad libitum*. All procedures followed NIH guidelines and were approved by Wright State University's Laboratory Animal Care and Use Committee (LACUC) – protocol numbers AUP 1145 and 1117.

Y-maze test

Y-maze protocol as stated in Study 1 was used to assess short-term working memory of rNLS +/+ mice. All mice were acclimated to testing room conditions 30 mins before start the test. Each mouse was tested for only one trial. Each trial consisted of 10 mins. At the start of a trial, a mouse was dropped in the middle of the chamber, where 3 of the arms intersected, to prevent starting point having an influence on the results. At the end of the trial, the mouse was removed from the Y-maze and the apparatus was cleaned with 70% (w/v) ethanol. Y-maze testing was conducted 3 weeks and 5 weeks after mice in each group were removed from doxycycline rodent chow and were expressing hTDP-43 genes. Number of alternations, number of entries and spontaneous alternations were assessed with results showing data from combined groups.

Data Analysis

For short-term memory assessment of rNLS +/+, SPSS® (IBM Corporation, New York USA) statistical software was used for statistical analysis of number of entries, number of alternations and spontaneous alternation. While, PRISM Graphpad (GraphPad Software, California USA) was used for all graph needs in this study. All data for this study had a normal distribution and did not reject the Levene's test ($p > 0.05$). Therefore, parametric statistical analysis was conducted for all measurements in this study. Independent t-test was conducted between rNLS -/- and rNLS +/+ groups with significance being 0.05 (α). In addition to an independent t-test, a two-way repeated ANOVA was also conduct to look at the difference across the two timepoints, 3 weeks and 5 weeks off doxycycline. All data are represented as mean $\pm$ SEM.

Results

Y-maze test detects short-term memory at 5 weeks off doxycycline

The purpose of this study was to assess if rNLS +/+ exhibits short-term memory loss during disease progression. Since previous literature has indicated brain atrophy occurs around 4 weeks off doxycycline (Walker et al., 2015), we decided to assess short-term memory 3 weeks and 5 weeks off doxycycline with the same set of animals.

Within each group, there is no statistical difference (p>0.05, Table) seen between rNLS -/- and rNLS +/+ for spontaneous alternation, number of entries and number of alternations. When Group A and Group B data was combined, the results show that there is no significant difference (p>0.05, p=0.409) in spontaneous alternation between rNLS -/- and rNLS +/+ at 3 weeks off doxycycline (Fig 14c). Our results also show that there is still no statistical difference (p>0.05, p=0.274 and p=0.475) in the number of entries and number of alternations between rNLS -/- and rNLS +/+ at week 3 off doxycycline (Fig 14a and Fig 14b).

At 5 weeks off doxycycline, rNLS +/+ has a significant decrease (p<0.05, p=0.011) in spontaneous alternation compared to rNLS -/- (Fig 15c). This suggests that rNLS +/+ exhibits short-term memory deficits at 5 weeks off doxycycline. The number of entries showed no statistical difference (p>0.05, p=0.055) between rNLS -/- and rNLS +/+ (Fig 15a), but the number of alternations was significantly lower (p<0.05, p=0.007) for rNLS +/+ compared to rNLS -/- 5 weeks off doxycycline (Fig 15b). Therefore, rNLS +/+ show short-term memory deficits when taken off doxycycline for 5 weeks.

A two-way repeated ANOVA test was done to compare the results of 3 weeks off to that of 5 weeks off doxycline. The results show that that number of entries and alterations

were significantly lower (p<0.05, p=0.036 and p=0.043) for rNLS +/+ group from 3 weeks off doxycycline to that 5 weeks off doxycycline (Fig 16a and b). Spontaneous alternation, for rNLS +/+ does not change from 3 week off doxycycline to that of 5-week off doxycycline (p>0.05, p=0.588) (Fig 16c). It does however, show that rNLS -/- has higher spontaneous alternation at 5 weeks off doxycline compared to 3 weeks off doxycycline (Fig 16c).

Table 3. p-values for Group A and Group B number of entries, number of alternations and spontaneous alternations.

Groups	Week Off Doxycycline	Measurement (p-value)
A	3	Entries (p=0.894) Alternations (p=0.445) Spontaneous Alterations (p=0.065)
	5	Entries (p=0.437) Alternations (p=0.074) Spontaneous Alterations (p=0.086)
B	3	Entries (p=0.197) Alternations (p=0.12) Spontaneous Alterations (p=0.289)
	5	Entries (p=0.067) Alternations (p=0.055) Spontaneous Alterations (p=0.084)
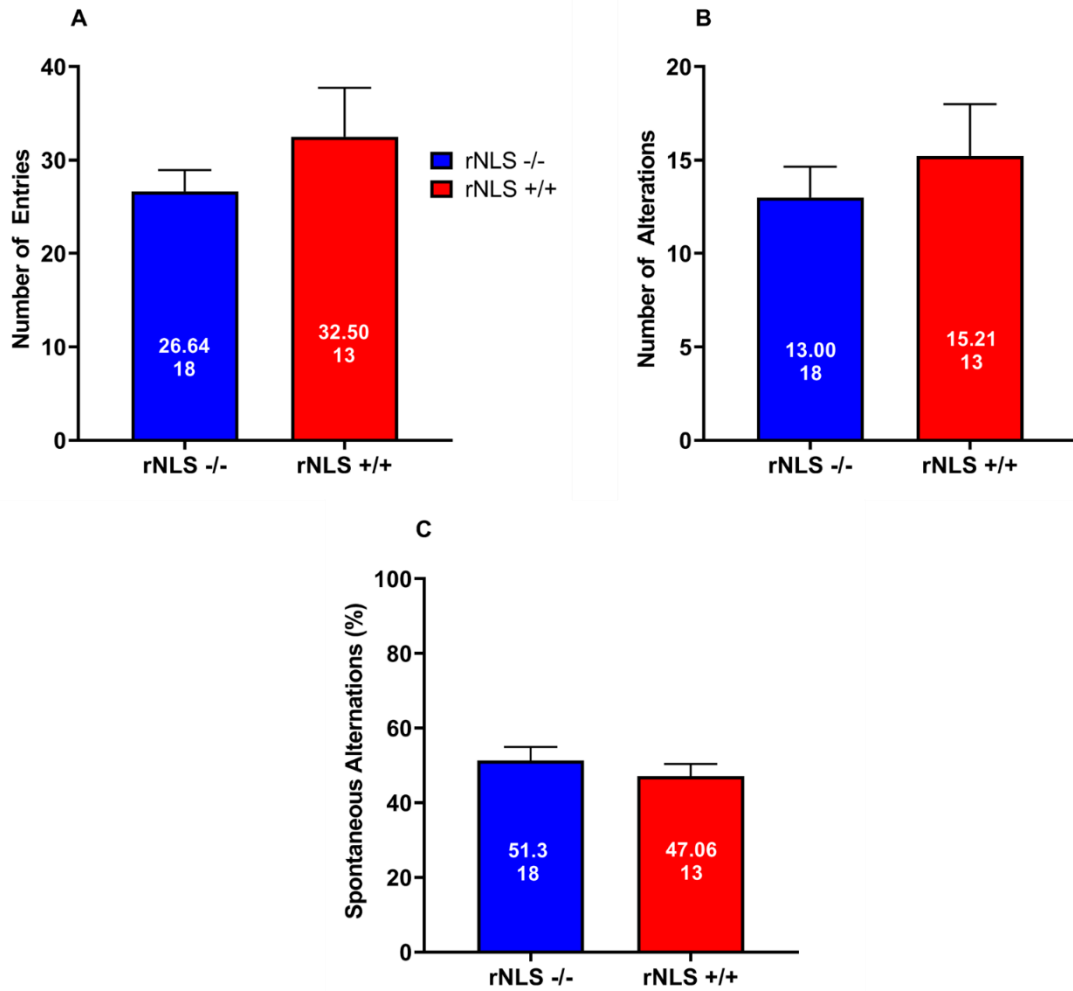
Figure 14. Y-maze assessment between rNLS -/- and rNLS +/+, 3 weeks off doxycycline.
Y-maze test results are shown for rNLS +/+ and rNLS -/- with (A) average number of entries, (B) average number of alternations and (C) spontaneous alternations (%) duration of the trial. Numbers inside the bars indicate mean (top) and sample size (bottom). Data represents mean $\pm$ SEM.
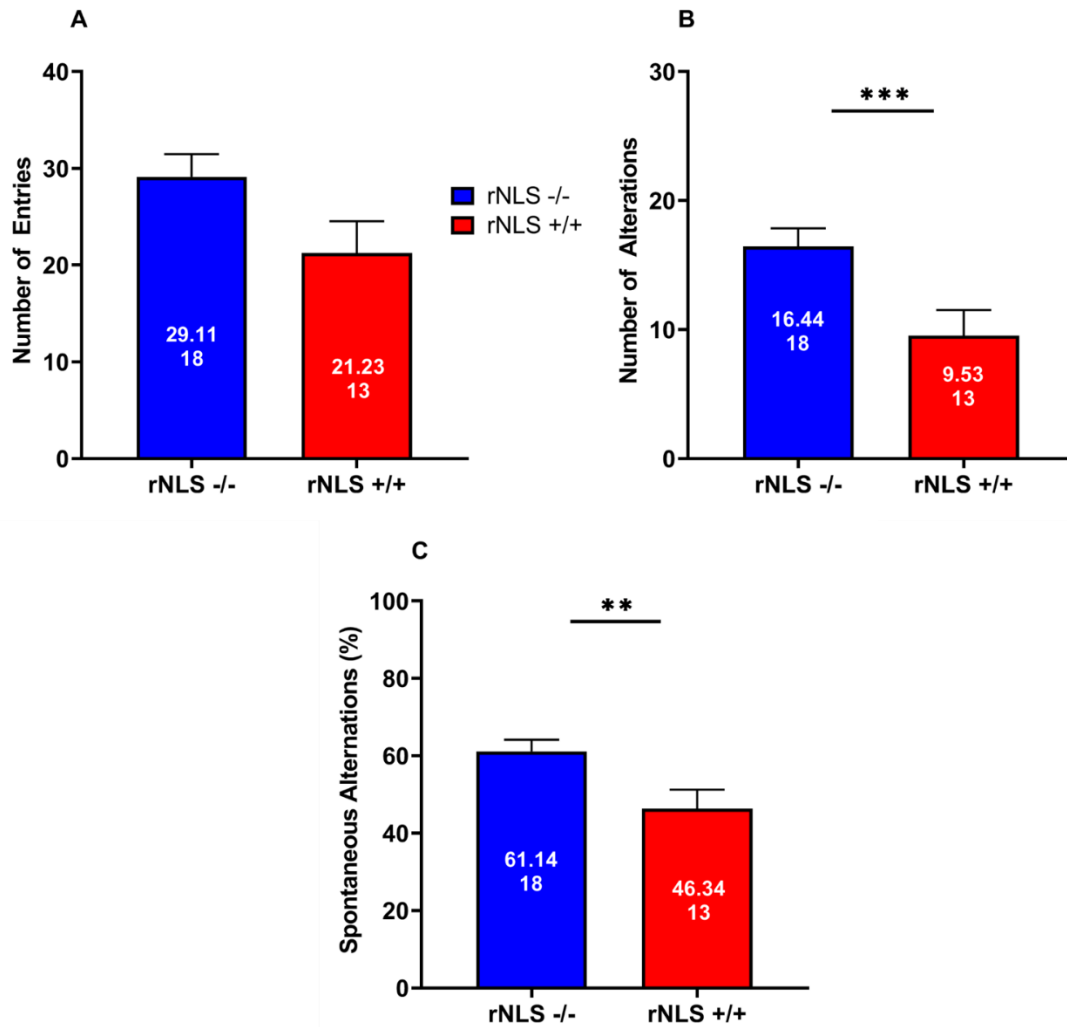
Figure 15. Y-maze assessment between rNLS -/- and rNLS +/+, 5 weeks off doxycycline.
Y-maze test results are shown for rNLS +/+ and rNLS -/- with (A) average number of entries, (B) average number of alternations and (C) spontaneous alternations (%) duration of the trial. Numbers inside the bars indicate mean (top) and sample size (bottom). ** denotes as $p<0.01$ and *** denotes at $p<0.001$. Data represents mean $\pm$ SEM.
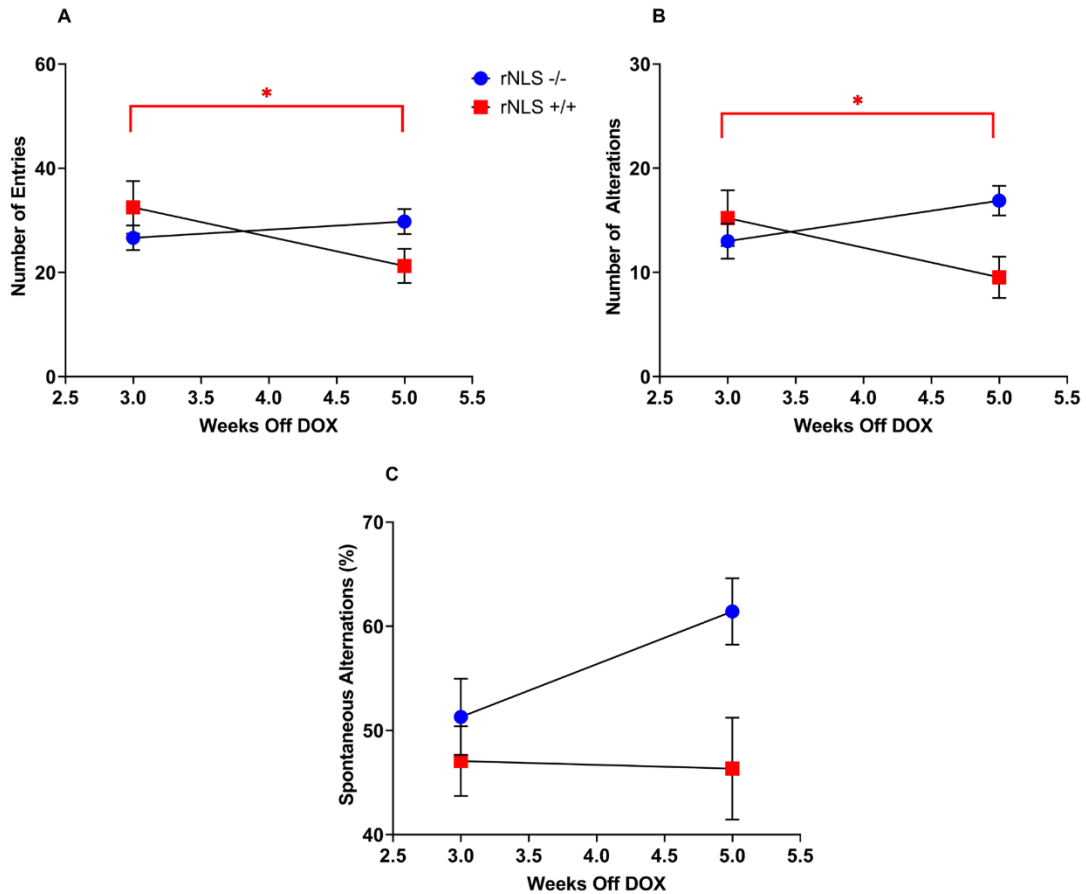
Figure 16. Y-maze assessment between rNLS -/- and rNLS +/+, timeline comparison between 3 and 5 weeks off doxycycline.
Y-maze test results are shown for rNLS +/+ and rNLS -/- at 3 and 5 weeks off doxycycline for (A) average number of entries, (B) average number of alternations and (C) spontaneous alternations (%) duration of the trial.. * denotes as $p < 0.05$ for rNLS +/+ group. Data represents mean $\pm$ SEM.

Specific Discussion

Y-maze test was conducted on rNLS +/+ to assess its short-term working memory. This mouse model was developed to express ALS and FTD symptoms (Walker et al., 2015). Previous literature has shown results that this mice model does show ALS like symptoms, however, no behavioral experiments have been conducted to determine if FTD like symptoms are present in this rNLS mice model (Walker et al., 2015). This

preliminary study was conducted to determine if rNLS +/+ mice exhibit short-term memory deficits and when it will exhibit these deficits off doxycycline.

Our results contribute to the notion that this rNLS mice model exhibits cognitive deficits in the form of short-term memory deficits. From our results, we saw a significant decrease in the spontaneous alternation between rNLS -/- and rNLS +/+ 5 weeks off doxycycline when Group A and Group B datasets were combined (Fig 15c). Interestingly, we don't see a significant decrease in the number of entries at this time point (Fig 15a). The number of entries depicts the locomotive active of the mice during testing. This suggests that the rNLS +/+ mice had a significant decrease in spontaneous alternation as a result of short-term working memory deficit and not from motor deficits presented by ALS. Our results also that when comparing the data of 3-week off doxycycline to 5-week off doxycycline there is hardly any change in spontaneous alternation between these two time points for rNLS +/+ (Fig 16c). Instead, you see a change in movement, where rNLS +/+ are less active and rNLS -/- are more active at the 5-week timepoint. This could suggest that rNLS mouse model develops cognitive deficits much later in disease progression or movement deficits of the rNLS +/+ occur before the onset of cognitive deficits, this alteration in movement also will make it difficult to assess cognition at later points.

Some of the results correspond to previous literature where a different rNLS mice model had been assessed through Y-maze and NOR (Alfieri et al., 2014). An earlier model rNLS mice model used had a tTA-*CamkIIa* promoter instead of a tTA-*NEFH* promoter. This resulted in TDP-43 aggregations expressed heavily in the brain causing symptoms of FTD (Alfieri et al., 2014). From that study, the results showed that there

was a decrease in spontaneous alternation, in the Y-maze, for rNLS one month off doxycycline compared to control group (Alfieri et al., 2014). Furthermore, the NOR test in that study also showed a significant decrease in the discrimination ratio between the rNLS one month off doxycycline and control group (Alfieri et al., 2014). This suggested that FTD symptoms are expressed in that rNLS mice model.

The Y-maze results from this study also resemble previous literature results and suggesting the possibility that this rNLS mice model shows cognitive deficits when mice are taken off doxycycline for a long time. However, due to COVID-19 pandemic we were unable to continue this study. For future directions on completing this study, a 3-week and 5-week off doxycycline rNLS +/+ mice must be tested on the NOR and Holeboard Discrimination Test. Validation of the model is also recommended to confirm that the cognitive deficits are due to hTDP-43 inclusions. To accomplish this a pathological analysis should be conducted by staining for hTDP-43 in the hippocampus of the mouse brain, in addition to obtaining brain weight measurement to measure atrophy of mice 3 weeks off doxycycline compared to 5 weeks off doxycycline.

Study 3: Comparison of FB and Cholera-Toxin B in Labelling of A-MNs

Brief Introduction

Neuroanatomical tracers have been frequently used to label neuronal structures since their discovery in 1971 by Kristensson & Olsson (Kristensson & Olsson, 1971)). Since then, numerous tracers of differing compositions have been developed. These include dextran conjugates such as Fluoro-Ruby (tetramethylrhodamine-dextran amine conjugate) (Nance & Burns, 1990), chemical tracers such as Fluoro-Gold (Schmued & Fallon, 1986), and enzymatic proteins such as horseradish peroxidase (Kristensson & Olsson, 1971). The usefulness of retrograde tracers is a) their ability to trace neural connections from synapses (i.e., their terminals) back to cell bodies (i.e., their sources), and b) their adaptability to different studies by changing the method of application (Haenggeli & Kato, 2002) and detection (Schmued et al., 1989) . Tracers have allowed researchers to identify neuroanatomical pathways (Horie et al., 2013)), improve our understanding of axonal transport mechanisms during states of health and disease (Chiasseu et al., 2017), and develop novel treatments for nerve injury (Acosta et al., 2017).

Of the various neuroanatomical tracers described in literature, FB and CTB are retrograde tracers that have been extensively used in labeling MNs. (Alstyne et al., 2018; Simon et al., 2017; Q.-G. Xu et al., 2010). FB is a chemical fluorescent dye that emits blue light upon excitation (Hayashi et al., 2007; Köbbert et al., 2000). CTB, on the other hand, is the beta-subunit of a bacterial toxin that is secreted by the bacterium *Vibrio cholera*e (Lencer & Tsai, 2003) . Although these tracers have several features in common, such as their retrograde transport ability and their fluorescence (Grkovic et al., 2005; Yoshikawa et al., 2011), they differ in some aspects. First, their uptake

mechanisms are different in that CTB uses receptor-mediated endocytosis by binding

onto monosialotetrahexosyl (GM1) gangliosides located on the neuronal membrane. This

increases the binding affinity of the tracer, leading to higher CTB uptake efficiency

(Köbbert et al., 2000; Lencer & Tsai, 2003). FB, in contrast, is passively taken up by

neurons and labels them through activate transport using endosomes (Köbbert et al.,

2000). Second, their compositions are different: CTB is a bacterial toxin that can be

conjugated, making it adaptable to any type of microscopy (Havton & Broman, 2005;

Yao et al., 2018), whereas FB cannot be conjugated and is thus only useful for

fluorescence microscopy (Hayashi et al., 2007; Köbbert et al., 2000). FB's fluorescence

property is somewhat limiting, because its blue fluorescence requires Ultraviolet (UV)

wavelength (360 nm) for excitation. This is a potential issue in cell culture studies,

because UV light can cause phototoxicity in labeled cells (Köbbert et al., 2000).

Additionally, FB can also interfere with cell adhesion in cell culture studies (Köbbert et

al., 2000).

  The purpose of this study is to compare FB and CTB under various

concentrations and survival days to determine which protocol is optimal for retrograde

labelling of α-MNs. This study can be related to the cognitive studies presented in study 1

and study 2, where either of these tracers will be used in future studies regarding the

novel rNLS mouse model to confirm of these novel rNLS mice are indeed appropriate

FTD/ALS mouse models. By retrograde labelling α-MNs located in the spinal cord, we

can investigate if innervate MNs are being affected by ALS disease progression.

Hypothesis

We hypothesis that CTB would be more efficient at labelling a higher quality and quantity of spinal alpha-motoneuron labelling. As well as, changing properties such as concentration and survival day will affect quantity and quality of motoneuron labelling.

Methods

Animals

WT (WT) B6SJL mice were used in the study as these were the most abundant type of mice available in our colony. Breeders were purchased from the Jackson Laboratory (stock #002726) and a line was established at Wright State University. 34 adult male mice (6-7 weeks of age) were used in this study, these mice were obtained from the colony and were randomly assigned to ten experimental groups. Each group tests a given tracer at a different concentration and number of survival days (Table 3 shows all groups). Mice were housed under appropriate conditions at WSU Laboratory Animal Resource (LAR) facility, prior to surgeries approximately 4 mice were housed per cage with cotton bedding material in a 12 hours light/dark cycle with water and food provided *ad libitum*. After surgeries, mice were then individually housed in single cages with 12 hours light/dark cycle with water and food provided *ad libitum* until euthanized.

All experiments and procedures were conducted in accordance with the Guiding Principles for Research Involving Animals and Human Beings as adopted by The American Physiological Society, and in compliance with the guidelines of Wright State University whose Laboratory Animal Care and Use Committee (LACUC) has approved these experiments (approved protocol numbers: AUP 1045 and 1117).

Table 4. WT B6SJL Male Mice Categorized Into Different Tracer Protocols.

Tracer	Concentration (%)	Survival days	Number of mice
CTB	0.05%	3-day	3
		5-day	3
	0.1%	3-day	3
		5-day	4
FB	0.1%	3-day	3
		5-day	3
	0.2%	3-day	3
		5-day	3
	2%	3-day	3
		5-day	3

Surgical Procedures and Tracer Injections

Surgical procedures were conducted in the morning to mid-afternoon in WSU's LAR sterile surgical suite. Mice were anesthetized with isoflurane at 3-5% for induction, then maintained at (2-3%) during surgery via nose cones. Four hindlimb muscles - soleus (Sol), tibialis anterior (TA), lateral and medial gastrocnemius (LG and MG) – were exposed by a small incision and separation of overlying biceps femoris muscle. All four muscles in a given mouse were injected with one of the following tracer/concentration protocols: 1) 5 µL of FB (FB) (Polyscience, Missouri, USA catalog 17740-1) at a) 0.1%, b) 0.2%, or c) 2%; in weight/volume; or 2) 5 µL of CTB-488 Alexa Fluor conjugate (Invitrogen, California, USA catalog C22841) at a) 0.05% or b) 0.1%; in weight/volume.

Injections were given through a 10 µl Hamilton syringe with a 33-gauge needle. Overall, each mouse received a total of 20 µL of one type/concentration of tracer injected into its four hindlimb muscles. Intraoperative monitoring was conducted every 5 minutes based off movement, respiration and color. Buprenorphine (0.0025 mL/g) was injected subcutaneously immediately after surgery followed by a subcutaneous injection of

Carprofen (0.01 mL/g) 24 hours after surgery for post-operative pain relief. Mice were then euthanized and perfused 3 or 5 days post-injection of tracers (survival days).

Perfusion and Dissection of Spinal Cord

All perfusions and dissections were conducted mid-morning and took place at WSU Microscopy Core Facility perfusion room. All mice were anaesthetized with a lethal dosage of Euthasol solution (150 mg/kg, pentobarbital sodium and phenytoin sodium) via intraperitoneal injection, either 3 or 5 days after injection of retrograde tracers into hindlimb muscles. After confirming lack of reflexive response via toe pinch, mice were transcardially perfused with vascular rinse (0.01 M phosphate buffer with 0.5% NaCl, 0.025% KCl, and 0.05% $NaHCO_3$, pH 7-8), followed by 4% paraformaldehyde in 0.1M phosphate buffer, pH 7-8. After fixation, mice had their spinal cord extracted from mid-thoracic to early sacral region. These extracted spinal cords were submerged into 4% paraformaldehyde for ~2 hours before being transferred into 15% (weight/volume) sucrose solution at 4°C overnight.

Identification of Spinal Cord segments and Sectioning

Extracted spinal cords were removed from 15% sucrose and pinned onto a Slyguard® padded dissection petri dish with large insect pins. Smaller insect pins were then used to mark the origins of the ventral roots from L3 to S1 (lower lumbar spinal cord region). After identifying the lower lumber spinal cord region, ventral roots were cut and spinal cord segments were painted using marking dyes (Bradley Products, Minnesota, USA) with contrasting colors. Two transverse cuts were made, at L2 and at S2. The lower

spinal cord regions were then placed into rubber molds with Tissue Freezing Medium™ (GeneralData, Ohio, USA catalog TFM-C) and frozen with cold isopentane. Frozen tissue blocks were removed and stored at -80°C until sectioning. Frozen tissue blocks were transversely sectioned at 45 µm at ~ -25 °C on a HM 550 ThermoFisher® Cryostat. Tissues were serially collected from L3 to L6 in 24-well plates filled with cryoprotectant.

Mounting and Immunohistochemistry

Approximately 3 days after perfusion, ~5-6 sections were collected from each spinal cord segment and transferred into Netwell® inserted 6 well-plates. Transverse sections were washed with 1x Phosphate Buffered Saline solution (PBS), pH 7.4 (ThermoFisher® Scientific Inc., New Jersey, USA catalog 10010023) 3 times at 10-minute intervals. This was followed by washing once in cupric sulfate (10 mM Cupric sulfate in 50 mM ammonium acetate) solution for 45 minutes to prevent the autofluorescence of endogenous protein, lipofuscin, within neurons. Sections were then rinsed in DDI-filled NetWell® 6 well-plates, followed by another minute of PBS washing before being mounted onto positively charged microscope slides and cover-slipped with Vectashield® antifade mounting medium (Vector Laboratories, California USA catalog H-1000). This process was repeated for all sections.

Additional sections from 2% FB 3-day and 0.1% CTB 3-day were labeled with Choline Acetyltransferase (ChAT) and Vesicular acetylcholine transporter (VaChT) to determine if the tracers were labeling cholinergic inputs on MNs. For this staining, sections were washed 3 times with PBS-T (0.01M PBS containing 0.1% Tritron-X, pH 7.3) followed by blockage with normal horse serum (10% PBS-T) for an hour. Sections

were then incubated with primary antibody, ChAT (mouse antibody, Novus Biologicals, catalog #NBP2-46620, Colorado, USA) at 1:100 dilution in PBS-T overnight at 4 °C. Additional sections were also labelled with VaChT (mouse antibody, Novus Biologicals, catalog #NBP2-59378, Colorado, USA) at a 1:400 dilution in PBS-T and incubated at 4 °C overnight. The following day, Alexa Fluor® 647 anti-mouse secondary antibody (Jackson ImmunoResearch Inc., catalog #715-605-150, Pennsylvania, USA) was diluted to 1:100 with PBS-T and sections were incubated for ~2 hours before being mounted onto positively charged microscope slides and cover slipped in Vectashield® antifade mounting medium.

For FB protocols (0.1% 5-day, 0.2% 5-day, 2% 3-day and 5-day) additional staining was conducted as small, round and blue fluorescent dots were seen after initial processing. To determine if these small and round structures are neuronal or non-neuronal, sections for these FB protocols were labelled with VAChT and NeuN. On the first day of staining, these sections were washed 3 times with PBS-T (0.01M PBS containing 0.1% Tritron-X, pH 7.3) followed by blockage with normal horse serum (10% PBS-T) for an hour. Sections were then incubated with primary antibodies, VaChT (mouse antibody, Novus Biologicals, catalog #NBP2-59378, Colorado, USA) at a 1:400 dilution in PBS-T and incubated overnight. The following day, Alexa Fluor® 647 anti-mouse secondary antibody (Jackson ImmunoResearch Inc., catalog #715-605-150, Pennsylvania, USA) was diluted to 1:100 with PBS-T for approximately 2 hours. After that, the sections were washed 3 times with PBS-T once more before primary antibody, NeuN, (guinea pig antibody, Millipore, catalog# ABN90, Washington, USA) at 1:300 in PBS-T was applied and left to incubate overnight. The next day, Alexa Fluor® 488 anti-

guinea pig secondary antibody (Jackson ImmunoResearch Inc., catalog #138058,

Pennsylvania, USA) was diluted to 1:100 with PBS-T for approximately 2 hours.

Afterwards, sections were mounted onto positively charged microscope slides and cover

slipped in Vectashield® antifade mounting

Imaging and Data Analysis

Images were obtained 4 days post-fixation using an FV1000 Olympus confocal

microscope objective lens at 20x with 1-µm z-steps. Only complete sections that

displayed both ventral horns without any major tears were imaged. Fluoview image

analysis software (Olympus Corporation, Pennsylvania USA) was used to measure the

labeling intensity ratio, labeling intensity difference, density of labeled cells and

percentage of non-neuronal co-labelling from images.

Labeling intensity ratio was obtained by circling the largest cross-sectional area of

a labeled MN with a complete nucleolus to obtain the average labeling intensity that was

compared to the average background intensity. Labeling intensity difference was

calculated as the difference between the average labelling intensity of a labelled MN and

the average background intensity. Density of labeled cells was calculated by counting the

number of labeled MNs within a 20x image and dividing it by the total volume of the

stack image; thereby allowing comparison of how many MNs are labeled among tracer

protocols. Non-MN labelling was seen as small, round, blue fluorescent dots in some FB

protocols. NeuN was used to determine if these dots were neuronal. Co-labelling

percentage was obtained by counting the number of non-neuronal labelled dots co-

labelled by NeuN only and dividing it by the entire count of non-MNs labelled dots in

selective FB protocols. These images were obtained using a 60x objective in order to better visualize the smaller fluorescent dots.

Neurolucida® 360 (MBF Bioscience, Vermont, USA) image analysis software was used to measure 3D properties of labeled somas and neurites. A neurite was defined as any projection out of the soma of a MN, as we could not determine if these projections were dendrites or axons without additional labeling. Analysis of neurites commenced with identifying somas; then using Neurolucida® 360 software to label neurites connected to their respective somas. Neurolucida® 360 Explorer software (MBF Bioscience, Vermont, USA) was then used to obtain three measurements: 1) neurite volume (μm^3), 2) total neurite length (μm), and 3) longest neurite path distance (μm). These parameters were selected because they assess different aspects of neuronal labeling quality by tracers. For instance, neurite volume provides a measure of how well a tracer fills the 3D structure of neurites, which is useful in studies aiming to reconstruct anatomical morphologies. Total neurite length was calculated as the summation of lengths of labeled neurites branching out of somas (see Figure. 4a), which provides a measure of how well a tracer labels somatic primary projections. The longest neurite path distance was calculated as the longest path formed by labeled neurites away from the soma, which provides a measure of how far a tracer is capable of labeling neurites away from the soma (see Figure. 4a). Previous literature has shown that MNs with largest cross-sectional area equal to or greater than 300 μm are deemed to be α-MNs (A. Ishihara et al., 2001; McHanwell & Biscoe, 1981). Therefore, in this study those labelled MNs with a largest cross-sectional area less than 300 μm are not included in these measurements, as they are not deemed to be α-MNs.

Statistical Analysis and Data Presentation

SPSS® (IBM Corporation, New York USA) statistical software was used for statistical analysis of all data. Prism GraphPad (GraphPad Software, California USA) was used for all graphing needs for this study. Data for all measurements were found not to be normally distributed as indicated by a failure of the normality test, Shapiro-Wilk test and therefore a logarithmic transformation was applied. Unequal variance was also indicated by Levene's test. In the end parametric analysis was used for all statistical analysis. using the logarthimical transformed data. Each experimental group (tracer, concentration, and number of survival days) was coded and tested with the One-way ANOVA Kruskal-Wallis test and the Tukey's post-hoc test. Threshold for significance (α) for all statistical analysis was 0.05. Any data with p-value >0.05 was deemed not statistically significant (N.S). All data are shown as mean $\pm$ SEM.

Three mice were excluded from the analysis due to insufficient tracer labeling. These mice were part of the 0.2% FB 3-day and 0.05% CTB 3-day groups and had less than 10 labeled cells in total. This is significantly less than other animals in the groups and from what is expected if the tracer has been successfully taken up at the muscle and retrogradely transported back to the spinal cord. Therefore, it was concluded that the tracer labeling was faulty in some way in these mice and their data was excluded. The sample sizes listed in table 1 show the number of animals that contributed successful data to each group and do not include the excluded animals. For each group, the data from each animal were compared and we confirmed that animals contributed comparably to the collected total sample.

Results

FB has a higher MN labeling intensity than CTB, and lower concentrations of FB are as effective as higher concentrations

The goals of the present study are: 1) to assess the effectiveness of different protocols of the retrograde tracers FB and CTB in labeling spinal α-MNs, and 2) to compare the labeling quality of tracers' standard concentrations (FB 2% and CTB 0.1%) versus lower concentrations, in an effort to avoid common issues such as leakage. To achieve that, a number of measurements were compared among experimental groups representing different tracers, concentrations, and survival days (see Table 3 for a summary of the experimental groups). All images were collected 4 days after mice were perfused (see Methods for detail). First, we compared the labeling intensity ratio among the experimental groups as shown in Figure 17a. The data showed that 0.2% FB 3-day provided the highest labeling intensity for FB (p<0.001), and 0.1% CTB 3-day provided the highest labeling intensity for CTB (p<0.001, Figure 17a) with the 0.2% FB 3-day protocol having the highest labeling intensity among all (i.e. higher than 0.1% CTB 3-day, p<0.001). Among all the examined protocols, three FB (0.1% 5-day, 0.2% 3-day, and 2% 3-day) had similar or higher mean intensity than that of the highest intensity CTB protocol (0.1% 3-day). This indicates that FB provides higher MN labeling intensity than that of CTB, and that FB has a wider range of effective MN labeling protocols than CTB. Additionally, FB and CTB 5-day protocols had generally similar (N.S in the 0.05% CTB) or lower neuronal labeling intensity than 3-day protocols (p<0.001), except at 0.1% FB which showed the opposite result. Importantly, the labeling intensity of 0.2% FB was not statistically different from that of the standard 2% FB concentration, in either 3-day or 5-

day protocols (N.S). This indicates that a 10-fold reduction of the standard FB concentration is equally effective in labeling spinal MNs. However, the lower concentration of CTB was statistically different than that of the standard 0.1% CTB 3-day and 5-day protocol.

The average background intensity could influence the outcome of labelling intensity ratio, a labelling intensity difference measure was also analyzed between all tracer protocols (Fig 17b). The results of this measurement further verify FB protocols having greater intensity by showing a significant difference in labelling intensity difference between all FB protocols to that of all CTB protocols (Fig 17b). Interestingly, it is also seen that there is no difference in labelling intensity difference of FB protocol when conditions, such as concentration and survival day are altered. However, this is not true for CTB as 0.1% CTB 5-day had the highest labelling intensity, which was significantly different ($p < 0.001$ and $p < 0.05$) compared to other CTB protocols (Fig 17b). In sum, our results show that: 1) FB provides higher labeling intensity of spinal MNs than CTB, 2) FB also has a greater number of effective labeling protocols than CTB, 3) 5-day protocols generally show lower labeling intensity than 3-day protocols in labelling intensity ratio, and 4) lower concentrations of FB provides equal, sometimes higher, MN labeling intensity than that of the standard concentrations.
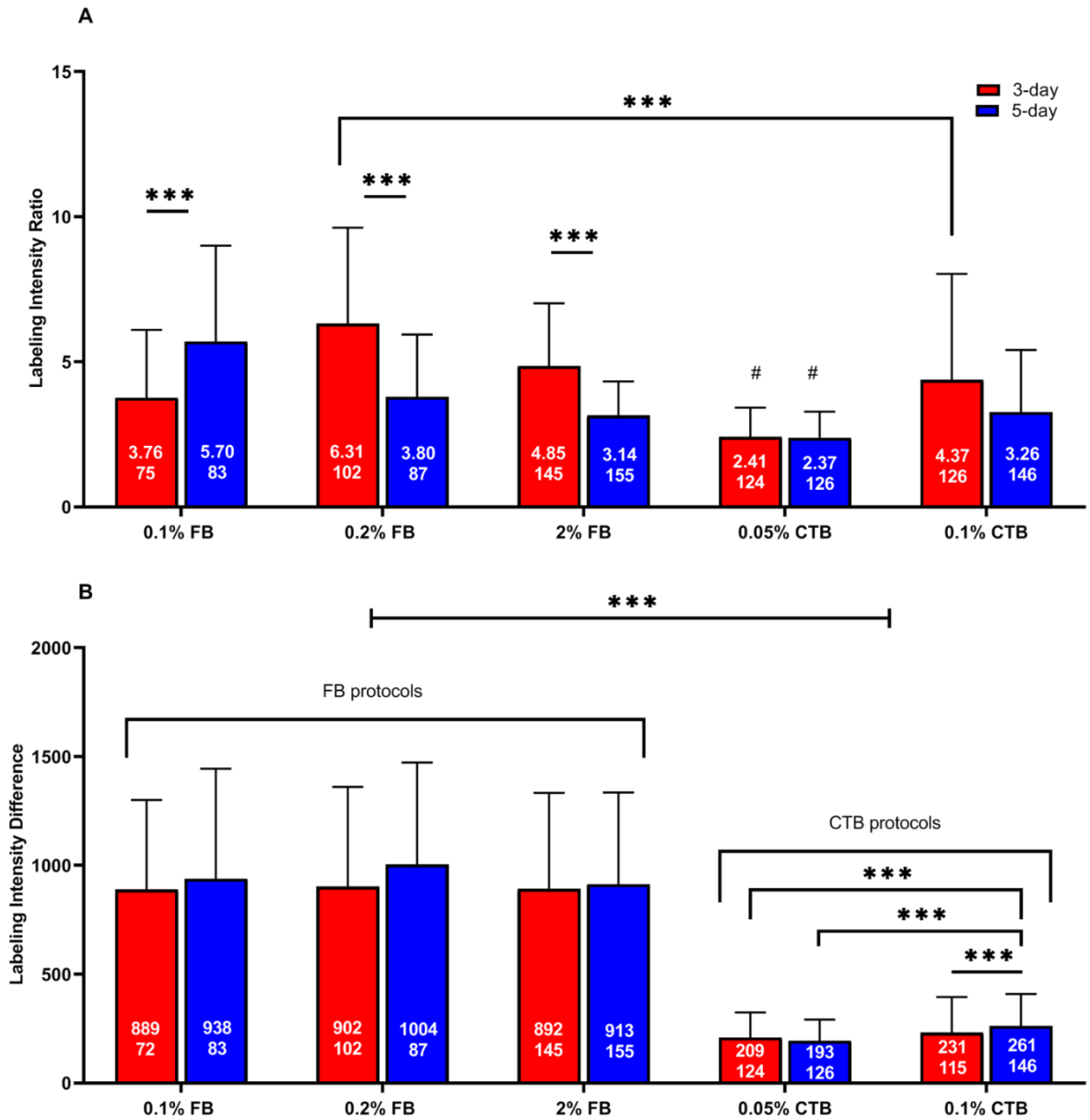
Figure 17. α-MN labeling intensity ratio and difference among tracer protocols.
(A) Intensity ratios (labeling/background intensity) (B) Intensity difference for all experimental groups measured 4 days after fixation. Data is mean ± SEM. The numbers inside the bars indicate the mean value (top) and the number of cells analyzed in that group (bottom). *** denotes $p<0.001$. The "#" symbol indicates that 0.05% CTB 3-day and 5-day are significantly different from all other experimental groups in labelling intensity ratio only.

CTB is more effective in labelling more α-MNs

To assess how successfully FB and CTB tracers are retrogradely transported from the muscle fibers to the spinal cord, we compared the number of α-MNs labeled among the experimental protocols. We injected tracers into multiple hindlimb muscles (Sol, TA, MG and LG) - to maximize the number of labeled cells and to achieve equal distribution of labeling across the lumbar spinal cord region (Bácskai et al., 2013) - and measured the density of labeled α-MNs (number of labeled α-MNs per unit tissue volume). Our data showed statistically significant differences in the density of labeled α-MNs among different FB and CTB protocol concentrations ($p<0.01$) (Fig 18). Specifically, the 0.05% CTB 3-day protocol had significantly higher labeled cell density than some FB protocols ($p<0.001$ and $p<0.05$) (Fig 18). This indicates that CTB generally labels more MNs than FB. Also, 3-day protocols generally had similar or higher cell density than 5-day protocols for both tracers (Figure 18, compare red to blue bars in all groups). With respect to tracer concentrations, FB protocols of low concentrations (0.1% and 0.2%) had comparable labeled cell density to that of the higher 2% FB standard concentration, and similarly the lower 0.05% CTB 3-day protocol had comparable labeled cell density to that of the 3-day higher 0.1% CTB standard concentration (Fig 18). These data further show no advantage for higher tracer concentrations than lower ones.

Together, these data show that 1) CTB generally labels more spinal MNs than FB, 2) 3-day protocols are as effective as 5-day protocols, and 3) protocols of low concentrations are as effective as, or sometimes better than, high concentration protocols.
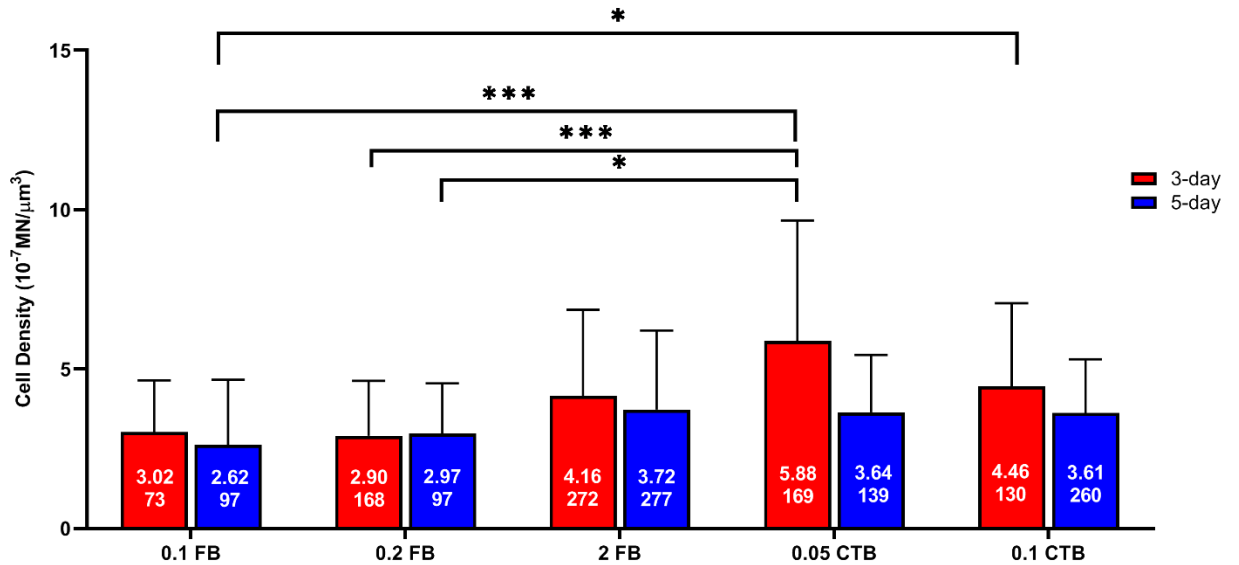
Figure 18. Density of labeled α-MNs among tracer protocols.
α-MN density was measured as the number of labeled MNs per unit tissue volume for all experimental groups. *** denotes $p<0.001$ and *denotes $p<0.05$. The numbers inside the bars indicate the mean value (top) and the number of cells analyzed in that group (bottom). Data represents mean $\pm$ SEM.

FB and CTB label α-MN anatomy comparably

To assess how well FB and CTB label the anatomy of α-MNs, we quantified and compared the 3D morphological properties of labeled α-MNs, including their somas and neuronal projections (neurites) among the experimental groups. To achieve that, we used the Neurolucida® 360 software to measure three parameters: 1) neurite volume, 2) total neurite length (i.e., total sum of neurite length, which would be =L1+L2+…+L10 in Figures 19a-b), and 3) longest neurite path distance (which would be =L4 in Figures 20a-b). These parameters were selected because they assess different aspects of the 3D neuronal labeling quality. For instance, neurite volume provides a measure of how well the tracer fills the 3D structure of neurites. Total neurite length provides a measure of how many neurites are labeled by the tracer and how well the tracer labels neurites along

their path. The longest neurite path distance provides a measure of how far a tracer is capable of labeling neurites away from the soma. Because a cell located near the edge of a section could have some of its neurites transected; thereby underestimating its neurites measurements, we – therefore – excluded cells located close to the section edge from the total and longest neurite length analysis.

For neurite volume, our data showed that regardless of concentration, 5-day FB protocols had higher labeling of neurites volume than 3-day FB protocols and higher than all CTB protocols (Fig 19). Specifically, statistical difference was seen between 3-day and 5-day protocols for all FB protocols ($p < 0.05$) and not for CTB tracers. With respect to tracer concentrations, 0.1% and 0.2% FB protocols were not statistically different from the higher 2% standard FB concentration (3-day or 5-day protocols), and similarly the 0.05% CTB protocols were not statistically different from the higher 0.1% standard CTB concentration (figure 19, the last four bars).
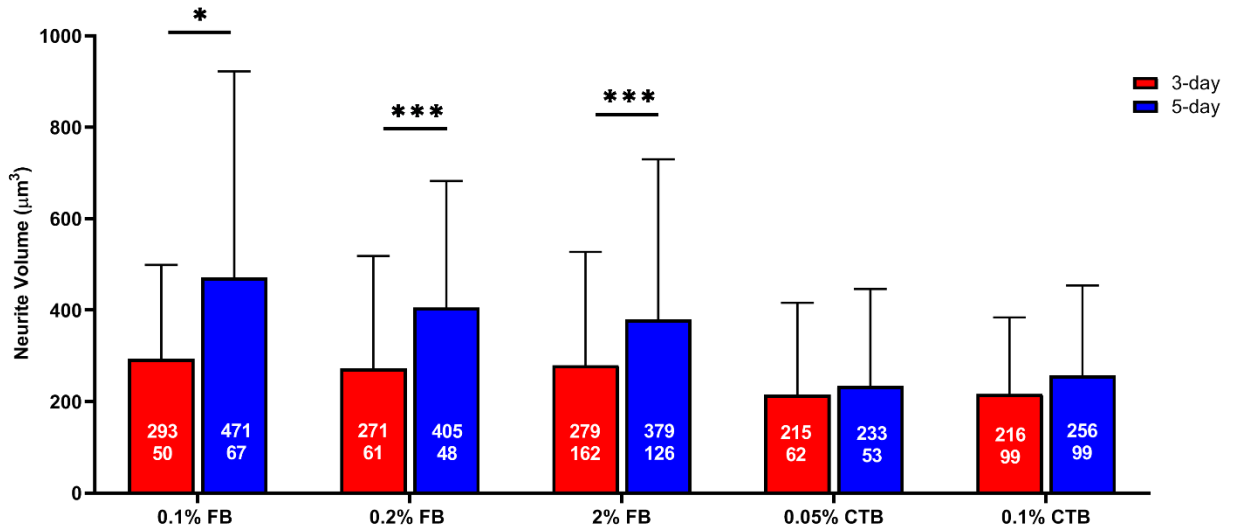

Figure 19. Neurite volume measurements among tracer protocols.
The numbers inside the bars indicate the mean values (top) and the number of analyzed neurites in each group (bottom). Data represents mean $\pm$ SEM.

With the total neurite length analysis, we continued to see similar trends with 3-day and 5-day protocols for both tracers having comparable total labeled neurite length (no statistical significance was noted between any blue and red bars at a given concertation in Figure 20c), and protocols of low and high concentrations having comparable total labeled neurite length (no statistical significance was noted among blue or red FB bars, or among blue or red CTB bars in Figure 20c). Between FB and CTB, protocols of both tracers had comparable total labeled neurite length, but 0.05% CTB protocols tended to show the lowest total neurite length values, whereas 0.1% FB 5-day and 0.1% CTB 5-day tended to show the highest total neurite length values (Fig 20c). When the longest neurite path length was compared among the experimental groups, no statistical difference was seen across all FB or CTB protocols (Fig 21c). Taken collectively, these results indicate that: 1) 5-day FB protocols are the most effective in labeling the neurite volume , 2) low FB and CTB concentration protocols are as effective as high concentration protocols in labeling neurite volume, total neurite length, and longest neurite path distance of α-MNs, and 3) short survival FB and CTB (i.e., 3-day) protocols are as effective as long survival (i.e., 5-day) protocols in labeling neurite volume, total neurite length, and longest neurite path distance of α-MNs.
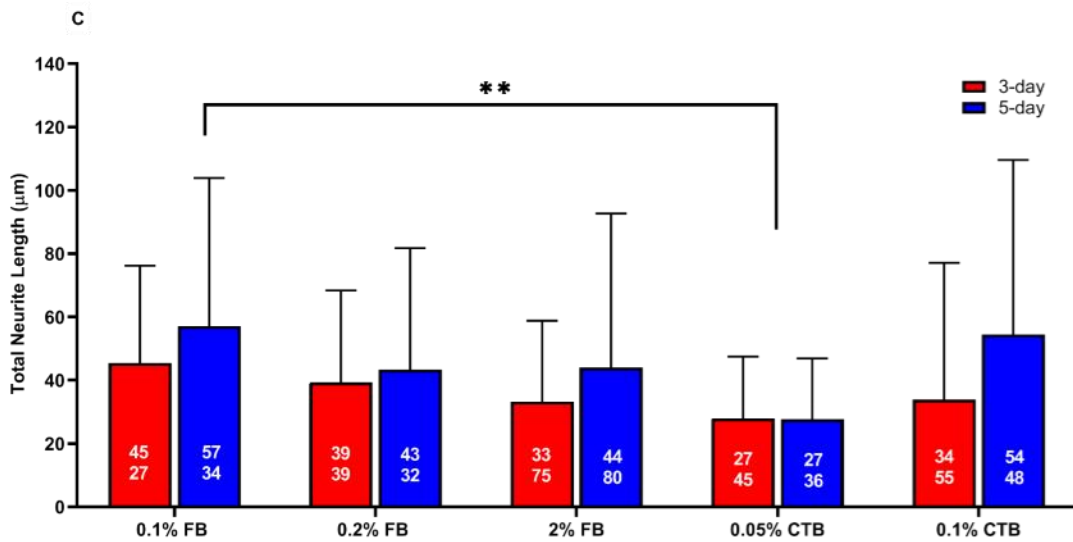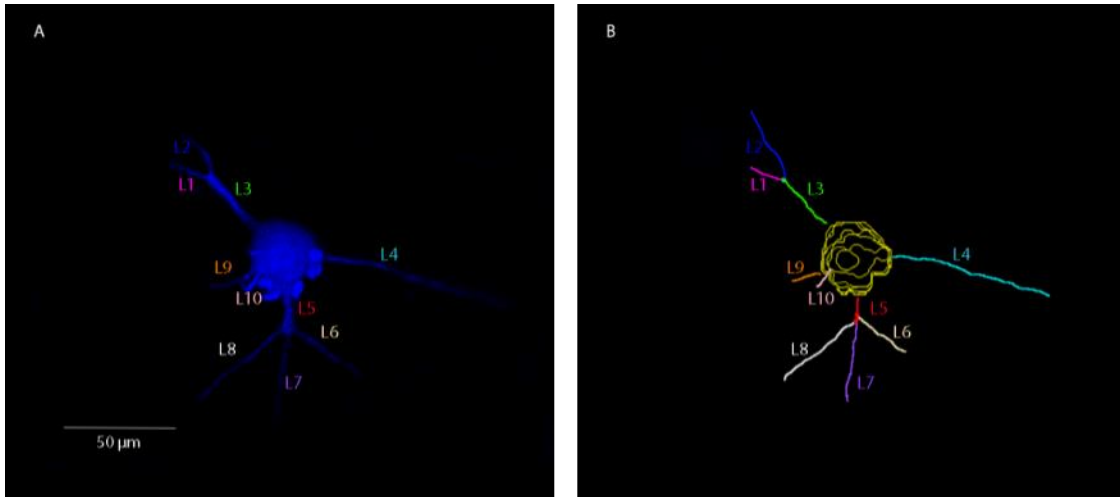
Figure 20. Total neurite length among tracer protocols.
(A) Image of neurite projection prior to reconstruction from tracer labeling. (B) Image of neurite projections reconstructed from tracer labeling. The total neurite length was calculated as the sum of L1, L2, ..., L10. (C) Total neurite length among tracer protocols. ** denotes $p<0.01$. The numbers inside the bars indicate the mean values (top) and the number of analyzed cells that had neurites (bottom). Data represents mean $\pm$ SEM.
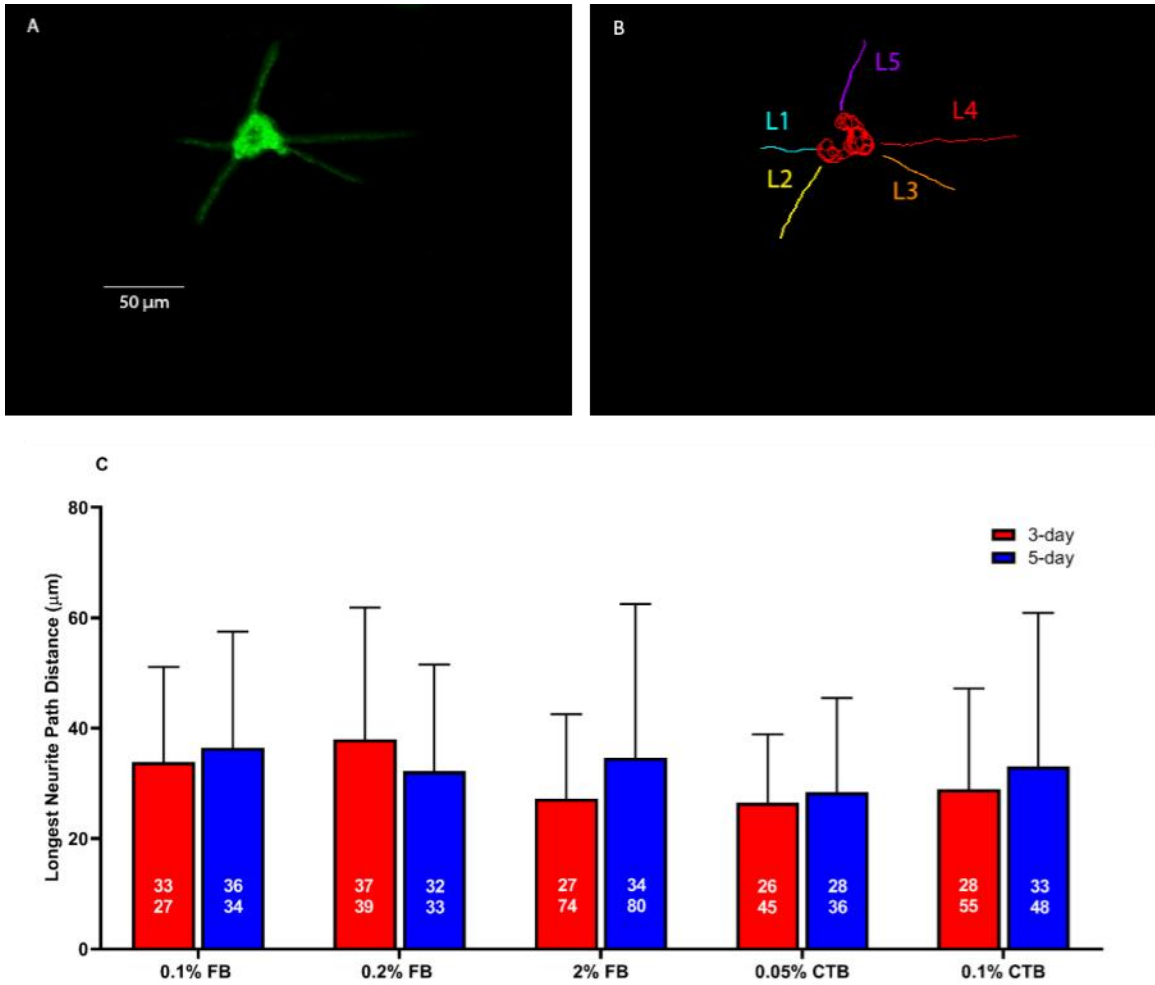
Figure 21. Longest neurite path distance among tracer protocols.
(A) Image of neurite projection prior to reconstruction from tracer labeling. (B) Image of
neurite projections reconstructed from tracer labeling. The longest neurite path distance
was determined to be L4, as it had the longest neurite length. (C) Longest neurite path
distance among tracer protocols. The numbers inside the bars indicate the mean values
(top) and the number of analyzed cells that had neurites (bottom). Data represents mean $\pm$
SEM.

FB and CTB label MNs, but not interneurons

As retrograde tracers, FB and CTB are expected to label α-MNs; they could also label γ-MNs or INs if transported via synapses. C-boutons are more likely to be found only on α-MNs, but can also be found on γ-MNs but not on INs (Witts et al., 2014). To determine if the labelled neurons are MNs and that only α-MNs were analyzed in this experiment., we stained spinal tissue with ChAT antibody to label C-boutons. and measured the LCA of all labelled MNs, removing those less than 300 μm, For ChAT labelling, We focused on 2% FB 3-day and 0.1% CTB 3-day protocols in these experiments because the high tracer concentrations in these protocols increases the risk of labeling non-MN cells and the high labeling intensity of these protocols maximizes the accuracy of this analysis (see Figure 17a); thereby enhancing the rigor of this investigation. Our confocal images and analysis showed that 100% of neurons labeled with FB or CTB also showed ChAT co-labeling (Fig 22). The results of ChAT labelling support that FB and CTB label MNs only, when intramuscularly injected. Importantly, similar results were obtained when VaChT – another specific C-bouton antibody to label MNs – was used in a separate tissue (data not shown), confirming that FB and CTB label MNs only.
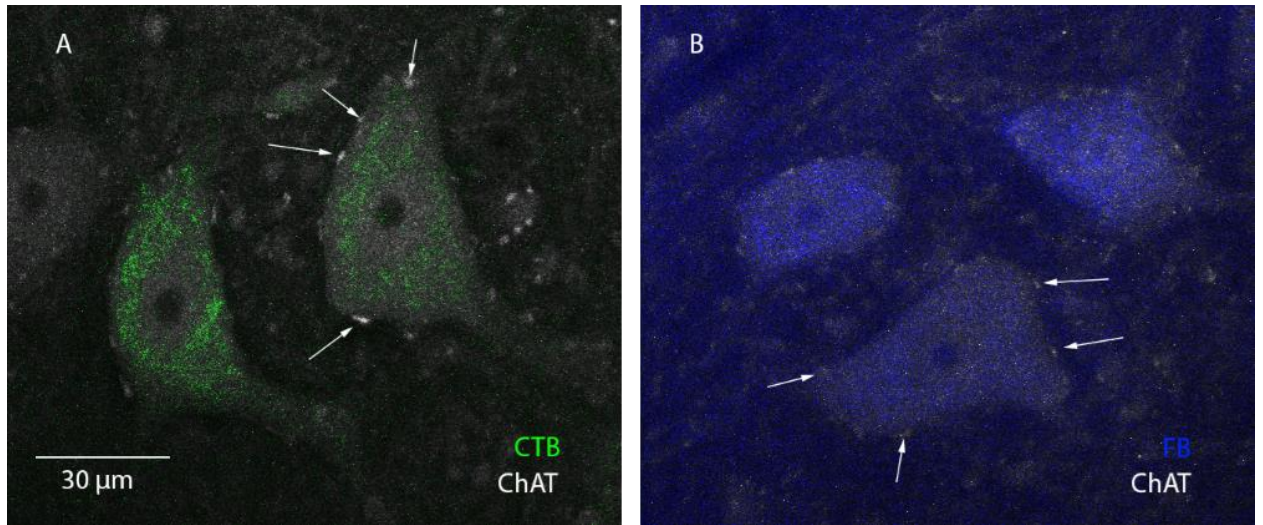
Figure 22. Co-labeling of ChAT with FB or CTB.
60x images of MNs labeled with 0.1% CTB 3-day (**A**) and 2% FB 3-day (B) co-labeled
with ChAT. White arrows indicate the location of C-bouton labeling. The scale bar
represents 30µm.

Tracer leakage with the standard 2% FB concentration.

Because FB has been shown to leak from labeled MNs to other cells in the spinal

cord (Köbbert et al., 2000), we examined images of all experimental groups for potential

leakage effects. Our analysis showed consistent appearance of FB leakage shown as

small, round, blue fluorescent dots that appear to be non-MN in the standard 2% FB

concentration (both 3-day and 5-day protocols, see the white arrows in Figure 23a) and in

the lower concentration of FB at 5-day. To determine if these small, round, blue

fluorescent dots could be neuronal and MN , we stained some FB sections from 0.1% FB

5-day, 0.2% FB 5-day, 2% FB 3-day and 5-day with NeuN and VAChT. After staining, a

NeuN co-labelled percentage was obtained from these sections without the inclusion of

those dots that also co-labelled with VAChT. This percentage depicts whether or not these dots are neuronal cells.

From our results in Table 3, it is seen that majority of FB protocols, had a small percentage of NeuN co-labelling, with the exception of 0.2% FB 5-day, suggesting that these small, round, blue fluorescent dots are indeed not motoneuron and are not neuronal. Furthermore, we also observed the presence of a halo like-effect specifically within 2% FB images, which appeared along with non-neuronal cell labeling.

Therefore, our NeuN analysis confirms that the small, round, blue fluorescent dots are non-neuronal and likely due to leakage from FB labeled α-MNs in the 2% FB protocols and in some cases lower concentration of FB at 5-day only (Fig 23). Interestingly, there was no non-MN cell labelingwith any concentration of CTB at 3 days or 5 days, or with lower concentrations (<2%) of FB at 3-days. Collectively, the results of these experiments and the experiments in the previous section on FB and CTB specificity in labeling α-MNs show that: 1) CTB and lower FB concentration (i.e., <2%) protocols at 3-days label α-MNs only without tracer leakage, 2) FB at either higher or lower concentration protocols can exhibit tracer leakage leading to labeling of additional non-neuronal labelling, in addition to the appearance of halo-like effects.

Table 5. NeuN Co-labelling Analysis. FB sections from 0.1% FB 5-day, 0.2% FB 5-day, 2% FB 3-day and 2% FB 5-day were stained with NeuN and VAChT to determine if blue, fluorescent dots were neuronal and/or MNs.

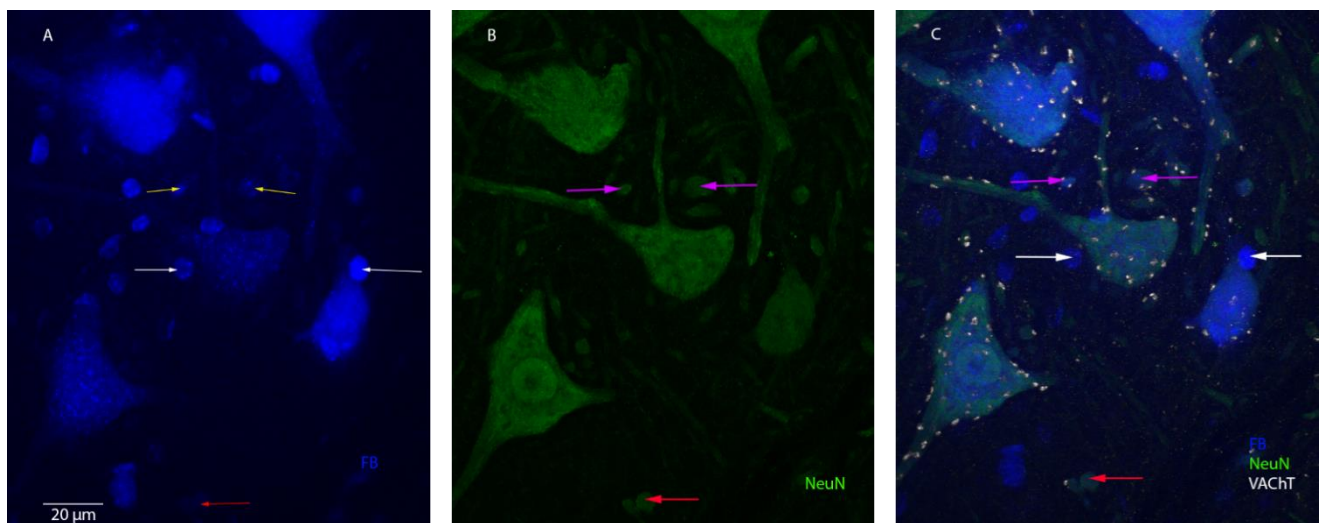| Protocol	Number of Non-neuronal labelling	Number of Co-labelled Non-neuronal labelling	Percentage Co-labelled (%)
0.1% FB 5-day	28	5	17.85
0.2% FB 5-day	11	7	63.63
2% FB 3-day	56	4	7.14
2% FB 5-day	87	3	3.44

Figure 23. Non-MN labeled cells in an image from 2% FB 3-day protocol. 60x image of **A)** FB labeling, **B)** NeuN labeling and **C)** FB, NeuN and VAChT labeling of non MN cells (red arrows), neuronal cells (white arrows) and γ-MN (yellow). The scale bar represents 20µm.

Specific Discussion

This study provides, for the first time, a systematic assessment and comparison of FB and CTB under different experimental conditions, such as tracer concentrations and survival days. These two retrograde tracers are widely used in labeling MNs. Seven different aspects of neuronal labeling quality were examined: 1) Labeling intensity ratio and difference, 2) density of labeled cells, 3) volume of labeled neurites, 4) total length of labeled neurites, 5) longest path distance of labeled neurites, 6) labeling specificity to MNs, and 7) tracer leakage through NeuN co-labelling analysis.

Our data show five major results: First, while FB and CTB protocols appear to differ in their labeling characteristics of α-MNs, the 0.2% FB 3-day protocol appears to offer good quality across 'all' labeling characteristics of α-MNs. Second, low tracer concentration protocols are equally effective in labeling α-MNs as the much higher tracer concentrations widely reported in literature, providing an economic advantage and avoiding major tracer leakage. Third, 3-day survival FB and CTB protocols are generally as effective as, and sometimes better than, 5-day survival protocols. Fourth, CTB and lower FB concentration protocols only label MNs. Fifth, the standard 2% FB concentration protocols (both 3-day and 5-day) suffer leakage problems, leading to large amounts of non-MN cell staining as well as halo-like effects in images. CTB protocols, on the other hand, do not appear to suffer leakage problems. Accordingly, these results provide a useful guide to selecting optimal protocols when using FB or CTB retrograde tracers.

High or low tracer concentration?

Although high tracer concentrations would be expected to provide high labeling quality, they also result in tracer leakage, thereby losing labeling specificity of the desired neuronal populations. This tradeoff makes the selection of FB and CTB protocols and concentrations particularly challenging because these tracers have been used in literature in various protocols and a wide range of concentrations with no study highlighting the advantages and disadvantages of different tracer concentrations or suggesting optimal protocols. Because of the absence of this knowledge, sub-optimal protocols and high tracer concentrations continue to be used in various studies ranging from injecting tracers into muscle, nerves and other locations of the rodents' body to label MNs and other various types of neurons.

For instance, in the last five years only, at least 13 studies have used high FB concentrations (>1.5%, and as high as 5%) (Atanasova et al., 2016; Chen et al., 2018; W. Gao et al., 2015; Hashimoto et al., 2018; Lee et al., 2016; Lee & Malykhina, 2017; Majima et al., 2017; N. Shimizu et al., 2018; T. Shimizu et al., 2018; Takaki et al., 2015; Wong et al., 2017; Yamamoto & Nakamuta, 2018; Zimmerman et al., 2020; Žygelyte et al., 2016) when only 6 studies have used low FB concentrations (<1.5%) (Chaves-Coira et al., 2016, 2018; Kanda et al., 2016; La et al., 2016; Okabe et al., 2017) This indicates that low FB concentrations (i.e., <1%) are still not popular and their advantages over high concentrations are still unknown though they have been used for many years (Ghosh et al., 2012; Kwon et al., 2002; Sagot et al., 1998)).

Data of the present study fill this knowledge gap and provide a direct comparison of the effects of high versus low tracer concentrations on the various aspects of neuronal

staining quality and, therefore, guide the selection of optimal tracer protocols and concentrations.

Shorter is better

It has been suggested that FB is the tracer of choice as compared to Fluoro-Gold (FG) and dextran conjugate tracers (Mini-Ruby, Fluoro-Ruby and Fluoro-Emerald), because FB labels a high number of MNs with persistent quality in labeling intensity for up to 24 weeks of survival time (Novikova et al., 1997)). Our results add to the positive characteristics of the FB tracer, but also establish that CTB is better than FB in staining more MNs, yet at the expense of neurite labeling. Interestingly, our results for labeling intensity ratio contradicts what is seen in literature that states labeling intensity for FB remains consistent with protocols of longer survival days from 8 weeks to 24 weeks (Choi et al., 2002; Novikova et al., 1997).

The only exception to this was with 0.1% FB, in which labeling intensity ratio was higher for the 5-day protocol than the 3-day protocol. Additionally, in most of our measurements, 3-day protocols were generally comparable to, and sometimes better than, 5-day protocols. However, upon reviewing the cell intensity difference data, our results also show that overall, regardless of the concentration and survival day, FB is optimal at labeling α-MNs greater than CTB (Figure 17b). In addition, this data also shows varying the concentration and survival day influences CTB protocols more than FB as 0.1% CTB 5-day had significantly higher labeling intensity difference compared to other CTB protocols.

Less is better

In intramuscular injection studies that utilize rodents such as ours, the standard concentration at which FB has been used is 2% (Khristy et al., 2009; Wong et al., 2017). Interestingly, our results show that a 0.2% FB protocol – a much lower concentration than what has been used before and 10-fold lower than the standard concentration – has comparable labeling quality. In addition to the economy of using less tracer, lowering the concentration of FB reduces leakage onto other non-MN cells and non-neuronal cells as well as the appearance of halo-like effects in images – two risks of higher tracer concentrations (Figures 23). To our knowledge, only one study has described the appearance of accidental neuronal staining caused by FB leakage in facial rat MNs. (Popratiloff et al., 2001).

In addition, the appearance of halo-like effects by FB is consistent with literature regarding other fluorescent tracers (Köbbert et al., 2000). The likely explanation for these effects is that they result from FB leaking from labeled neurons (Köbbert et al., 2000). Interestingly, from our NeuN analysis majority of these cells are also not neuronal as there was a low percentage of NeuN co-labelling. In addition, we also found that those that are co-labelled with NeuN could simply be small γ-MNs, as they were co-labelled with VAChT, or dendrites from MNs whose somas are not located in the section.

Thus, the finding that significantly lower FB concentrations at 3-day have comparable neuronal staining quality to that of higher concentrations, while avoiding leakage is novel to this study. On the other hand, lowering the CTB concentration could have adverse effects: When the CTB standard concentration was decreased by half in our experiments, labeling intensity ratio was reduced while the intensity difference was comparable across concentrations (see figure 17). The lower concentration did yield

fewer neurites labeled relative to the CTB standard concentration (see Figures 20 and 21). Although previous studies examined different survival times of the 0.1% CTB concentration (Hirakawa et al., 1992) , there is no data in literature comparing the effects of different CTB concentrations on the quality of neuronal labeling, thus, these results represent additional novel data. In sum, lowering FB concentration does not decrease neuronal labeling quality, but does avert non-α-MN cell labeling and halo-like effects. Conversely, lowering CTB concentration decreases neuronal labeling quality.

FB protocols and 0.1% CTB protocols are similarly effective in labeling the volume and length of α-MN somas and neurites (see Figures 19-21). Previously, CTB was found to label long neurites significantly better than Fluorogold (Yao et al., 2018). Fluorogold has been speculated to be potentially harmful for labeled neurons in the long term (Naumann et al., 2000) which would suggest that CTB and FB would preferably over Fluorogold. The effectiveness of FB and CTB tracers in labeling somas and neurites renders them useful in studying neurodegenerative diseases, such as ALS in which α-MNs experience changes in size (Dukkipati et al., 2018). However, FB and CTB labeling are only good for measuring the morphological properties of the α-MN soma and primary projections: In our images, all neurite projections from labeled α-MNs had few or no branches. Thus, intracellular fillings – as opposed to intramuscular fillings via retrograde tracers – would be the method of choice to study the full dendritic anatomy of α-MNs.

Final Discussion

Final Discussion

The discovery of TDP-43 aggregates in ALS and FTD patients provided a possibility of how these two opposite diseases are related (T. Ishihara et al., 2010; Neumann et al., 2006). To be able to study and assess the characterization of ALS-FTD in a mouse model, proper experiments must be developed and/or optimized.

The rNLS mouse model is a unique model that allows researchers to control disease progression by the removal of doxycycline in the mouse's diet (Walker et al., 2015). In a previous rNLS mice model, a *CamkIIa* promotor was used to express TDP-43 aggregates in neurons of the brain (Alfieri et al., 2014). A study on this rNLS model suggested that the expression of TDP-43 aggregates in the brain had resulted in FTD like symptoms by showing cognitive deficits in behavioral experiments (Alfieri et al., 2014). The use of a *CamkIIa* promotor limited aggregates to only the forebrain and therefore full ALS like symptoms were not seen (Alfieri et al., 2014). This then leads to the development of a novel rNLS8 mice model, which had a *NEFH* promoter had been used instead of a *CamkIIa*, which resulted in an overexpression of hTDP-43 into the brain as well as spinal cord resulting in ALS symptoms (Walker et al., 2015). In addition to TDP-43 aggregates in the spinal cord, it was also said that this model had a ten-fold increase of TDP-43 inclusions than what was seen in *CamkIIa* model (Walker et al., 2015).

Since the creation of this novel rNLS mice model, more research has been focused on ALS symptoms on this study such as motor function deficits (Walker et al., 2015), MNs loss (Spiller, Cheung, et al., 2016), motor function recovery after the suppression of hTDP-43 overexpression and axonal dieback (Spiller, Restrepo, et al., 2016). While minimal study has been conducted on the brain of this mouse model, so far

it is known that ~28% of neurons are lost in the brain and that other non-neuronal structures are also affected leading to gliosis, which is the reactive change in glial cells in response to damage in the CNS, in the brain (Walker et al., 2015). Despite, the current literature regarding the brain of this mouse model, there has been no behavioral experiments conducted on this rNLS mouse model and additional characterization should be warranted on this rNLS mouse model to confirm if it is an ideal FTD/ALS mouse model. Therefore, the purpose of this thesis is to optimize protocols that would be advantageous for researchers to use to properly to characterize this rNLS mouse model.

To be able to properly assess the cognitive function of the rNLS mice model, we had to first to develop proper protocols for the following behavioral experiments: the Y-maze test, the NOR test and the Holeboard Discrimination test. These behavioral experiments are designed to assess short-term memory and learning of mice (Arias et al., 2015; Labots et al., 2015; Prieur & Jadavji, 2019). It was important for this study to assess short-term memory and learning as the novel rNLS mouse model had shown evidence hTDP-43 inclusions in the hippocampus, without any behavioral testing conducted to determine if cognitive deficits appear (Walker et al., 2015). The reasons why these tests were chosen were because of different short-term memory it assessed. Y-maze test assessed spatial working memory, NOR test assessed recognition memory and Holeboard Discrimination test assessed spatial reference memory as well as learning. The creditbility of these tests expands from the constant usage in literature (Castilla-Ortega et al., 2010; Fukuda et al., 2019; Griffiths et al., 2019; Labots et al., 2015; Onaolapo & Onaolapo, 2015; Rossi et al., 2018; Sampedro-Piquero et al., 2019; J. Xu et al., 2018).

For the first study, we determined that the results obtained are optimal through the use of literature. Results that are consistently seen in published literature were similar to our results for the Y-maze and NOR tests. For example, our spontaneous alternation for the Y-maze was ~65%, numerous literature has suggested that their spontaneous alternation for the control was ~60-70% (Barakat et al., 2018; Hiramatsu et al., 2010; Paretkar & Dimitrov, 2018). Similarly, literature has mentioned that the discrimination ratio for NOR was ~0.4-0.7 (Denninger et al., 2018; Sik et al., 2003), our discrimination ratio at the final protocol was ~0.65 for our control group. For Holeboard Discrimination test, other literature had reference memory errors of ~7 on Day 1 and ~2 on Day 4. A working memory errors of ~9 on Day 1 and ~3 on Day 4 and completion time of ~100 sec on Day 1 to roughly less than 60 sec on Day 4 (Kuc et al., 2006). Interestingly, our results were consistently lower in comparison to the literature. However, the downward/upward trends with a statistical difference ($p<0.05$) from Day 1 to Day 4 for reference memory error, completion time, 1st time to treat and the number of treats, all indicate that the mice had learned the object of the experiment. Therefore, our protocols that were developed for the Y-maze test, NOR Test and Holeboard Discrimination Test are deemed to be optimal.

Furthermore, to determine the accuracy of our Y-maze and NOR, we used a positive control. Scopolamine was injected at either 1 mg/kg or 3 mg/kg in 12 BCJL6-WT mice 30 mins before the commencement of a testing experiment (see methods for details). This drug is an acetylcholine antagonist that mimics short-term memory deficits commonly seen in Alzheimer's disease by decreasing the amount of acetylcholine in the brain (Esquerda-Canals et al., 2017). Many published studies have used scopolamine-

induced mice as a common positive control in AD-related studies (Balmus & Ciobica, 2017; H.-B. Kim et al., 2017; Skalicka-Wozniak et al., 2018).

Our results with scopolamine injected mice showed that our Y-maze and NOR tests are appropriate in assessing short-term memory deficits in mice (Figs 8 and 10). Therefore, Y-maze and NOR tests with the current protocol are suitable for short-term memory assessment because it can detect short-term memory deficits. Future directions of this study should involve conducting a positive control experiment for the Holeboard Discrimination test to confirm that test is also suitable to detect short-term memory and learning deficits in mouse.

Differences in behavior protocols are commonly seen in the literature. Usually, changes to the protocols are minor such as altering the time of experiment or number of times the experiment is running (Post et al., 2011; Stover et al., 2015). The need for altering behavior protocols stems from the possibility that different strains of mice behave differently when assessed in behavioral experiments. For example, a study conducted by Sik et al. looked at four different strains of mice with regards to the NOR test (Sik et al., 2003). From this study, researchers were able to conclude that strains like Swiss mice are more capable of being behaviorally assessed regarding the NOR test than other strains like 129/SVs (Sik et al., 2003). These strain differences in performance could be because of stress and anxiety, as it is an important factor that could influence any experiment (Heyser et al., 1999; Kuc et al., 2006; Sik et al., 2003). Some strains of mice are more capable of handling anxiety and stress from behavioral experiments than other strains of mice (Kuc et al., 2006; Sik et al., 2003). In addition to background strain difference, environmental factors such as husbandry, setup and experimental procedures

could also influence results of behavioral experiments by contributing stress. Several literatures have indicated that the changes in environment housing and experimental procedures can alter the reproducibility of results due to stress. One study conducted by Gerdin et al looked at the effects of experimental and husbandry procedures on C57BL/6Nac mice regarding stress. In this study, mice had undergone a surgical procedure, numerous cage changes and overnight fasting. Their results suggested that mice experience higher blood glucose, higher blood pressure and lower body weight due to stress caused by these experimental and husbandry procedures (Gerdin et al., 2012).

Therefore, differences in behavioral protocols such as strain differences, husbandry and experimental procedures could have a significant impact on the performance of mice in cognitive behavioral testing. Since hybrid animals such as our background strain of mice are not commonly used in research for behavioral experiments, altering experimental protocols is necessary to address non-variable effects such as anxiety and stress-related differences. Also, differences in protocol were necessary for Holeboard Discrimination test as fasting was not feasible for this experiment, since this particular mouse model would have FTD/ALS, which would result in significant weight loss and possibly death, if fasted.

For our second study, we hypothesized that this novel rNLS mice model, that contain the tTA-*NEFH* promoter with tetO-hTDP-43ΔNLS transgene will develop short-term memory deficits. Our results showed that when rNLS +/+ mouse group were 5 weeks off doxycycline, they experience short-term memory deficits because of the significant decrease in spontaneous alternation compared to rNLS -/- mouse group (Fig 15c). This decrease in spontaneous alternation is a result of short-term memory deficits

and not motor deficit due to ALS disease progression. This was determined because the number of entries for the rNLS +/+ mice at 5 weeks off doxycycline were not statistically different from the control, rNLS -/- (Fig 15a). Previous literature has determined that these rNLS mice with the *NEFH* promoter exhibit motor deficits as early as 2 weeks off doxycycline (Spiller, Cheung, et al., 2016; Walker et al., 2015). Qualitatively it is also seen that our cohorts of mice were starting show symptoms of ALS before behavioral experimentation. Therefore, it is probable that FTD symptoms in this rNLS mice model occur after ALS symptoms, which is common in patients with ALS-FTD (Lillo & Hodges, 2009).

Previous studies have assessed cognition through behavioral experiments on doxycycline suppressible mice. The most relevant study was, where rNLS mice with *CamkIIa* promoter was used instead of a *NEFH* promotor (Alfieri et al., 2014). In that study, a significant difference was seen in the Y-maze test when rNLS mice were 1 month off doxycycline (Alfieri et al., 2014). The results presented by that study is similar to this study, which suggest that FTD like symptoms occur when doxycycline suppression happens for a long period.

Interestingly, another study that had also utilized a doxycycline suppression system had shown similar results. Alfieri, Silva and Igaz, 2016 had used mice that had the genetics tTA-*CamkIIa* promoter with tetO-TDP-43WT12, this would cause overexpression of hTDP-43 in the forebrain neurons. In this study, it was determined that 1 month off doxycycline had resulted in cognitive deficits as Y-maze showed significantly lower spontaneous alternation (Alfieri et al., 2016). In the end, our preliminary results suggest that rNLS mice with *NEFH* promoter appear to show short-

term memory deficits, after ALS symptom onset. However, plans of NOR and Holeboard test will confirm the presence of short-term memory deficits.

The third study was conducted to optimize tracer protocols of two commonly used retrograde tracers, FB and CTB, to label α-MNs by intramuscular injection. The labeled neurons located in the ventral horn of the spinal cord section were α-MNs that are innervated to muscles. When ALS disease affects a significant number of these innervated α-MNs, mice will start to show symptoms of ALS (Martin et al., 2017). These symptoms usually start with tremors that will gradually progress into paralysis (Rowland & Shneider, 2001). Interestingly, ALS symptom onset and disease progression tend to vary between different mouse models of ALS (Philips & Rothstein, 2015). Differences in disease progression are due to the type of transgenic mutation inserted within a mouse as well as how much are these mutations are expressed (Philips & Rothstein, 2015). For example, SOD1 G93A has overexpression of SOD1, which affects excitatory mechanism in the CNS resulting in excitotoxicity (Kaur et al., 2016). Whereas, TDP-43 mouse models revolve around affecting RNA-dependent mechanism by the loss of nuclear TDP-43 and/or overexpression of aggregated TDP-43 (Philips & Rothstein, 2015). Therefore, having proper tracer protocols will allow researchers to properly label innervated α-MNs in various ALS mice models. These α-MNs can then be assessed through fluorescent microscopy in future experiments.

This study was conducted by comparing FB and CTB under various conditions like different concentrations and survival days. It was hypothesized in this study that CTB would be more efficient at labeling MNs due to its high affinity for neurons through receptor-mediated endocytosis (Lencer & Tsai, 2003). But our results suggest that there is

no overall difference between FB and CTB for all of the seven parameters used for assessment. This study also reveals that FB has more experimental protocols that are useful for alpha-motoneuron labelling compared to CTB. Also, it was noticed that altering the survival days after tracer injection could alter labeling qualities after reviewing labeling intensity ratio data. For example, lowering the survival day from 5-day to 3-day had resulted in an equal or higher quality of motoneuron labeling (Fig 17). This was the case for most of the experimental groups except for 0.1% FB (Fig 17).

Lowering the concentration of FB − 10-fold than what is used as standard concentration is capable of labeling MNs just as efficient (Fig 17), if not better because adverse effect like tracer leakage was limited to what is seen at standard concentration of FB (Fig 23). Tracer leakage is an important adverse effect to be aware of as it can cause staining of non-neuronal cells (Choi et al., 2002). In this study, non-neuronal cells were also labelled as the result of FB leakage at the standard concentration (ie. $\geq$ 2%) and in some cases lower concentrations (0.1% and 0.2%), however, only at 5-day survival day timepoint. From our NeuN analysis, it can be said that these small, blue fluorescent dots could be either γ-MNs, remanent of dendrites from somas not included in the sections or sequestering of FB dye after leakage. Interestingly, the advantage of lowering concentration is not for CTB, as a lower concentration of CTB revealed less quality in motoneuron labelling (Figs 17a, 20 and 21).

Tracer protocol optimization is necessary as anatomical tracers like FB and CTB are commonly used in various research, especially in neurodegenerative disease related studies (Fernández-Espejo & Bis-Humbert, 2018; Nouraei et al., 2018; Vaughan et al., 2015; Wang et al., 2016). An example of a study using retrograde tracer in a

neurodegenerative disease setting would be a study conducted by Mohajeri et al., where Fluoro-gold was intramuscularly injected in an ALS mouse model, SOD1 G93A. The researchers in that study had injected retrograde tracer Fluoro-gold (FG), intramuscularly injecting into hindlimb muscles at various time points (Mohajeri et al., 1998). From that study, they saw that α-MNs were lost 4 weeks before symptom onset and that FG also adequately labelled gamma-MNs (γ-MNs) (Mohajeri et al., 1998). Interestingly, other studies have described FG as a toxic retrograde tracer that harms labelled neurons (Naumann et al., 2000). Therefore, our study provides creditability and reliability in support of two retrograde tracers, FB and CTB, because these tracers would be better for neurodegenerative studies.

This study is also unique in various other aspects as it provides more information about the intramuscular injection of retrograde tracers like FB and CTB, and their ability to label α-MNs. Firstly, this study provides further clarification of intramuscular labeling in mice. A previous study has shown that differences in FB labeling arise when different species of rodents are used even with the same method of application (Hayashi et al., 2007). Hayashi et al. mentioned that FB labeling is generally lower in rats when compared against mice after the tracer was intramuscular injected into hindlimbs. Secondly, our study looked at several different parameters to assess labeling quality. Many kinds of literature have only relied mostly on the number of neurons labelled and not so much any other variable to determine the efficiency of tracer labelling (Novikova et al., 1997; Schmued & Fallon, 1986). Our study utilized parameters like labeling intensity ratio, labelling intensity difference, neurite volume, total and longest neurite path distance in addition to cell density.

Neurite measurements are not commonly seen in tracer comparison literature, only one paper as recently used the neurite projections as measurements (Yao et al., 2018). Neurite projections are important as it provides as a 3D morphological anatomy of the labeled MNs, which provide information that can be used in various other disciplines of science.

In conclusion, these studies were developed to optimize protocols for short-term memory assessment through behavioral experiments and to label innervated MNs by intramuscular injection of retrograde tracers, FB and CTB. These studies are important because having accurate protocols will allow researchers to be able to properly characterize ALS and FTD in mice models that contain both of these neurogenerative diseases like the rNLS mice model. In future experiments, we will thoroughly characterize rNLS mice model through the use of the methods developed in this thesis.

REFERENCES

1. Acosta, M. C., Copley, P. A., Harrell, J. R., & Wilhelm, J. C. (2017). Estrogen signaling is necessary for exercise-mediated enhancement of motoneuron participation in axon regeneration after peripheral nerve injury in mice. *Developmental Neurobiology*, *77*(10), 1133–1143. https://doi.org/10.1002/dneu.22501

2. Alfieri, J. A., Pino, N. S., & Igaz, L. M. (2014). Reversible behavioral phenotypes in a conditional mouse model of TDP-43 proteinopathies. *The Journal of Neuroscience: The Official Journal of the Society for Neuroscience*, *34*(46), 15244–15259. https://doi.org/10.1523/JNEUROSCI.1918-14.2014

3. Alfieri, J. A., Silva, P. R., & Igaz, L. M. (2016). Early Cognitive/Social Deficits and Late Motor Phenotype in Conditional WT TDP-43 Transgenic Mice. *Frontiers in Aging Neuroscience*, *8*, 310. https://doi.org/10.3389/fnagi.2016.00310

4. Alstyne, M. V., Simon, C. M., Sardi, S. P., Shihabuddin, L. S., Mentis, G. Z., & Pellizzoni, L. (2018). Dysregulation of Mdm2 and Mdm4 alternative splicing underlies motor neuron death in spinal muscular atrophy. *Genes & Development*. https://doi.org/10.1101/gad.316059.118

5. Antunes, M., & Biala, G. (2012). The NOR memory: Neurobiology, test procedure, and its modifications. *Cognitive Processing*, *13*(2), 93–110. https://doi.org/10.1007/s10339-011-0430-z

6. Arias, N., Méndez, M., & Arias, J. L. (2015). The recognition of a novel-object in a novel context leads to hippocampal and parahippocampal c-Fos involvement. *Behavioural Brain Research*, *292*, 44–49. https://doi.org/10.1016/j.bbr.2015.06.012

7. Atanasova, D. Y., Dimitrov, N. D., & Lazarov, N. E. (2016). Expression of nitric oxide-containing structures in the rat carotid body. *Acta Histochemica*, *118*(8), 770–775. https://doi.org/10.1016/j.acthis.2016.09.007

8. Bácskai, T., Fu, Y., Sengul, G., Rusznák, Z., Paxinos, G., & Watson, C. (2013). Musculotopic organization of the motor neurons supplying forelimb and shoulder

girdle muscles in the mouse. *Brain Structure & Function*, *218*(1), 221–238. https://doi.org/10.1007/s00429-012-0396-3

9. Balmus, I.-M., & Ciobica, A. (2017). Main Plant Extracts' Active Properties Effective on Scopolamine-Induced Memory Loss. *American Journal of Alzheimer's Disease and Other Dementias*, *32*(7), 418–428. https://doi.org/10.1177/1533317517715906

10. Bang, J., Spina, S., & Miller, B. L. (2015). Non-Alzheimer's dementia 1. *Lancet (London, England)*, *386*(10004), 1672–1682. https://doi.org/10.1016/S0140-6736(15)00461-4

11. Barakat, R., Lin, P.-C., Park, C. J., Best-Popescu, C., Bakry, H. H., Abosalem, M. E., Abdelaleem, N. M., Flaws, J. A., & Ko, C. (2018). Prenatal Exposure to DEHP Induces Neuronal Degeneration and Neurobehavioral Abnormalities in Adult Male Mice. *Toxicological Sciences*, *164*(2), 439–452. https://doi.org/10.1093/toxsci/kfy103

12. Bennion Callister, J., & Pickering-Brown, S. M. (2014). Pathogenesis/genetics of frontotemporal dementia and how it relates to ALS. *Experimental Neurology*, *262*, 84–90. https://doi.org/10.1016/j.expneurol.2014.06.001

13. Cascella, R., Capitini, C., Fani, G., Dobson, C. M., Cecchi, C., & Chiti, F. (2016). Quantification of the Relative Contributions of Loss-of-function and Gain-of-function Mechanisms in TAR DNA-binding Protein 43 (TDP-43) Proteinopathies. *The Journal of Biological Chemistry*, *291*(37), 19437–19448. https://doi.org/10.1074/jbc.M116.737726

14. Castilla-Ortega, E., Sánchez-López, J., Hoyo-Becerra, C., Matas-Rico, E., Zambrana-Infantes, E., Chun, J., De Fonseca, F. R., Pedraza, C., Estivill-Torrús, G., & Santin, L. J. (2010). Exploratory, anxiety and spatial memory impairments are dissociated in mice lacking the LPA1 receptor. *Neurobiology of Learning and Memory*, *94*(1), 73–82. https://doi.org/10.1016/j.nlm.2010.04.003

15. Chaves-Coira, I., Barros-Zulaica, N., Rodrigo-Angulo, M., & Núñez, Á. (2016). Modulation of Specific Sensory Cortical Areas by Segregated Basal Forebrain Cholinergic Neurons Demonstrated by Neuronal Tracing and Optogenetic Stimulation in Mice. *Frontiers in Neural Circuits*, *10*. https://doi.org/10.3389/fncir.2016.00028

16. Chaves-Coira, I., Rodrigo-Angulo, M. L., & Nuñez, A. (2018). Bilateral Pathways from the Basal Forebrain to Sensory Cortices May Contribute to Synchronous Sensory Processing. *Frontiers in Neuroanatomy*, *12*. https://doi.org/10.3389/fnana.2018.00005

17. Chen, B. K., Madigan, N. N., Hakim, J. S., Dadsetan, M., McMahon, S. S., Yaszemski, M. J., & Windebank, A. J. (2018). GDNF Schwann cells in hydrogel scaffolds promote regional axon regeneration, remyelination and functional improvement after spinal cord transection in rats. *Journal of Tissue Engineering and Regenerative Medicine*, *12*(1), e398–e407. https://doi.org/10.1002/term.2431

18. Chiasseu, M., Alarcon-Martinez, L., Belforte, N., Quintero, H., Dotigny, F., Destroismaisons, L., Vande Velde, C., Panayi, F., Louis, C., & Di Polo, A. (2017). Tau accumulation in the retina promotes early neuronal dysfunction and precedes brain pathology in a mouse model of Alzheimer's disease. *Molecular Neurodegeneration*, *12*(1), 58. https://doi.org/10.1186/s13024-017-0199-3

19. Chiò, A., Logroscino, G., Traynor, B. J., Collins, J., Simeone, J. C., Goldstein, L. A., & White, L. A. (2013). Global epidemiology of amyotrophic lateral sclerosis: A systematic review of the published literature. *Neuroepidemiology*, *41*(2), 118–130. https://doi.org/10.1159/000351153

20. Choi, D., Li, D., & Raisman, G. (2002). Fluorescent retrograde neuronal tracers that label the rat facial nucleus: A comparison of Fast Blue, Fluoro-ruby, Fluoro-emerald, Fluoro-Gold and DiI. *Journal of Neuroscience Methods*, *117*(2), 167–172. https://doi.org/10.1016/s0165-0270(02)00098-5

21. Colombrita, C., Zennaro, E., Fallini, C., Weber, M., Sommacal, A., Buratti, E., Silani, V., & Ratti, A. (2009). TDP-43 is recruited to stress granules in conditions of oxidative insult. *Journal of Neurochemistry*, *111*(4), 1051–1061. https://doi.org/10.1111/j.1471-4159.2009.06383.x

22. Coyne, A. N., Zaepfel, B. L., & Zarnescu, D. C. (2017). Failure to Deliver and Translate-New Insights into RNA Dysregulation in ALS. *Frontiers in Cellular Neuroscience*, *11*, 243. https://doi.org/10.3389/fncel.2017.00243

23. Denninger, J. K., Smith, B. M., & Kirby, E. D. (2018). NOR and Object Location Behavioral Testing in Mice on a Budget. *Journal of Visualized Experiments: JoVE*, *141*. https://doi.org/10.3791/58593

24. Dukkipati, S. S., Garrett, T. L., & Elbasiouny, S. M. (2018). The vulnerability of spinal motoneurons and soma size plasticity in a mouse model of amyotrophic lateral sclerosis. *The Journal of Physiology*, *596*(9), 1723–1745. https://doi.org/10.1113/JP275498

25. Duncan, A., Heyer, M. P., Ishikawa, M., Caligiuri, S. P. B., Liu, X.-A., Chen, Z., Micioni Di Bonaventura, M. V., Elayouby, K. S., Ables, J. L., Howe, W. M., Bali, P., Fillinger, C., Williams, M., O'Connor, R. M., Wang, Z., Lu, Q., Kamenecka, T. M., Ma'ayan, A., O'Neill, H. C., … Kenny, P. J. (2019). Habenular TCF7L2 links nicotine addiction to diabetes. *Nature*, *574*(7778), 372–377. https://doi.org/10.1038/s41586-019-1653-x

26. Esquerda-Canals, G., Montoliu-Gaya, L., Güell-Bosch, J., & Villegas, S. (2017). Mouse Models of Alzheimer's Disease. *Journal of Alzheimer's Disease: JAD*, *57*(4), 1171–1183. https://doi.org/10.3233/JAD-170045

27. Fernández-Espejo, E., & Bis-Humbert, C. (2018). Excess amounts of 3-iodo-l-tyrosine induce Parkinson-like features in experimental approaches of Parkinsonism. *Neurotoxicology*, *67*, 178–189. https://doi.org/10.1016/j.neuro.2018.06.002

28. Fukuda, T., Ayabe, T., Ohya, R., & Ano, Y. (2019). Matured hop bitter acids improve spatial working and object recognition memory via nicotinic acetylcholine receptors. *Psychopharmacology*, *236*(9), 2847–2854. https://doi.org/10.1007/s00213-019-05263-7

29. Gao, J., Wang, L., Huntley, M. L., Perry, G., & Wang, X. (2018). Pathomechanisms of TDP-43 in neurodegeneration. *Journal of Neurochemistry*. https://doi.org/10.1111/jnc.14327

30. Gao, W., Liu, Q., Li, S., Zhang, J., & Li, Y. (2015). End-to-side neurorrhaphy for nerve repair and function rehabilitation. *The Journal of Surgical Research*, *197*(2), 427–435. https://doi.org/10.1016/j.jss.2015.03.100

31. Garcia, Y., & Esquivel, N. (2018). Comparison of the Response of Male BALB/c and C57BL/6 Mice in Behavioral Tasks to Evaluate Cognitive Function. *Behavioral Sciences (Basel, Switzerland)*, *8*(1). https://doi.org/10.3390/bs8010014

32. Gerdin, A.-K., Igosheva, N., Roberson, L.-A., Ismail, O., Karp, N., Sanderson, M., Cambridge, E., Shannon, C., Sunter, D., Ramirez-Solis, R., Bussell, J., & White, J. K. (2012). Experimental and husbandry procedures as potential modifiers of the results of phenotyping tests. *Physiology & Behavior*, *106–20*(5), 602–611. https://doi.org/10.1016/j.physbeh.2012.03.026

33. Ghosh, A., Peduzzi, S., Snyder, M., Schneider, R., Starkey, M., & Schwab, M. E. (2012). Heterogeneous spine loss in layer 5 cortical neurons after spinal cord injury. *Cerebral Cortex (New York, N.Y.: 1991)*, *22*(6), 1309–1317. https://doi.org/10.1093/cercor/bhr191

34. Griffiths, B. B., Sahbaie, P., Rao, A., Arvola, O., Xu, L., Liang, D., Ouyang, Y., Clark, D. J., Giffard, R. G., & Stary, C. M. (2019). Pre-treatment with microRNA-181a Antagomir Prevents Loss of Parvalbumin Expression and Preserves NOR Following Mild Traumatic Brain Injury. *Neuromolecular Medicine*, *21*(2), 170–181. https://doi.org/10.1007/s12017-019-08532-y

35. Grkovic, I., Fernandez, K., McAllen, R. M., & Anderson, C. R. (2005). Misidentification of cardiac vagal pre-ganglionic neurons after injections of retrograde tracer into the pericardial space in the rat. *Cell and Tissue Research*, *321*(3), 335–340. https://doi.org/10.1007/s00441-005-1145-1

36. Guo, L., & Shorter, J. (2017). Biology and Pathobiology of TDP-43 and Emergent Therapeutic Strategies. *Cold Spring Harbor Perspectives in Medicine*, *7*(9). https://doi.org/10.1101/cshperspect.a024554

37. Haenggeli, C., & Kato, A. C. (2002). Rapid and reproducible methods using fluorogold for labelling a subpopulation of cervical motoneurons: Application in the wobbler mouse. *Journal of Neuroscience Methods*, *116*(2), 119–124. https://doi.org/10.1016/s0165-0270(02)00035-3

38. Hashimoto, M., Yamanaka, A., Kato, S., Tanifuji, M., Kobayashi, K., & Yaginuma, H. (2018). Anatomical Evidence for a Direct Projection from Purkinje Cells in the Mouse Cerebellar Vermis to Medial Parabrachial Nucleus. *Frontiers in Neural Circuits*, *12*. https://doi.org/10.3389/fncir.2018.00006

39. Hasselmo, M. E., Hinman, J. R., Dannenberg, H., & Stern, C. E. (2017). Models of spatial and temporal dimensions of memory. *Current Opinion in Behavioral Sciences*, *17*, 27–33. https://doi.org/10.1016/j.cobeha.2017.05.024

40. Havton, L. A., & Broman, J. (2005). Systemic administration of cholera toxin B subunit conjugated to horseradish peroxidase in the adult rat labels preganglionic autonomic neurons, motoneurons, and select primary afferents for light and electron microscopic studies. *Journal of Neuroscience Methods*, *149*(2), 101–109. https://doi.org/10.1016/j.jneumeth.2005.03.014

41. Hayashi, A., Moradzadeh, A., Hunter, D. A., Kawamura, D. H., Puppala, V. K., Tung, T. H. H., Mackinnon, S. E., & Myckatyn, T. M. (2007). Retrograde Labeling in Peripheral Nerve Research: It Is Not All Black and White. *Journal of Reconstructive Microsurgery*, *23*(7), 381–389. https://doi.org/10.1055/s-2007-992344

42. Heyser, C. J., McDonald, J. S., Polis, I. Y., & Gold, L. H. (1999). Strain distribution of mice in discriminated Y-maze avoidance learning: Genetic and procedural differences. *Behavioral Neuroscience*, *113*(1), 91–102. https://doi.org/10.1037//0735-7044.113.1.91

43. Hirakawa, M., McCabe, J. T., & Kawata, M. (1992). Time-related changes in the labeling pattern of motor and sensory neurons innervating the gastrocnemius muscle, as revealed by the retrograde transport of the cholera toxin B subunit. *Cell and Tissue Research*, *267*(3), 419–427. https://doi.org/10.1007/BF00319364

44. Hiramatsu, M., Takiguchi, O., Nishiyama, A., & Mori, H. (2010). Cilostazol prevents amyloid β peptide(25-35)-induced memory impairment and oxidative stress in mice. *British Journal of Pharmacology*, *161*(8), 1899–1912. https://doi.org/10.1111/j.1476-5381.2010.01014.x

45. Horie, M., Meguro, R., Hoshino, K., Ishida, N., & Norita, M. (2013). Neuroanatomical study on the tecto-suprageniculate-dorsal auditory cortex pathway in the rat. *Neuroscience*, *228*, 382–394. https://doi.org/10.1016/j.neuroscience.2012.10.047

46. Igaz, L. M., Kwong, L. K., Lee, E. B., Chen-Plotkin, A., Swanson, E., Unger, T., Malunda, J., Xu, Y., Winton, M. J., Trojanowski, J. Q., & Lee, V. M.-Y. (2011). Dysregulation of the ALS-associated gene TDP-43 leads to neuronal death and degeneration in mice. *The Journal of Clinical Investigation*, *121*(2), 726–738. https://doi.org/10.1172/JCI44867

47. Ishihara, A., Ohira, Y., Tanaka, M., Nishikawa, W., Ishioka, N., Higashibata, A., Izumi, R., Shimazu, T., & Ibata, Y. (2001). Cell Body Size and Succinate Dehydrogenase Activity of Spinal Motoneurons Innervating the Soleus Muscle in Mice, Rats, and Cats. *Neurochemical Research*, *26*(12), 1301–1304. https://doi.org/10.1023/A:1014245417017

48. Ishihara, T., Ariizumi, Y., Shiga, A., Yokoseki, A., Sato, T., Toyoshima, Y., Kakita, A., Takahashi, H., Nishizawa, M., & Onodera, O. (2010). [FTLD/ALS as TDP-43 proteinopathies]. *Rinsho Shinkeigaku = Clinical Neurology*, *50*(11), 1022–1024. https://doi.org/10.5692/clinicalneurol.50.1022

49. Jaiswal, M. K. (2019). Riluzole and edaravone: A tale of two amyotrophic lateral sclerosis drugs. *Medicinal Research Reviews*, *39*(2), 733–748. https://doi.org/10.1002/med.21528

50. Janssens, J., & Van Broeckhoven, C. (2013). Pathological mechanisms underlying TDP-43 driven neurodegeneration in FTLD–ALS spectrum disorders. *Human Molecular Genetics*, *22*(R1), R77–R87. https://doi.org/10.1093/hmg/ddt349

51. Kabashi, E., Lin, L., Tradewell, M. L., Dion, P. A., Bercier, V., Bourgouin, P., Rochefort, D., Bel Hadj, S., Durham, H. D., Vande Velde, C., Rouleau, G. A., & Drapeau, P. (2010). Gain and loss of function of ALS-related mutations of TARDBP (TDP-43) cause motor deficits in vivo. *Human Molecular Genetics*, *19*(4), 671–683. https://doi.org/10.1093/hmg/ddp534

52. Kanda, H., Clodfelder-Miller, B. J., Gu, J. G., Ness, T. J., & DeBerry, J. J. (2016). Electrophysiological properties of lumbosacral primary afferent neurons innervating urothelial and non-urothelial layers of mouse urinary bladder. *Brain Research*, *1648*, 81–89. https://doi.org/10.1016/j.brainres.2016.06.042

53. Kapeli, K., Martinez, F. J., & Yeo, G. W. (2017). Genetic mutations in RNA-binding proteins and their roles in ALS. *Human Genetics*, *136*(9), 1193–1214. https://doi.org/10.1007/s00439-017-1830-7

54. Kaur, S. J., McKeown, S. R., & Rashid, S. (2016). Mutant SOD1 mediated pathogenesis of Amyotrophic Lateral Sclerosis. *Gene*, *577*(2), 109–118. https://doi.org/10.1016/j.gene.2015.11.049

55. Khristy, W., Ali, N. J., Bravo, A. B., de Leon, R., Roy, R. R., Zhong, H., London, N. J. L., Edgerton, V. R., & Tillakaratne, N. J. K. (2009). Changes in GABAA receptor subunit gamma2 in extensor and flexor motoneurons and astrocytes after spinal cord transection and motor training. *Brain Research*, *1273*, 9–17. https://doi.org/10.1016/j.brainres.2009.03.060

56. Kim, E., Ko, H. J., Jeon, S. J., Lee, S., Lee, H. E., Kim, H. N., Woo, E.-R., & Ryu, J. H. (2016). The memory-enhancing effect of erucic acid on scopolamine-induced cognitive impairment in mice. *Pharmacology, Biochemistry, and Behavior*, *142*, 85–90. https://doi.org/10.1016/j.pbb.2016.01.006

57. Kim, H.-B., Lee, S., Hwang, E.-S., Maeng, S., & Park, J.-H. (2017). P-Coumaric acid enhances long-term potentiation and recovers scopolamine-induced learning and memory impairments. *Biochemical and Biophysical Research Communications*, *492*(3), 493–499. https://doi.org/10.1016/j.bbrc.2017.08.068

58. Köbbert, C., Apps, R., Bechmann, I., Lanciego, J. L., Mey, J., & Thanos, S. (2000). Current concepts in neuroanatomical tracing. *Progress in Neurobiology*, *62*(4), 327–351. https://doi.org/10.1016/s0301-0082(00)00019-8

59. Kovacs, G. G. (2016). Molecular Pathological Classification of Neurodegenerative Diseases: Turning towards Precision Medicine. *International Journal of Molecular Sciences*, *17*(2). https://doi.org/10.3390/ijms17020189

60. Kraeuter, A.-K., Guest, P. C., & Sarnyai, Z. (2019). The Y-Maze for Assessment of Spatial Working and Reference Memory in Mice. *Methods in Molecular Biology (Clifton, N.J.)*, *1916*, 105–111. https://doi.org/10.1007/978-1-4939-8994-2_10

61. Kristensson, K., & Olsson, Y. (1971). Retrograde axonal transport of protein. *Brain Research*, *29*(2), 363–365. https://doi.org/10.1016/0006-8993(71)90044-8

62. Kuc, K. A., Gregersen, B. M., Gannon, K. S., & Dodart, J.-C. (2006). Holeboard discrimination learning in mice. *Genes, Brain, and Behavior*, *5*(4), 355–363. https://doi.org/10.1111/j.1601-183X.2005.00168.x

63. Kwon, B. K., Liu, J., Messerer, C., Kobayashi, N. R., McGraw, J., Oschipok, L., & Tetzlaff, W. (2002). Survival and regeneration of rubrospinal neurons 1 year after spinal cord injury. *Proceedings of the National Academy of Sciences*, *99*(5), 3246–3251. https://doi.org/10.1073/pnas.052308899

64. La, J.-H., Feng, B., Kaji, K., Schwartz, E. S., & Gebhart, G. F. (2016). Roles of isolectin B4-binding afferents in colorectal mechanical nociception. *Pain*, *157*(2), 348–354. https://doi.org/10.1097/j.pain.0000000000000380

65. Labots, M., Van Lith, H. A., Ohl, F., & Arndt, S. S. (2015). The modified hole board—Measuring behavior, cognition and social interaction in mice and rats. *Journal of Visualized Experiments: JoVE*, *98*. https://doi.org/10.3791/52529

66. Lee, S., & Malykhina, A. P. (2017). Neuro-tracing approach to study kidney innervation: A technical note. *Kidney Research and Clinical Practice*, *36*(1), 86–94. https://doi.org/10.23876/j.krcp.2017.36.1.86

67. Lee, S., Yang, G., Xiang, W., & Bushman, W. (2016). Retrograde double-labeling demonstrates convergent afferent innervation of the prostate and bladder. *The Prostate*, *76*(8), 767–775. https://doi.org/10.1002/pros.23170

68. Lencer, W. I., & Tsai, B. (2003). The intracellular voyage of cholera toxin: Going retro. *Trends in Biochemical Sciences*, *28*(12), 639–645. https://doi.org/10.1016/j.tibs.2003.10.002

69. Lillo, P., & Hodges, J. R. (2009). Frontotemporal dementia and motor neurone disease: Overlapping clinic-pathological disorders. *Journal of Clinical Neuroscience: Official Journal of the Neurosurgical Society of Australasia*, *16*(9), 1131–1135. https://doi.org/10.1016/j.jocn.2009.03.005

70. Ling, S.-C., Polymenidou, M., & Cleveland, D. W. (2013). Converging mechanisms in ALS and FTD: Disrupted RNA and protein homeostasis. *Neuron*, *79*(3), 416–438. https://doi.org/10.1016/j.neuron.2013.07.033

71. Liu, W., Miller, B. L., Kramer, J. H., Rankin, K., Wyss-Coray, C., Gearhart, R., Phengrasamy, L., Weiner, M., & Rosen, H. J. (2004). Behavioral disorders in the frontal and temporal variants of frontotemporal dementia. *Neurology*, *62*(5), 742–748.

72. Ludolph, A. C., & Brettschneider, J. (2015). TDP-43 in amyotrophic lateral sclerosis—Is it a prion disease? *European Journal of Neurology*, *22*(5), 753–761. https://doi.org/10.1111/ene.12706

73. Lueptow, L. M. (2017). NOR Test for the Investigation of Learning and Memory in Mice. *Journal of Visualized Experiments: JoVE*, *126*. https://doi.org/10.3791/55718

74. Majima, T., Tyagi, P., Dogishi, K., Kashyap, M., Funahashi, Y., Gotoh, M., Chancellor, M. B., & Yoshimura, N. (2017). Effect of Intravesical Liposome-Based Nerve Growth Factor Antisense Therapy on Bladder Overactivity and Nociception in a Rat Model of Cystitis Induced by Hydrogen Peroxide. *Human Gene Therapy*, *28*(7), 598–609. https://doi.org/10.1089/hum.2016.121

75. Martin, S., Al Khleifat, A., & Al-Chalabi, A. (2017). What causes amyotrophic lateral sclerosis? *F1000Research*, *6*. https://doi.org/10.12688/f1000research.10476.1

76. McHanwell, S., & Biscoe, T. J. (1981). The sizes of motoneurons supplying hindlimb muscles in the mouse. *Proceedings of the Royal Society of London. Series B, Biological Sciences*, *213*(1191), 201–216. https://doi.org/10.1098/rspb.1981.0062

77. Medina, D. X., Orr, M. E., & Oddo, S. (2014). Accumulation of C-terminal fragments of transactive response DNA-binding protein 43 leads to synaptic loss and cognitive

deficits in human TDP-43 transgenic mice. *Neurobiology of Aging*, *35*(1), 79–87. https://doi.org/10.1016/j.neurobiolaging.2013.07.006

78. Mohajeri, M. H., Figlewicz, D. A., & Bohn, M. C. (1998). Selective loss of alpha motoneurons innervating the medial gastrocnemius muscle in a mouse model of amyotrophic lateral sclerosis. *Experimental Neurology*, *150*(2), 329–336. https://doi.org/10.1006/exnr.1998.6758

79. Nance, D. M., & Burns, J. (1990). Fluorescent dextrans as sensitive anterograde neuroanatomical tracers: Applications and pitfalls. *Brain Research Bulletin*, *25*(1), 139–145. https://doi.org/10.1016/0361-9230(90)90264-z

80. Naumann, T., Härtig, W., & Frotscher, M. (2000). Retrograde tracing with Fluoro-Gold: Different methods of tracer detection at the ultrastructural level and neurodegenerative changes of back-filled neurons in long-term studies. *Journal of Neuroscience Methods*, *103*(1), 11–21. https://doi.org/10.1016/s0165-0270(00)00292-2

81. Neumann, M., Sampathu, D. M., Kwong, L. K., Truax, A. C., Micsenyi, M. C., Chou, T. T., Bruce, J., Schuck, T., Grossman, M., Clark, C. M., McCluskey, L. F., Miller, B. L., Masliah, E., Mackenzie, I. R., Feldman, H., Feiden, W., Kretzschmar, H. A., Trojanowski, J. Q., & Lee, V. M.-Y. (2006). Ubiquitinated TDP-43 in frontotemporal lobar degeneration and amyotrophic lateral sclerosis. *Science (New York, N.Y.)*, *314*(5796), 130–133. https://doi.org/10.1126/science.1134108

82. Ng, L., Khan, F., Young, C. A., & Galea, M. (2017). Symptomatic treatments for amyotrophic lateral sclerosis/motor neuron disease. *The Cochrane Database of Systematic Reviews*, *1*, CD011776. https://doi.org/10.1002/14651858.CD011776.pub2

83. Nouraei, N., Mason, D. M., Miner, K. M., Carcella, M. A., Bhatia, T. N., Dumm, B. K., Soni, D., Johnson, D. A., Luk, K. C., & Leak, R. K. (2018). Critical appraisal of pathology transmission in the α-synuclein fibril model of Lewy body disorders. *Experimental Neurology*, *299*(Pt A), 172–196. https://doi.org/10.1016/j.expneurol.2017.10.017

84. Novikova, L., Novikov, L., & Kellerth, J. O. (1997). Persistent neuronal labeling by retrograde fluorescent tracers: A comparison between Fast Blue, Fluoro-Gold and

various dextran conjugates. *Journal of Neuroscience Methods*, *74*(1), 9–15. https://doi.org/10.1016/s0165-0270(97)02227-9

85. Okabe, N., Himi, N., Maruyama-Nakamura, E., Hayashi, N., Narita, K., & Miyamoto, O. (2017). Rehabilitative skilled forelimb training enhances axonal remodeling in the corticospinal pathway but not the brainstem-spinal pathways after photothrombotic stroke in the primary motor cortex. *PloS One*, *12*(11), e0187413. https://doi.org/10.1371/journal.pone.0187413

86. Olney, N. T., Spina, S., & Miller, B. L. (2017). Frontotemporal Dementia. *Neurologic Clinics*, *35*(2), 339–374. https://doi.org/10.1016/j.ncl.2017.01.008

87. Onaolapo, A. Y., & Onaolapo, O. J. (2015). Caffeine's influence on object recognition and working-memory in prepubertal mice and its modulation by gender. *Pathophysiology: The Official Journal of the International Society for Pathophysiology*, *22*(4), 223–230. https://doi.org/10.1016/j.pathophys.2015.09.001

88. Ou, S. H., Wu, F., Harrich, D., García-Martínez, L. F., & Gaynor, R. B. (1995). Cloning and characterization of a novel cellular protein, TDP-43, that binds to human immunodeficiency virus type 1 TAR DNA sequence motifs. *Journal of Virology*, *69*(6), 3584–3596.

89. Pankevich, D. E., & Bale, T. L. (2008). Stress and sex influences on food-seeking behaviors. *Obesity (Silver Spring, Md.)*, *16*(7), 1539–1544. https://doi.org/10.1038/oby.2008.221

90. Paretkar, T., & Dimitrov, E. (2018). The central amygdala corticotropin-releasing hormone (CRH) neurons modulation of anxiety-like behavior and hippocampus-dependent memory in mice. *Neuroscience*, *390*, 187–197. https://doi.org/10.1016/j.neuroscience.2018.08.019

91. Philips, T., & Rothstein, J. D. (2015). Rodent Models of Amyotrophic Lateral Sclerosis. *Current Protocols in Pharmacology*, *69*, 5.67.1-5.67.21. https://doi.org/10.1002/0471141755.ph0567s69

92. Popratiloff, A. S., Neiss, W. F., Skouras, E., Streppel, M., Guntinas-Lichius, O., & Angelov, D. N. (2001). Evaluation of muscle re-innervation employing pre- and post-

axotomy injections of fluorescent retrograde tracers. *Brain Research Bulletin*, *54*(1), 115–123. https://doi.org/10.1016/s0361-9230(00)00411-1

93. Post, A. M., Wultsch, T., Popp, S., Painsipp, E., Wetzstein, H., Kittel-Schneider, S., Sontag, T. A., Lesch, K.-P., & Reif, A. (2011). The COGITAT holeboard system as a valuable tool to assess learning, memory and activity in mice. *Behavioural Brain Research*, *220*(1), 152–158. https://doi.org/10.1016/j.bbr.2011.01.054

94. Prieur, E., & Jadavji, N. (2019). Assessing Spatial Working Memory Using the Spontaneous Alternation Y-maze Test in Aged Male Mice. *BIO-PROTOCOL*, *9*. https://doi.org/10.21769/BioProtoc.3162

95. Ratti, A., & Buratti, E. (2016). Physiological functions and pathobiology of TDP-43 and FUS/TLS proteins. *Journal of Neurochemistry*, *138 Suppl 1*, 95–111. https://doi.org/10.1111/jnc.13625

96. Rossi, P., Cesaroni, V., Brandalise, F., Occhinegro, A., Ratto, D., Perrucci, F., Lanaia, V., Girometta, C., Orrù, G., & Savino, E. (2018). Dietary Supplementation of Lion's Mane Medicinal Mushroom, Hericium erinaceus (Agaricomycetes), and Spatial Memory in WT Mice. *International Journal of Medicinal Mushrooms*, *20*(5), 485–494. https://doi.org/10.1615/IntJMedMushrooms.2018026241

97. Rowland, L. P., & Shneider, N. A. (2001). Amyotrophic lateral sclerosis. *The New England Journal of Medicine*, *344*(22), 1688–1700. https://doi.org/10.1056/NEJM200105313442207

98. Sagot, Y., Rossé, T., Vejsada, R., Perrelet, D., & Kato, A. C. (1998). Differential Effects of Neurotrophic Factors on Motoneuron Retrograde Labeling in a Murine Model of Motoneuron Disease. *Journal of Neuroscience*, *18*(3), 1132–1141. https://doi.org/10.1523/JNEUROSCI.18-03-01132.1998

99. Sampedro-Piquero, P., Mañas-Padilla, M. C., Ávila-Gámiz, F., Gil-Rodríguez, S., Santín, L. J., & Castilla-Ortega, E. (2019). Where to place the rewards? Exploration bias in mice influences performance in the classic hole-board spatial memory test. *Animal Cognition*, *22*(3), 433–443. https://doi.org/10.1007/s10071-019-01256-3

100.   Schmued, L. C., & Fallon, J. H. (1986). Fluoro-Gold: A new fluorescent retrograde axonal tracer with numerous unique properties. *Brain Research*, *377*(1), 147–154. https://doi.org/10.1016/0006-8993(86)91199-6

101.   Schmued, L. C., Kyriakidis, K., Fallon, J. H., & Ribak, C. E. (1989). Neurons containing retrogradely transported Fluoro-Gold exhibit a variety of lysosomal profiles: A combined brightfield, fluorescence, and electron microscopic study. *Journal of Neurocytology*, *18*(3), 333–343. https://doi.org/10.1007/BF01190836

102.   Scotter, E. L., Chen, H.-J., & Shaw, C. E. (2015). TDP-43 Proteinopathy and ALS: Insights into Disease Mechanisms and Therapeutic Targets. *Neurotherapeutics: The Journal of the American Society for Experimental NeuroTherapeutics*, *12*(2), 352–363. https://doi.org/10.1007/s13311-015-0338-x

103.   Shimizu, N., Wada, N., Shimizu, T., Suzuki, T., Takaoka, E.-I., Kanai, A. J., de Groat, W. C., Hirayama, A., Hashimoto, M., Uemura, H., & Yoshimura, N. (2018). Effects of nerve growth factor neutralization on TRP channel expression in laser-captured bladder afferent neurons in mice with spinal cord injury. *Neuroscience Letters*, *683*, 100–103. https://doi.org/10.1016/j.neulet.2018.06.049

104.   Shimizu, T., Majima, T., Suzuki, T., Shimizu, N., Wada, N., Kadekawa, K., Takai, S., Takaoka, E., Kwon, J., Kanai, A. J., de Groat, W. C., Tyagi, P., Saito, M., & Yoshimura, N. (2018). Nerve growth factor-dependent hyperexcitability of capsaicin-sensitive bladder afferent neurones in mice with spinal cord injury. *Experimental Physiology*, *103*(6), 896–904. https://doi.org/10.1113/EP086951

105.   Shiotsuki, H., Yoshimi, K., Shimo, Y., Funayama, M., Takamatsu, Y., Ikeda, K., Takahashi, R., Kitazawa, S., & Hattori, N. (2010). A rotarod test for evaluation of motor skill learning. *Journal of Neuroscience Methods*, *189*(2), 180–185. https://doi.org/10.1016/j.jneumeth.2010.03.026

106.   Shrager, Y., Bayley, P. J., Bontempi, B., Hopkins, R. O., & Squire, L. R. (2007). Spatial memory and the human hippocampus. *Proceedings of the National Academy of Sciences of the United States of America*, *104*(8), 2961–2966. https://doi.org/10.1073/pnas.0611233104

107. Sieben, A., Van Langenhove, T., Engelborghs, S., Martin, J.-J., Boon, P., Cras, P., De Deyn, P.-P., Santens, P., Van Broeckhoven, C., & Cruts, M. (2012). The genetics and neuropathology of frontotemporal lobar degeneration. *Acta Neuropathologica*, *124*(3), 353–372. https://doi.org/10.1007/s00401-012-1029-x

108. Sik, A., van Nieuwehuyzen, P., Prickaerts, J., & Blokland, A. (2003). Performance of different mouse strains in an object recognition task. *Behavioural Brain Research*, *147*(1–2), 49–54. https://doi.org/10.1016/s0166-4328(03)00117-7

109. Simon, C. M., Dai, Y., Van Alstyne, M., Koutsioumpa, C., Pagiazitis, J. G., Chalif, J. I., Wang, X., Rabinowitz, J. E., Henderson, C. E., Pellizzoni, L., & Mentis, G. Z. (2017). Converging Mechanisms of p53 Activation Drive Motor Neuron Degeneration in Spinal Muscular Atrophy. *Cell Reports*, *21*(13), 3767–3780. https://doi.org/10.1016/j.celrep.2017.12.003

110. Sj, C., & Jr, S. R. (2014). Assessing rodent hippocampal involvement in the NOR task. A review. *Behavioural Brain Research*, *285*, 105–117. https://doi.org/10.1016/j.bbr.2014.08.002

111. Skalicka-Wozniak, K., Budzynska, B., Biala, G., & Boguszewska-Czubara, A. (2018). Scopolamine-Induced Memory Impairment Is Alleviated by Xanthotoxin: Role of Acetylcholinesterase and Oxidative Stress Processes. *ACS Chemical Neuroscience*, *9*(5), 1184–1194. https://doi.org/10.1021/acschemneuro.8b00011

112. Smid, H. M., & Vet, L. E. (2016). The complexity of learning, memory and neural processes in an evolutionary ecological context. *Current Opinion in Insect Science*, *15*, 61–69. https://doi.org/10.1016/j.cois.2016.03.008

113. Spiller, K. J., Cheung, C. J., Restrepo, C. R., Kwong, L. K., Stieber, A. M., Trojanowski, J. Q., & Lee, V. M.-Y. (2016). Selective Motor Neuron Resistance and Recovery in a New Inducible Mouse Model of TDP-43 Proteinopathy. *The Journal of Neuroscience: The Official Journal of the Society for Neuroscience*, *36*(29), 7707–7717. https://doi.org/10.1523/JNEUROSCI.1457-16.2016

114.   Spiller, K. J., Khan, T., Dominique, M. A., Restrepo, C. R., Cotton-Samuel, D., Levitan, M., Jafar-Nejad, P., Zhang, B., Soriano, A., Rigo, F., Trojanowski, J. Q., & Lee, V. M.-Y. (2019). Reduction of matrix metalloproteinase 9 (MMP-9) protects motor neurons from TDP-43-triggered death in rNLS8 mice. *Neurobiology of Disease*, *124*, 133–140. https://doi.org/10.1016/j.nbd.2018.11.013

115.   Spiller, K. J., Restrepo, C. R., Khan, T., Stieber, A. M., Kwong, L. K., Trojanowski, J. Q., & Lee, V. M.-Y. (2016). Progression of motor neuron disease is accelerated and the ability to recover is compromised with advanced age in rNLS8 mice. *Acta Neuropathologica Communications*, *4*. https://doi.org/10.1186/s40478-016-0377-5

116.   Stover, K. R., Campbell, M. A., Van Winssen, C. M., & Brown, R. E. (2015). Early detection of cognitive deficits in the 3xTg-AD mouse model of Alzheimer's disease. *Behavioural Brain Research*, *289*, 29–38. https://doi.org/10.1016/j.bbr.2015.04.012

117.   Takaki, F., Nakamuta, N., Kusakabe, T., & Yamamoto, Y. (2015). Sympathetic and sensory innervation of small intensely fluorescent (SIF) cells in rat superior cervical ganglion. *Cell and Tissue Research*, *359*(2), 441–451. https://doi.org/10.1007/s00441-014-2051-1

118.   Teegarden, S. (2020). Behavioral Phenotyping in Rats and Mice. *Materials and Methods*. /method/Behavioral-Phenotyping-in-Rats-and-Mice.html

119.   Tremblay, C., St-Amour, I., Schneider, J., Bennett, D. A., & Calon, F. (2011). Accumulation of TAR DNA Binding Protein-43 (TDP-43) in Mild Cognitive Impairment and Alzheimer Disease. *Journal of Neuropathology and Experimental Neurology*, *70*(9), 788–798. https://doi.org/10.1097/NEN.0b013e31822c62cf

120.   Vaughan, S. K., Kemp, Z., Hatzipetros, T., Vieira, F., & Valdez, G. (2015). Degeneration of proprioceptive sensory nerve endings in mice harboring amyotrophic lateral sclerosis-causing mutations. *The Journal of Comparative Neurology*, *523*(17), 2477–2494. https://doi.org/10.1002/cne.23848

121.   Voigt, A., Herholz, D., Fiesel, F. C., Kaur, K., Müller, D., Karsten, P., Weber, S. S., Kahle, P. J., Marquardt, T., & Schulz, J. B. (2010). TDP-43-mediated neuron loss in vivo requires RNA-binding activity. *PloS One*, *5*(8), e12247. https://doi.org/10.1371/journal.pone.0012247

122.   Vorhees, C. V., & Williams, M. T. (2014). Assessing Spatial Learning and Memory in Rodents. *ILAR Journal*, *55*(2), 310–332. https://doi.org/10.1093/ilar/ilu013

123.   Walker, A. K., Spiller, K. J., Ge, G., Zheng, A., Xu, Y., Zhou, M., Tripathy, K., Kwong, L. K., Trojanowski, J. Q., & Lee, V. M.-Y. (2015). Functional recovery in new mouse models of ALS/FTLD after clearance of pathological cytoplasmic TDP-43. *Acta Neuropathologica*, *130*(5), 643–660. https://doi.org/10.1007/s00401-015-1460-x

124.   Wang, Z.-Y., Lian, H., Zhou, L., Zhang, Y.-M., Cai, Q.-Q., Zheng, L.-F., & Zhu, J.-X. (2016). Altered Expression of D1 and D2 Dopamine Receptors in Vagal Neurons Innervating the Gastric Muscularis Externa in a Parkinson's Disease Rat Model. *Journal of Parkinson's Disease*, *6*(2), 317–323. https://doi.org/10.3233/JPD-160817

125.   Witts, E. C., Zagoraiou, L., & Miles, G. B. (2014). Anatomy and function of cholinergic C bouton inputs to motor neurons. *Journal of Anatomy*, *224*(1), 52–60. https://doi.org/10.1111/joa.12063

126.   Wong, H., Hossain, S., & Cairns, B. E. (2017). Delta-9-tetrahydrocannabinol decreases masticatory muscle sensitization in female rats through peripheral cannabinoid receptor activation. *European Journal of Pain (London, England)*, *21*(10), 1732–1742. https://doi.org/10.1002/ejp.1085

127.   Xu, J., Wang, K., Yuan, Y., Li, H., Zhang, R., Guan, S., & Wang, L. (2018). A Novel Peroxidase Mimics and Ameliorates Alzheimer's Disease-Related Pathology and Cognitive Decline in Mice. *International Journal of Molecular Sciences*, *19*(11). https://doi.org/10.3390/ijms19113304

128.   Xu, Q.-G., Forden, J., Walsh, S. K., Gordon, T., & Midha, R. (2010). Motoneuron survival after chronic and sequential peripheral nerve injuries in the rat. *Journal of Neurosurgery*, *112*(4), 890–899. https://doi.org/10.3171/2009.8.JNS09812

129.   Yamamoto, Y., & Nakamuta, N. (2018). Morphology of P2X3-immunoreactive nerve endings in the rat tracheal mucosa. *The Journal of Comparative Neurology*, *526*(3), 550–566. https://doi.org/10.1002/cne.24351

130.   Yao, F., Zhang, E., Gao, Z., Ji, H., Marmouri, M., & Xia, X. (2018). Did you choose appropriate tracer for retrograde tracing of retinal ganglion cells? The differences between cholera toxin subunit B and Fluorogold. *PloS One*, *13*(10), e0205133. https://doi.org/10.1371/journal.pone.0205133

131.   Yoshikawa, A., Atobe, Y., Takeda, A., Kamiya, Y., Takiguchi, M., & Funakoshi, K. (2011). A Retrograde Tracing Study of Compensatory Corticospinal Projections in Rats with Neonatal Hemidecortication. *Developmental Neuroscience*, *33*(6), 539–547. https://doi.org/10.1159/000335526

132.   Young, J. J., Lavakumar, M., Tampi, D., Balachandran, S., & Tampi, R. R. (2018). Frontotemporal dementia: Latest evidence and clinical implications. *Therapeutic Advances in Psychopharmacology*, *8*(1), 33–48. https://doi.org/10.1177/2045125317739818

133.   Zarei, S., Carr, K., Reiley, L., Diaz, K., Guerra, O., Altamirano, P. F., Pagani, W., Lodin, D., Orozco, G., & Chinea, A. (2015). A comprehensive review of amyotrophic lateral sclerosis. *Surgical Neurology International*, *6*, 171. https://doi.org/10.4103/2152-7806.169561

134.   Zimmerman, R., Smith, A., Fech, T., Mansour, Y., & Kulesza, R. J. (2020). In utero exposure to valproic acid disrupts ascending projections to the central nucleus of the inferior colliculus from the auditory brainstem. *Experimental Brain Research*, *238*(3), 551–563. https://doi.org/10.1007/s00221-020-05729-7

135.   Žygelyte, E., Bernard, M. E., Tomlinson, J. E., Martin, M. J., Terhorst, A., Bradford, H. E., Lundquist, S. A., Sledziona, M., & Cheetham, J. (2016). RetroDISCO: Clearing technique to improve quantification of retrograde labeled motor neurons of intact mouse spinal cords. *Journal of Neuroscience Methods*, *271*, 34–42. https://doi.org/10.1016/j.jneumeth.2016.05.017